DEPARTMENT of ELECTRICAL ENGINEERING
SCHOOL of ENGINEERING and SCIENCE
NEW YORK UNIVERSITY
UNIVERSITY HEIGHTS BRONX, NEW YORK 10453

UNCLASSIFIED
Security Classification

DOCUMENT CONTROL DATA - R & D
(Security classification of title, body of abstract and indexing annotation must be entered when the overall report is classified)

1. ORIGINATING ACTIVITY (Corporate author) New York University, School of Engineering and Science Department of Electrical Engineering University Heights, Bronx, N.Y. 10453	2a. REPORT SECURITY CLASSIFICATION UNCLASSIFIED 2b. GROUP

3. REPORT TITLE
"Impulse Response of a Kinetically Described Non-Uniform Plasma Bounded in Sheaths"

4. DESCRIPTIVE NOTES (Type of report and inclusive dates)
Technical Report

5. AUTHOR(S) (First name, middle initial, last name)
Rudolf A. Frisch
B. R. Cheo

6. REPORT DATE October 1971	7a. TOTAL NO. OF PAGES 101 + ix	7b. NO. OF REFS 28
8a. CONTRACT OR GRANT NO. N00014-67-A-0467-0018 b. PROJECT NO. NR 371-147/24-4/70(427) c. d.	9a. ORIGINATOR'S REPORT NUMBER(S) 402-9 9b. OTHER REPORT NO(S) (Any other numbers that may be assigned this report) None	

10. DISTRIBUTION STATEMENT
"Reproduction in whole or part is permitted for any purpose of the United States Government"

11. SUPPLEMENTARY NOTES None	12. SPONSORING MILITARY ACTIVITY Director, Electronics Program Physical Sciences Division Office of Naval Research Department of the Navy, Arlington, VA 22217

13. ABSTRACT

The impulse response of a kinetically defined, non-uniform electron plasma slab bounded by sheaths is obtained. The one-dimensional Vlasov-Poisson system is considered. Electron-free boundaries are specified for all time. Possible equilibrium states are studied; under relatively loose mathematical conditions the electron distribution is separable and the only possible velocity distribution is Gaussian. Admissible initial conditions are investigated. The equilibrium plasma is stimulated by an impulse electric field which imparts upon all electrons an equal additional velocity. A numerical scheme is developed which permits to obtain reliable solutions for certain time periods after which numerical instabilities begin to appear. Throughout this study, considering plasma slabs with an equilibrium temperature around 300000K and a plasma frequency of approximately 1 GHz at the center of the slab, reliable solutions were obtained for the spans ranging from 2 plasma periods for strong stimuli to 20 plasma periods in linear operation.

It is found that for excitations in the linear region the Fourier Spectrum of the impulse response contains three strong resonances at and below the background plasma frequency at the center of the slab as well as a series of smaller resonances above this frequency. The former are Tonks-Dattner resonances and it is shown that each one is associated with a well-definable region within the slab. The highest of the three high-amplitude resonances is a cold plasma oscillation while the other two are shown to be thermomodes in the sense of Baldwin and Ignat. In the non-linear responses corresponding to strong stimuli, early bunching and wave-particle interaction are observed.

DD FORM 1 NOV 1473

UNCLASSIFIED
Security Classification

14. KEY WORDS	LINK A ROLE	LINK A WT	LINK B ROLE	LINK B WT	LINK C ROLE	LINK C WT
Impulse Response						
Inhomogeneous Vlasov Plasma						
Slab Resonances						
Sheath						
Numerical Methods						

TECHNICAL REPORT 402-9

IMPULSE RESPONSE OF A KINETICALLY DESCRIBED NON-UNIFORM PLASMA BOUNDED BY SHEATHS

Rudolf A. Frisch
B.R. Cheo

October 1971

Prepared By
NEW YORK UNIVERSITY
SCHOOL OF ENGINEERING AND SCIENCE
Department of Electrical Engineering
University Heights
Bronx, New York 10453

For
Office of Naval Research
under
Grant N00014-67-A-0467-0018
Physical Sciences Division

ABSTRACT

The impulse response of a kinetically defined, non-uniform electron plasma slab bounded by sheaths is obtained. The one-dimensional Vlasov-Poisson system is considered. Electron-free boundaries are specified for all time. Possible equilibrium states are studied; under relatively loose mathematical conditions the electron distribution is separable and the only possible velocity distribution is Gaussian. Admissible initial conditions are investigated. The equilibrium plasma is stimulated by an impulse electric field which imparts upon all electrons an equal additional velocity. A numerical scheme is developed which permits to obtain reliable solutions for certain time periods after which numerical instabilities begin to appear. Throughout this study, considering plasma slabs with an equilibrium temperature around 30000°K and a plasma frequency of approximately 1 GHz at the center of the slab, reliable solutions were obtained for time spans ranging from 2 plasma periods for strong stimuli to 20 plasma periods in linear operation.

It is found that for excitations in the linear region the Fourier spectrum of the impulse response contains three strong resonances at and below the background plasma frequency at the center of the slab as well as a series of smaller resonances above this frequency. The former are Tonks-Dattner resonances and it is shown that each one is associated with a well-definable region within the slab. The highest of the three high-amplitude resonances is a cold plasma oscillation while the other two are shown to be thermomodes in the sense of Bladwin and Ignat. In the non-linear responses corresponding to strong stimuli, early bunching and wave-particle interaction are observed.

ACKNOWLEDGMENT

The authors are grateful to the members of the Electrophysics Group of the Department of Electrical Engineering of New York University for many fruitful discussions.

Appreciation is also extended to the staff of New York University's Bronx Campus UHMC Computer facility for their efforts to make the necessary large amounts of computer time available as well as their assistance to optimize the usage of their Univac 1108.

The authors also wish to thank the secretarial staff of the Department of Electrical Engineering for their assistance in typing the manuscript.

This work was supported by the Office of Naval Research, under Contract N00014-67-A-0467-0018.

TABLE OF CONTENTS

LIST OF TABLES

LIST OF ILLUSTRATIONS

LIST OF SYMBOLS

NOTE:

1. All units are expressed in the MKS International system unless noted.
2. Notation in the appendices is independently defined therein.
3. Indexing superscripts and subscripts are not listed.

a	Thermal velocity of electrons in the plasma slab in equilibrium
d	Half-width of slab
D	$\partial/\partial t$ (Operator)
e	Electron charge, absolute value
E	Electric field
E(x)	Ditto, in the equilibrium state
E(x,t)	Ditto, time dependent
$\{E_n\}$	Set formed by E(x) and its first n derivatives
f	In Parts IV and V: Frequency referenced to T_p^{-1}
f	In Parts I-III: Electron distribution function
f(x,v)	Ditto, in the equilibrium state
f(x,v,t)	Ditto, time-dependent
f_n	Frequency, referenced to T_p^{-1}
f_p	Plasma frequency
f_{po}	Ditto, at center of plasma slab in equilibrium
h	Discrete time interval
h(x)	Defining function of $\varphi(x)$, in order that $\varphi(x)$ can be used as initial condition (See Eq. 35)
J	Total number of time intervals covered by a numerical experiment

m	Electron mass
M	Half-number of intervals covering the width of the slab
n,n(x)	Ion density
n_e	Electron density (See also $\varphi(x)$)
$n_e(x,t)$	Ditto, time-dependent
N	Half-number of intervals in (truncated) velocity-space
N^j	Total number of electrons per unit area of slab, normalized to unity at t=0
N^{jc}	N^j=1.004 (See text, Section III.b)
N_T	Total number of electrons per unit area of slab
N_o	Electron density at center of plasma slab in equilibrium
Q_{nj}	Coefficients of powers of w (See Eq. 28)
R_n	n-th partial time derivative of E(x,t) at t=0.
s	Order of infinity of the voltage on the boundaries (walls)
t	In Parts IV and V: Time referenced to T_p
t	In Parts I-III: Time
t_n	Time referenced to the plasma period T_p
T_p	Plasma period at center of slab in equilibrium
u	Fixed value of the velocity imparted to all electrons by the impulse electric field at t=0
v	Electron velocity
v_n	Absolute value of the limits of truncated velocity space
V	In Parts IV and V: Identical to V_n (See ibidem.)
V	In Parts I-III: Voltage
V(x)	Ditto, in equilibrium state V(0)=0
V(t)	Ditto, between $-x_{min}$ and x_{min}

V_n	Voltage normalized to the parameters of the standard experiment (See Eq. 62)
w	$v+u$
x	distance from center of slab
x_{min}	First minimum of ion density nearest to boundary (wall) $x=d$
y	Distance from wall
ε_o	Free space permittivity
$\lambda_D, \lambda_D(x)$	Debye length in equilibrium state
λ_{Do}	Ditto, at center of slab
$\varphi, \varphi(x)$	Electron density in the plasma slab in equilibrium (See also n_e, $n_e(x,t)$)
$\{\varphi_n\}$	Set formed by $\varphi(x)$ and its first n derivatives
$\psi(v)$	Velocity distribution in the plasma in equilibrium, normalized to $\int_{-\infty}^{+\infty}\psi(v)dv = 1$
ω_p	Plasma angular velocity
ω_{po}	Ditto at center of plasma slab in equilibrium

I. INTRODUCTION AND HISTORICAL BACKGROUND

The study of plasmas is of great interest because it covers a wide spectrum of phenomena which are applicable to many fields from fundamental research to industrial applications. To mention a few areas of investigation, the studies of plasmas ranges from the microcosmic interatomic behavior of a system of charged and neutral particles to the macrocosmic behavior of waves in interstellar spaces. Serious work is being done, based on plasma theory, to obtain a controlled and controllable nuclear fusion pile. Plasma theory has influenced both semiconductor and gaseous electronics. Plasma-magneto-hydrodynamic based energy conversion seems to be within the realms of large-scale applicability.

The mathematical formulation of plasma phenomena is based on Maxwell's laws of electromagnetic field theory and the laws of mechanics. Through a completely stochastic formulation of particle distribution functions in the six-dimensional phase space of mechanics one arrives at the Maxwell-Klimontovich system[1,2]. By ensemble-averaging the system and assuming small fluctuations one obtains the non-linear Maxwell-Vlasov system[1,2]. Taking the moments of the particle distribution function with respect to velocity the fluid model is obtained which treats the plasma like a gas of charged particles. Since only a finite number of moments can be used the fluid model cannot contain the same amount of information as the Maxwell-Vlasov or the Maxwell-Klimontovich system; it restricts itself to a few macroscopic observables.

The kinetic model is non-linear as is the fluid model in an Eulerian frame of reference. The fluid model consists of a system of partial differential equations while the kinetic model is more complicated and consists of a system of partial-differential-integral equations. In a Lagrangian reference frame the fluid model is linear; during back transformation to the Eulerian frame however singularities prevail except under the most favorable circumstances[3]. One is therefore obliged to look for the solution of non-linear systems with all the difficulties this presents.

Since the fluid model represents essentially macroscopic data, it cannot explain phenomena which appear on a macroscopic level but can only be explained by the microscopic behavior of the system. The classical case is the Landau damping which cannot be understood with the fluid model alone. The approximations and limitations inherent to the fluid model are well known and have been well explained by Vandenplas and Gould and by Obermann[4,5]. Attempts to improve the fluid model have not been abandoned; Feix proposed to use the Fourier-Hermite transform to obtain fluid equations[6]. A better link to kinetic theory was shown. However certain limitations in this model still exist. For example, such important phenomena as particle-wave interaction cannot be studied with the fluid model.

The mathematical analysis of the kinetic model is far from trivial even when studied in the linearized form. While for the linearized fluid model spectral analysis after Fourier-Laplace transform of space and time variables yields a finite number of modes for a homogeneous, isotropic, uniform and unbounded plasma, the linearized kinetic model reveals the

existence of a continuous spectrum covering the real frequency axis (Van Kampen modes[7]). To complicate matters, the real frequency axis is the boundary of the region of convergence of the Laplace transform and is therefore a branch of the complex frequency domain. Hilbert transform-Plemelj decomposition techniques therefore are required if one wants to work with real frequencies. One is confronted with the inherent difficulties of a system which contains a singular integral even after the algebraization effected by the Fourier-Laplace transform of space and time.

If these are the difficulties which confront the scientist in the case of an homogeneous, isotropic, uniform and unbounded plasma after linearization of the system, the difficulties become compounded when the plasma becomes bounded and is non-uniform and fluctuations become large enough to invalidate the linearization. Various perturbation methods have been used to study the non-linear system when the fluctuations are small[8]. Einaudi and Sudan have reviewed available perturbation techniques in their several forms and pointed out their limitations[9]. Marcuvitz has utilized the two-time method to study plasma turbulence phenomena[10], Barston[11,12], Crawford and Kino[13] have used variational techniques to study non-uniform cold plasma systems. Trocheris has studied the implicit conditions in the "quasi-linear" equations using both the two-time method and variational principles[14]. In general these methods have only a limited range of validity.

Most of the work done in the above direction has been formulated

in the ($\underline{k}$,ω) formulation (spin-space) of the problem. The reasons for this procedure are not only and exclusively the above mentioned mathematical fact that transform techniques change a differential system into an algebraic one. On the experimental side, due to technical circumstances, interest was constrained either to oscillatory phenomena or to aspects of long duration with respect to a plasma period $T_p=2\pi/\omega_p$. The results therefore have been mostly expressed in terms of spin space variables.

The investigation of strongly non-linear phenomena was not only hampered by the usual mathematical difficulties posed by non-linear systems. These were compounded by the fact that laboratory experiments are conducted in bounded and very often non-uniform plasmas. The corresponding mathematical systems become extremely cumbersome even in the linear approximation. Comparison between experimental and theoretical results are often made only qualitatively. This general difficulty is reflected in the literature. Comprehensive treatises on plasmas became available since the late fifties[15,16]. Vandenplas basic text on bounded plasmas[17] lagged by almost ten years and even so restricts itself almost completely to the fluid model; the kinetic model is used for basic considerations and to show that the fluid model is a satisfactory representation of the system.

Recently, Marcuvitz was able to make the crossover from the frequency domain to the time domain from the linearized kinetic model. For this purpose, he constructed the complete eigenbasis of the Fourier-Laplace transformed equations[18] and this in spite of the fact that the eigenmodes are defined on a branch of the complex frequency plane and thus

need Plemelj formulae for definition. On this eigenbase a very convenient formulation for the recently discovered temporal plasma wave echo was obtained. The echo was formulated through perturbation expansion in such a fashion that the n-th order term depends recursively on the terms up to order (n-1) but does not contain the independent variable explicitly and thus presents no secular terms[19]. Unfortunately, obtaining even the first-order term for a Maxwellian plasma by numerical methods proved to be prohibitive in terms of computer time even on a Univac 1108 or CDC 6600[20]; the Fourier transform on a digital computer is extremely slow and has remained so in spite of all efforts to the contrary. Marcuvitz also attempted to obtain an eigenbasis in the second Riemann sheet defined by the problem[21]. The corresponding set of eigenvalues consists of enumerably infinite complex values with an accumulation point at infinity; this set (whose least damped mode incidentally is the Landau mode) has not yet been completely determined. Both eigenbases were proven to be complete.

The advent of the high-speed digital computer changed the situation to some extent. Not only could one attempt the solution of non-linear systems, be they algebraic, differential, integral or mixed types by numerical methods; it also became possible to associate numerical techniques with analytical results and thus investigate at least numerical behavior in the range of validity and to point to directions for further theoretical and experimental investigations. In the early sixties, Dawson developed a model in which the motion of charged "sheets" in a slab bounded

by two parallel walls is followed: The movement of the sheets is governed by the basic laws of physics[22]. This model was analyzed in depth by Feix[6] and has continued to be used by others [23]. Results proved to be in satisfactory agreement with experimental data in the linear region. It is presently being further investigated by Brooks and Cheo of the electrophysics group at New York University on a nonuniform slab and it is hoped that results can be extended into the strongly non-linear region[24].

Several attempts were made to obtain solutions to plasma problems in the time domain. Armstrong[25] studied the relaxation problem of a nonuniform electron plasma with a uniform ion background in a plasma slab (see Equations I.8 and I.9, Appendix I) using Fourier and Fourier-Hermite series for space and velocity respectively since these yielded the longest time span before numerical instabilities began to prevail. As expected, the smaller the deviation of the initial electron distribution the better the solution since the small disturbance parameter is needed to obtain rapid convergence of the Fourier series. A stable scheme for the problem was not obtained but results agreed with analytical data in the linear and quasi-linear region. The solution for stronply non-linear problems was not adduced.

During 1970, a very high amplitude and very fast pulse generator, called bouncing ball generator (BBG), became available at New York University. This generator was constructed by P. Pleshko in connection with his Ph.D. thesis work supervised by Prof. I. Palocz at New York University[26]. The BBG is capable of generating pulses having 3db width of approximately

1.2×10^{-10} sec. with an amplitude of well over 10^3 volts (appro. 1.5 KV) into a 50 ohm load (peak power appr. 45 KW). This capability of combined high amplitude and short duration and the use of high resolution sampling scopes have enabled a series of transient studies on laboratory plasmas at both linear and non-linear levels. One of the structures chosen for the experimental work is the Tonks-Dattner structure. In this structure a plasma column was placed between a parallel plate system which is connected to the BBG. The pulses from the BBG (width appr. 0.1 of a plasma period) impart sufficient energy to the electrons and result in stimulated oscillations of velocities reaching 10^7 m/sec, well into the non-linear region. Such a system has great advantages over microwave CW excitations since the average power is very small inspite of the high amplitude oscillation. Thus the problem of additonal heating is avoided. Furthermore, the observations are made within a short period following each pulse (appr. 5.0×10^{-8} sec.). This is short compared with average collision times of the system. Thus no ionization or recombination can take place. This situation offers an attractive situation for theoretical study: The output of the BBG can be reasonably well simulated by a Dirac delta-function; collisional, ionization and recombination models are not necessary in this context.

It is the purpose of this work to present the results of a theoretical effort which to some degree parallels experimental developments obtained and being obtained at the Electrical Engineering Department of New York University.

For this study, the following problem is considered: A non-uniform kinetically described plasma in equilibrium is bounded by two parallel planes and contained by an imposed electric field. The plasma is excited by an impulsive electric field (in the form of a Dirac delta-function) uniform in space and perpendicular to the planes. The resulting phenomena and responses are obtained by solving numerically the system formed by Maxwell's divergence law and Boltzmann-Vlasov equations. The necessary calculations have been performed on a high-speed digital computer using a numerical scheme which has been developed for this purpose. Results, in particular the electric field and voltage, are studied in the time domain. Subsequent Fourier transforms lead to frequency domain data which are then analyzed and discussed. Of particular interest are Tonks-Dattner resonances in the voltage spectrum which are shown to originate in definite regions of the slab.

In the next section, the model is defined, formulated, analyzed and discussed from the mathematical point of view. Boundary conditions and initial conditions are established. Section III presents the development of the numerical scheme used for the necessary computations and discusses this numerical scheme. Section IV presents obtained results for relatively small impulses resulting in responses which can be considered linear to a good degree of approximation. Also discussed is the effect of variation of parameters necessary to define the plasma. Finally, in Section V, results are adduced for large impulse-excitations and some observed non-linearities are discussed.

II. MATHEMATICAL ANALYSIS

A. General Considerations

From the mathematical point of view, one is confronted in the general case of a plasma containing n kinds of particles with a system of 8+n scalar equations, four of which are partial-differential-integral of the first order, the others being partial differential of first order. These equations relate 6+n dependent scalar variables to seven independent variables (See Appendix I.). The problems of existence, uniqueness and well-posedness are tremendous and in order to attempt a solution at all, even by numerical methods, one has to reduce the problem to simpler proportions. One considers therefore a system with 2 kinds of particles only, electrons and ions. One assumes further that the time span considered in the problem is relatively short and therefore the ions can be considered immobile.

While it would be desirable to obtain a solution in cylindrical coordinates since most experimental work is done in this geometry, it is the plasma slab which offers the minimum significant number of both dependent and independent variables. The basic equations of the kinetic model for the plasma slab have been derived in Appendix I. It should be noted that Equation I.9 represents the non-linear Boltzmann-Vlasov equation while Equation I.8 represents Maxwell's divergence law. The electrostatic approximation is not necessary to the system I.8,9.

The first question is what should be the conditions at the boundary of the slab? In the experimental work the plasma is contained by physical walls together with the plasma sheath; an appropriate simulation of this is

given by an externally imposed electric field (associated with an ion distribution) which rises rapidly to infinity at the walls. This high field intensity extends over only a very short distance (of the order of less than one Debye length) from the wall. This field therefore simulates both the impenetrable walls and the sheath. (For ease of language, the parallel planes which are the boundaries of the plasma will be called "walls" although their physical existence is immaterial to the present model due to the presence of the electric field.)

The initial conditions are stipulated as follows: Suppose that at t=0-, the electron distribution function is given by f(x,v,0-). At time t=0 one applies an impulse electric field in the form of a Dirac delta-function. Assuming a non-relativistic formulation, this impulse will accrue the velocity of every electron by an increment of u in the negative direction. In other words, if an electron at t=0- had a velocity v, at t=0+, this electron will have a velocity v+u. Therefore the initial condition of f(x,v,t) at t=0+ is f(x,v+u,0-). f(x,v,0-) is considered an equilibrium state of the system.

The electric field vector E(x,t) depends on the charge distributions through Maxwell's divergence equation. Since no particle has time to move from t=0- to t=0+, the electric field is continuous at t=0.

To summarize, one considers the following Maxwell-Vlasov system as a mixed initial value - boundary condition problem (formulated in MKS International units)

$$\frac{\partial E^*(x,t)}{\partial x} = -\frac{e}{\epsilon_o}\int_{-\infty}^{+\infty} f^*(x,v,t)dv + \frac{e}{\epsilon_o} n^*(x) \qquad (1a)$$

$$\frac{\partial f^*(x,v,t)}{\partial t} + v\frac{\partial f^*(x,v,t)}{\partial x} - \frac{e}{m} E^*(x,t)\frac{\partial f^*(x,v,t)}{\partial v} = 0 \qquad (1b)$$

defined on the domain

$$t > 0 \quad , \quad -d < x < d \quad , \quad -\infty < v < \infty \qquad (2a)$$

subject to the initial conditions

$$f^*(x,v,0+) = f^*(x,v+u,0-) \qquad (2b)$$

$$\frac{\partial^n f^*(x,v,t)}{\partial^n t} \equiv 0 \qquad t < 0 \qquad (2c)$$

and the boundary conditions:

$$f^*(d,v,t) = f^*(-d,v,t) = 0 \qquad t > 0 \qquad (2d)$$

$$f^*(x,\infty,t) = f^*(x,-\infty,t) = 0 \qquad t > 0 \qquad (2e)$$

$$\frac{\partial^n f^*(d,v,t)}{\partial^n t} = \frac{\partial^n f^*(-d,v,t)}{\partial^n t} = 0 \qquad \text{any } n,\ t > 0 \qquad (2f)$$

$$\frac{\partial^n f^*(x,\infty,t)}{\partial^n t} = \frac{\partial^n f^*(x,-\infty,t)}{\partial^n t} = 0 \qquad \text{any } n,\ t > 0 \qquad (2g)$$

The functions E*, f* and n* of (1) are expressed in the MKS International (or a similarly rationalized) system. It is more convenient to normalize by introducing

$$f(x,v,t) = \frac{1}{N_o} f^*(x,v,t) \tag{3}$$

$$E(x,t) = \frac{e}{m} E^*(x,t) \tag{4}$$

$$n(x) = \frac{1}{N_o} n^*(x) \tag{5}$$

$$\omega_{po}^2 = \frac{N_o e^2}{m\varepsilon_o} \tag{6}$$

(1) then becomes

$$\frac{1}{\omega_{po}^2} \frac{\partial E}{\partial x} = - \int_{-\infty}^{+\infty} f dv + n \tag{7}$$

$$\frac{\partial f}{\partial t} + v \frac{\partial f}{\partial x} - E \frac{\partial f}{\partial v} = 0 \tag{8}$$

N_o is a particle number density and thus ω_{po} is a plasma angular velocity. (N_o will be chosen to be the electron density at x=0 in an equilibrium state and ω_{po} thus will be the plasma angular velocity at x=0, t=0- of electrons.)

The problem is of the mixed type in the sense that both boundary conditions and initial values are specified. They are still expressed by (2) but without the asterisk. Physically expressed, the boundary conditions specify that at no time there are electrons on the walls of the slab nor do electrons with infinite velocity exist.

It is possible to gain some insight into some properties of the system (7,8). A short analysis has been performed and it can be shown that

$f(x,v,t)$ can be seen to be hyperboloidal in the sense that there are two characteristic manifolds (in this case two-dimensional planes) through each point of (x,v,t)-space but degenerate in the sense that the quadratic form defined by the respective partial differential equation degenerates into two straight lines and does not define a true conic. It can also be seen that any plane perpendicular to the x-axis is a characteristic plane. Thus any plane t=constant represents a characteristic plane. (It follows that an initial value problem defined at t=0 with boundary conditions defined as above constitutes a variation of "Goursat's problem" which solves initial value problems defined on a characteristic at t=0.) Therefore the initial conditions to be stipulated on a characteristic will have to be stipulated with great care since they will constitute another constraint on the problem. In fact, one has to ask if the initial values together with the boundary conditions in (2) do not overspecify the problem or what can be done to avoid this situation. This again might constitute another constraint.

As mentioned before, the initial conditions at time t=0+ result from an equilibrium state at t=0-. The investigation into this problem is not trivial since one has to expect that the system (7,8) will impose conditions on this initial state which is defined on a characteristic of the system.

B. Study of the Equilibrium States and Possible Initial Conditions

To look for a steady state of the system (7,8) one sets $\partial f(x,v,t)/\partial t = 0$. (8) then yields

$$E(x) = \frac{v \frac{\partial}{\partial x} f(x,v)}{\frac{\partial}{\partial v} f(x,v)} \tag{9}$$

$$f(x,v) = f(x,v,0-) \tag{10}$$

$$E(x) = E(x,0-) \tag{11}$$

It is shown (See Appendix II) that $f(x,v)$ is separable under relatively loose restrictions on $E(x)$; i.e., that

$$f(x,v) = \varphi(x)\psi(v) \tag{12}$$

and it is shown ibidem that with K and A being constants

$$\psi(v) = K \exp(-Av^2) \tag{13}$$

Thus the only distribution in the equilibrium state is the Maxwellian (13). For convenience one stipulates

$$\int_{-\infty}^{+\infty} \psi(v)dv = 1 \tag{14}$$

and therefore (13) becomes

$$\psi = \frac{1}{a\sqrt{2\pi}} \exp\left(-\frac{v^2}{2a^2}\right) \tag{15}$$

a being the termal velocity of the electrons. Appendix II also proves that $\varphi(x) > 0$ for all x except on the boundary.

One further choses $\varphi(0) = 1$. Using (3,12) the unnormalized equilibrium electron distribution function is $f^*(x,v) = N_o\varphi(x)\psi(v)$ and N_o can be seen to be the number of electrons per unit volume at x=0 in the

equilibrium state. Therefore ω_{po} defined by (6) has indeed become the plasma angular velocity at x=0 in the equilibrium state.

Appendix II proves that for (12) true one has, under suitable mathematical conditions

$$E = -a^2 \frac{d\varphi}{dx}\frac{1}{\varphi} = -a^2 \frac{d}{dx}(\ell n \varphi) \tag{16}$$

and

$$n = \varphi - \lambda_{Do}^2 \frac{d^2}{dx^2}(\ell n \varphi) \qquad \lambda_{Do} = \frac{a}{\omega_{po}} \tag{17}$$

with λ_{Do} the Debye length at the origin. Since the electron density varies with x, so will the Debye length $\lambda_D(x)$. In particular, since $f(x,v,t) = 0$ on the walls of the slab, $\lambda_D(x)$ becomes infinity. This variation of the Debye length becomes significant from the physical point of view. The phenomena described by (7,8) are macroscopic in the sense that they refer to behavior outside of a Debye sphere centered on a given particle; thus one might neglect to a certain point occurrences within one Debye length from the boundary. If as can be shown, n(x) has a local maximum at the boundary, then within the slab there exists at least one point x_{min} where $n(x_{min})$ is a local minimum. If one of these minima occur near the boundary of the slab in the sense that the distance $y = d - x_{min}$ be of the order of λ_D or less, it is reasonable to study the phenomena within the slab located between $+x_{min}$ and $-x_{min}$. The region between the minima and the walls can be assumed to represent the sheath.

The voltage V(x) follows from (16) by integration. If one assumes for the arbitrary integration constant $V(0) = 0$ one has

$$V(x) = -a^2 \ln \varphi \qquad (18)$$

If $\varphi(x)$ is even and monotonically decreasing from the center to the walls, one sees that the voltage is even and monotonically increasing from the center to the boundary and, as follows from the boundary condition, becomes infinity at the boundary. The electric field for its part is odd and thus zero in the center of the slab. The behavior of $E(x)$ and $V(x)$ near the boundary cannot be predicted without more detailed information about $\varphi(x)$.

The question arises which of the possible equilibrium states can be initial states which will follow the prescribed boundary conditions after the perturbing electric field has been applied. As seen before, the initial conditions have to be prescribed on a characteristic surface of the system and thus act as a constraint on the problem. Physically speaking, the initial electric field (which is the electric field of the equilibrium state) has to be such that even with further developments it is strong enough to avoid contact of electrons with the wall surfaces. It has been shown that the electric field $E(x)$ of an equilibrium state which is an admissible initial condition has to behave near the boundary with an order $1+s$ in $1/y$ where y is the distance from the boundary and s is positive finite. In fact, $\varphi(x)$ has to be of a given functional form. The following outlines the procedure to obtain the obtained result:

Assume now that one has a equilibrium state background for $t < 0$ given by (10) with (14)

$$f(x,v) = \frac{1}{a\sqrt{2\pi}} \varphi(x) \exp\left(-\frac{v^2}{2a^2}\right) \tag{19}$$

At time t=0 one applies an electric field $E_d(t) = (mu/e)\delta(t)$. This will change the velocity of all electrons by an increment of u(in the negative direction) between t=0- and t=0+. Since at t=0- the electron distribution function was given by (19), it follows that at time 0+ the distribution function will be

$$f(x,v,0+) = \frac{1}{a\sqrt{2\pi}} \varphi(x) \exp\left[-\frac{(v+u)^2}{2a^2}\right] \tag{20}$$

As mentioned before, the requirement that the boundary of the slab remain free of electrons at all times, places restrictions on the functional form of $\varphi(x)$. To investigate this behavior, the following procedure has been adopted.

One sets

$$w = v + u \tag{21}$$

and expands f(x,w,t) in a McLaurin series with x and v fixed

$$f(x,w,t) = \sum_{n=o}^{\infty} \frac{t^n}{n!} \frac{\partial^n}{\partial t^n} f(x,w,0^+) \tag{22}$$

Similarly one writes

$$E(x,t) = \sum_{n=o}^{\infty} \frac{t^n}{n!} \frac{\partial^n}{\partial t^n} E(x,0^+) \tag{23}$$

From time-independent Boltzmann-Vlasov one has

$$\frac{\partial f}{\partial t} = u\, \psi(w) \frac{d\varphi}{dx} \tag{24}$$

and obtains

$$\frac{\partial^2 E}{\partial t \partial x} = - \omega_{po}^2 \, u \, \frac{d\varphi}{dx} \tag{25}$$

integration with respect to x yielding

$$\frac{\partial E}{\partial t} = - \omega_{po}^2 \, u \, \varphi + \text{constant} \tag{26}$$

Examination of (7) now permits one to assume that also E(x,t) should remain time-invariant on the walls and all its partial time derivatives equal to zero. This is based on the fact that at no time electrons of whatever speed can reach the wall. Thus since $\varphi(x) = 0$ on the wall, the constant in (26) vanishes and (26) becomes

$$\frac{\partial E}{\partial t} = - \omega_{po}^2 \, u \, \varphi \tag{27}$$

Similarly, one obtains the second partial time derivatives of f(x,v) and E(x). The recursive formulae for the higher order partial time derivatives of these two equilibrium state functions have been also obtained and it can be shown that they are of the form

$$\frac{\partial^{n+1} f}{\partial t^{n+1}} = u \, \psi(w) \sum_{j=0}^{n} Q_{nj} w^j \tag{28}$$

$$\frac{\partial^{n+1} E}{\partial t^{n+1}} = - R_n \tag{29}$$

where

$$w = v + u \tag{30}$$

$$Q_{nj} = Q_{nj}(u, \omega_{po}^2, \{\varphi\}_n, \{E\}_n) \tag{31}$$

$$R_n = R_n(u,\omega_{po}^2,\{\varphi\}_n,\{E\}_n) \tag{32}$$

$$\{\varphi\}_n = (\varphi, \frac{d\varphi}{dx}, \ldots\ldots, \frac{d^n\varphi}{dx^n}) \tag{33}$$

$$\{E\}_n = (E, \frac{\partial E}{\partial t}, \ldots\ldots, \frac{\partial^n E}{\partial t^n}) \tag{34}$$

From the form of the terms Q_{nj} and R_n it has been deduced that the functions $\varphi(x)$ which fulfill the requirement that all partial time derivatives of the electric field and the distribution function at time t=0+ are zero have to be of the form

$$\varphi(x) = K \exp(-1/h(x)) \qquad K \text{ Constant} \tag{35}$$

where h(x) has the properties

a. h(x) is even (36a)

b. h(x) is positive everywhere in the slab and vanishes on the boundary and on the boundary only (36b)

c. h(x) belongs to the class of functions with an infinite number of derivatives (36c)

d. h(x) goes to zero as y^{-s}, s positive finite y=d-x being the distance to the wall.* (36d)

From (16) it can be seen that E(x) will go to infinity as $y^{-(s+1)}$.

K is defined by $\varphi(0) = 1$ as

$$K = \exp(1/h(0)) \tag{37}$$

*Complete proof of the development from Equation (21) to (36) as well as explicit recursion formulae (28-34) can be obtained from the author.

As an example of functions satisfying the above one has

$$\cos^s \frac{\pi x}{2d} \quad ; \quad (a^2 - x^2)^s \qquad s > 0 \tag{38}$$

s being finite. These functions have a zero of order s on the wall and satisfy all conditions (36).

A particularly attractive h(x) out of (38) is of course $h(x) = a^2-x^2$ since all its derivatives of higher than second order vanish. However, preliminary calculations show that due to the form of the terms of the derivatives of the corresponding $\varphi(x)$ which contain a factor of the form

$$\varphi(x)/h^n(x) \tag{39}$$

with n smaller or equal to the order of the derivative of $\varphi(x)$, the derivatives, although zero on the boundary, have a maximum near the boundary which increases with increasing order and which also gets nearer to the boundary with increasing order. This behavior unfortunately affects the numerical solution. It proved therefore to be of advantage to use an equilibrium state where only the first time-derivative of f(x,w,t) vanishes at t=0+. This leads to loss of electrons as time goes on. This loss, however, has proved to be negligibly small compared with other numerical inaccuracies.

III. NUMERICAL SCHEME

A. Development of the Numerical Scheme

In order to solve (7,8) over a reasonable time compared with a plasma period T_p, a numerical scheme is developed. One has the truncated Taylor series (note that v not w is used)

$$f(x,v,t+\Delta t) \cong f(x,v,t) + \sum_{j=1}^{K} \frac{\partial^j}{\partial t^j}[f(x,v,t)](\Delta t)^j \frac{1}{j!} \tag{40}$$

$$E(x,t+\Delta t) \cong E(x,t) + \sum_{j=1}^{K} \frac{\partial^j}{\partial t^j}[E(x,t)](\Delta t)^j \frac{1}{j!} \tag{41}$$

for fixed x and v. One uses K=1 for the first approximation.

Time discretization is based on the constant interval $h=\Delta t$. Then for a non-negative integer j

$$f(x,v,[j+1]h) \cong f(x,v,jh) + h \frac{\partial}{\partial t}[f(x,v,jh)] \tag{42}$$

$$E(x,[j+1]h) \cong E(x,jh) + h \frac{\partial}{\partial t}[E(x,jh)] \tag{43}$$

the remainders being $0(h^2)$. Similarly x and v are discretized. One has therefore

$$t = jh \qquad j = 0,1,2.....J \tag{44a}$$

$$x = m\Delta x \qquad m = 0,\overline{+}1,\overline{+}2.....\overline{+}M \tag{44b}$$

$$v = n\Delta v \qquad n = 0,\overline{+}1,\overline{+}2.....\overline{+}N \tag{44c}$$

where Jh is the total time to be considered and NΔx = d, d being the half-width of the slab. N is chosen to cover a deviation of

$$v_n = 4\sqrt{2}a \tag{45}$$

from the average velocity. For a Gaussian this truncation introduces an error of $0(e^{-16})$.

One now sets

$$f(m\Delta x, n\Delta v, jh) \equiv f^j_{m,n} \quad ; \quad E(m\Delta x, jh) \equiv E^j_m \tag{46}$$

and (40-41) become

$$f^{j+1}_{m,n} = f^j_{m,n} + h\,\frac{\partial}{\partial t} f^j_{m,n} \tag{47}$$

$$E^{j+1}_m = E^j_m + h\,\frac{\partial}{\partial t} E^j_m \tag{48}$$

One now uses (8) and sets using central differences

$$\frac{\partial}{\partial t} f^j_{m,n} \simeq -\frac{1}{2\Delta x} v_n (f^j_{m+1,n} - f^j_{m-1,n}) + \frac{1}{2\Delta v} E^j_m (f^j_{m,n+1} - f^j_{m,n-1}) \tag{49}$$

One sets further

$$\frac{\partial}{\partial t} f^j_{m,n} \equiv D \cdot f^j_{m,n} \tag{50}$$

and (49) becomes

$$f^{j+1}_{m,n} = f^j_{m,n} + hD \cdot f^j_{m,n} \tag{51}$$

In order to use (48), one sets (31) in a discrete form with respect to v (which replaces w)

$$\frac{\partial^2 E}{\partial x \partial t} \approx - \omega_{po}^2 \Delta v \sum_{-N}^{+N} {}_n \; D \cdot f^j_{m,n} \tag{52}$$

and then replaces the integral over x by the sum

$$\frac{\partial}{\partial t}[E^j_m] = - \omega_{po}^2 \Delta x \Delta v \sum_{-(M-1)}^{m} {}_k \sum_{-N}^{+N} {}_n \; D \cdot f^j_{k,n} \tag{53}$$

or alternatively by the summation

$$\frac{\partial}{\partial t}[E^j_m] = + \omega_{po}^2 \Delta x \Delta v \sum_{M-1}^{m} {}_k \sum_{-N}^{+N} {}_n \; D \cdot f^j_{k,n} \tag{54}$$

where the constant of integration was set to zero due to the argument previously developed (See after Equation 26). (53) and (54) show quite clearly that for an arbitrary initial condition the imposed boundary conditions can overspecify; (53,54) might easily lead to different results for the same m. If however a proper initial condition is used, the two equations can be used to reduce numerical error.

If one sets similarly to (50)

$$\frac{\partial}{\partial t} E^j_m = D \cdot E^j_m \tag{55}$$

(48) can be written

$$E^{j+1}_m = E^j_m + h \; D \cdot E^j_m \tag{56}$$

(51,56) constitute a "memoryless" advancing in time from jh to (j+1)h using exclusively the information contained in the system at time jh. From the numerical point of view, however, "leapfrogging" seems to yield

better results and better stability in the sense to be explained in the next section. One replaces (51,56) by

$$f^{j+1}_{m,n} = f^{j-1}_{m,n} + 2h\ D \cdot f^{j}_{m,n} \tag{57}$$

$$E^{j+1}_{m} = E^{j-1}_{m} + 2h\ D \cdot E^{j}_{m} \tag{58}$$

except for j=0 when (51,56) continue to be used.

B. Considerations on Numerical Stability

There is no known technique applicable to the present problem for a study of stability criteria in the sense of Von Neumann. It is possible, by manipulating the system (7,8), to arrive at a quasi-linear partial differential equation of third order for the function f(x,v,t) which can be analyzed for Von Neumann stability in a heuristic sense. However, besides losing two levels of information, the stability analysis will only yield results in a "local" sense offering no assurance of global stability.

A large number however of computer runs has shown that a macroscopic parameter exists which will define the area in which obtained results are reliable. This parameter is the total number of particles per unit area of slab. This number is

$$N_T(t) = N_o \int_{-d}^{+d} dx \int_{-\infty}^{+\infty} dv\, f(x,v,t)$$

$$\cong N_o \Delta x \Delta v \sum_{-M+1}^{M-1} \sum_{-N}^{+N} f^j_{m,n}$$

$$= N_T(jh) \tag{59}$$

One defines the "normalized" electron quantity

$$N^j = N_T(jh)/N_T(0) \tag{60}$$

which ideally should be constant and equal to one. However, besides numerical instability, there is a factor to be considered which will allow N^j to vary at least to some degree. This is the replacement of a continuous electric field E(x,t) by the discretized field E(m,t). E(x,t) should go to infinity with an order (1+s) as x goes to the wall. (s=1 was considered.) This is impossible to simulate on any computer. Even working with the finest possible mesh in x-space, the electric field near the boundary cannot be made infinite. Therefore some electrons are lost to the boundary. This is, in fact, observed during a very small time compared to T_p but then N^j begins to increase (and sometimes to oscillate very slightly). Computer runs were made with several values of M and N using either (51,56) or (57,58) or any combination thereof. The physical parameters of the plasma were

$$N_o = 10^{16} \text{ electrons per cu. meter} \tag{61a}$$

$$a = 10^6 \text{ m/sec} \tag{61b}$$

$$d = 5.10^{-3} \text{m} \tag{61c}$$

$$\varphi(x) = \cos^2 \frac{\pi x}{2d} \tag{61d}$$

and for several values of h ranging from $T_p/20$ to $T_p/240$ and (where T_p is the plasma period of the center of the slab in equilibrium) for several values of u ranging from .1a to a. As long as N^j was less than 1.004, results for the same parameters were practically the same independent of the used scheme. However scheme (57,58) (which in some way is similar to the Dufort-Frankel scheme of the diffusion equation) always reached 1.004 after much more time than any other scheme, and thus can be taken as "more stable". After several dozen of comparative runs, all schemes were discarded in favor of (57,58). The macroscopic parameter evaluated in this stage, except N^j, was the voltage both wall-to-wall and from $-x_{min}$ to x_{min}.

The problem thus became to extend the time (in terms of T_p) at which N^j reached the value 1.004. Call this time N^{jc}. This time is in strong dependence of the strength of the impulse given by u/a as can be expected since this value is a measure of the non-linearity introduced into the system. For decreasing u/a, N^{jc} increases with constant h,M,N. N^{jc} also increases with increasing M and N for constant h provided h be sufficiently small. The total amount of time at which $N^j = N^{jc}$ also

increases for decreasing h with constant M and N for some time after which a decrease of h yields no further improvement. Thus the technique to extend the time at which N^{jc} is reached seems to consist in increasing M and N (interestingly best results correspond to M=N) and then decreasing h until no further improvement is obtained. Unhappily, this also requires an increase in computer core space and processor time. If one doubles M and N and halves h, the computer core requirement increases by a factor of 4 and CPU time by 8. Although New York University's Heights Univac 1108 is a very fast and large machine, the program is operating near the core capacity of the 1108 and uses a considerable amount of CPU time per run.

The increase of the number of electrons was investigated. Essentially, it consists in the fact that in the "corners" of the (x,v)-space the numerical values of the central differences in (49) show a relatively large error compared to true analytical values. The two errors can reinforce each other, deform $D^{\cdot}f^{j}_{m,n}$ and thus distort $f^{j+1}_{m,n}$ and then E^{j+1}_{m}. With time, these errors propagate through the whole slab and lead to a catastrophic explosion of N^{j}. However, as long as N^{j} does not pass 1.004 by a considerable amount, the resulting distortion seems to be negligible; it certainly does not affect voltages, electron density and electric field and discrepancies in velocity space are practically restricted to the corners of (x,v)-space.

In order to get an idea about the variation of N^{j} and the time at which N^{jc} is reached, Table I shows a few results obtained for the plasma (61). This plasma in equilibrium has at the center of the slab a frequency

TABLE I

Values of N^j at times t/T_p for various sets of values $T_p/\Delta t$, $d/\Delta x$, $4a\sqrt{2}/\Delta v$ and u/a
$a = 10^6$, $d = 0.005$

$\frac{u}{a}$	$\frac{d}{\Delta x}$	$\frac{4a\sqrt{2}}{\Delta v}$	$\frac{T_p}{\Delta t}$	N^j	$\frac{t}{T_p}$
0.1	50	50	320	1.004	8.050
0.2	60	60	400	1.004	5.657
0.5	60	60	400	1.004	2.867
1.0	60	60	400	1.004	2.055
0.1	50	50	320	1.0073	10.0
0.05	50	50	320	1.0034	10.0
0.01	50	50	320	1.0005	10.0
0.01	50	50	320	1.0009	15.0
0.01	50	50	320	1.001	20.0
0.1	60	60	100	1.0095	0.180

of approximate 1GHz and a temperature of approximately 30000°K. The first group of results in Table I shows values of N^{jc} for various values of the involved parameters, in particular for values of u/a from 0.1 to 1.0. The second group shows values of N^{j} for decreasing values of u/a. The last set points out that a very strong sensitivity seems to exist in terms of the relationship between M,N and h. This sensitivity is in accordance with similar phenomena observed for other systems of partial differential equations solved by numerical difference methods.

The values shown in Table I are pretty characteristic. They vary with the half-width d although not in straight proportion. N^{jc} increases with d while N^{j} decreases with constant t/T_p or t/T_p increases with constant N^{j}, all other parameters being constant. It follows from Table I that unhappily at the present time it is not possible to investigate the effect of very strong impulses resulting in, say, u/a = 1 for relatively long periods of time. Even so, some non-linearities resulting from the increase of u/a up to a value equal to unity have been observed and will be reported in the respective section.

The quest for extension of N^{jc} also explains the use of (61d). This function proved to yield larger N^{jc} than (35) with $h(x) = a^2 - x^2$ although (61d) does not satisfy conditions (35,36). As mentioned before, this should result in some (additional) loss of electrons to the boundary but the observed numerical results in this direction have been negligible.

IV. RESULTS IN THE LINEAR REGION DUE TO SMALL AMPLITUDE EXCITATIONS

A. Basic Features of Voltage Behavior and the Fourier Transform

In accordance with the arguments presented in section II.b (following (17)), the voltage henceforth will be understood to be the voltage between the two minimum density points located at $\pm x_{min}$. This avoids the numerical difficulties caused by the singular field at the walls. It gives an accurate description of the voltage between the walls since the singular electric fields cancel out. In the equilibrium state, the voltage between any two points symmetric with respect to the center of the slab is always zero and will remain so at t=0+ due to the continuity of the electric field. Thus the voltage at t=0 will always be zero.

It is convenient to introduce a "standard experiment". The equilibrium plasma for this experiment will be the plasma slab defined by (61). The excitation for the "standard experiment" will be supplied by an impulse electric field yielding an electron velocity increment of $u=10^5$ towards the wall at x=-d. The stimulus $u=10^5$ has been chosen for the "standard experiment" since this value proves to be approximately the upper limit of the linear region.

Some data for the "standard" plasma slab in equilibrium are listed in Table 2.

All numerical experiments henceforth will be performed on plasmas having N_o and $\varphi(x)$ given by (61a,d). The equilibrium thermal velocity a,

TABLE 2

Equilibrium Plasma Data

Standard Experiment

Electron density N_o at center of slab: 10^{16} el/m^3

Thermal velocity a : 10^6 m/sec

Electron density law : $N_o \cos^2 \frac{\pi}{2} \frac{x}{d}$

Velocity distribution : Gaussian

At center of slab:

Plasma angular velocity ω_{po}: $5.6452.10^9$ rad/sec

Plasma frequency f_{po} : $0.89846.10^9$ KHz

Plasma period T_p : 1.1130 n sec

Debye length : $0.177142.10^{-3}$ m

For a slab with halfwidth of 0.005m, at $\pm x_{min}$ (minimum ion density points):

Electron density, relative to same at center: 0.07870

Ion density, ditto : 0.1574

Ion/electron ratio : 2.000

Voltage : 14.45 volts

Electron Debye length = $0.6314.10^{-3}$ m

$x_{min} = 0.9048.10^3 \simeq 0.18d \simeq 1.433$ local Debye lengths

the slab half-width d and the stimulus u will be varied according to need. For brevity every numerical experiment will be described by these three parameters.

For easy comparison of results and convenience, one defines the normalized voltage and time

$$V_n = \frac{u}{10^5} \frac{0.005}{d} V \tag{62}$$

$$t_n = t/T_p \tag{63}$$

Henceforth, the terms "voltage" and "time" will always mean the normalized voltage and normalized time as defined. The subscript "n" will be dropped.

Fig. 1 shows the behavior of the voltage over ten plasma periods for the "standard experiment". Table 3 shows the values of the voltage peaks and their time of occurrence. Computer calculations were performed using 100 intervals in both x-space and v-space and a time interval of 1/320 plasma periods (M=N=50, h=1/320, see (44) et seq.). Finer intervals were tried but did not yield any improvement in the linear region. Peak times shown in Table 3 are therefore correct to 0.003.

Examination of Fig. 1 and Table 3 shows a rather puzzling behavior. One would expect a reasonable periodic oscillation damped according to some reasonable damping law. Examination of Fig. 1 reveals, to mention a few aspects, that the third peaks, both positive and negative, are larger than the respective second peaks. The fifth positive peak is larger than the 2nd, 4th and 5th and almost as large as the 3rd. Time spans between adjacent

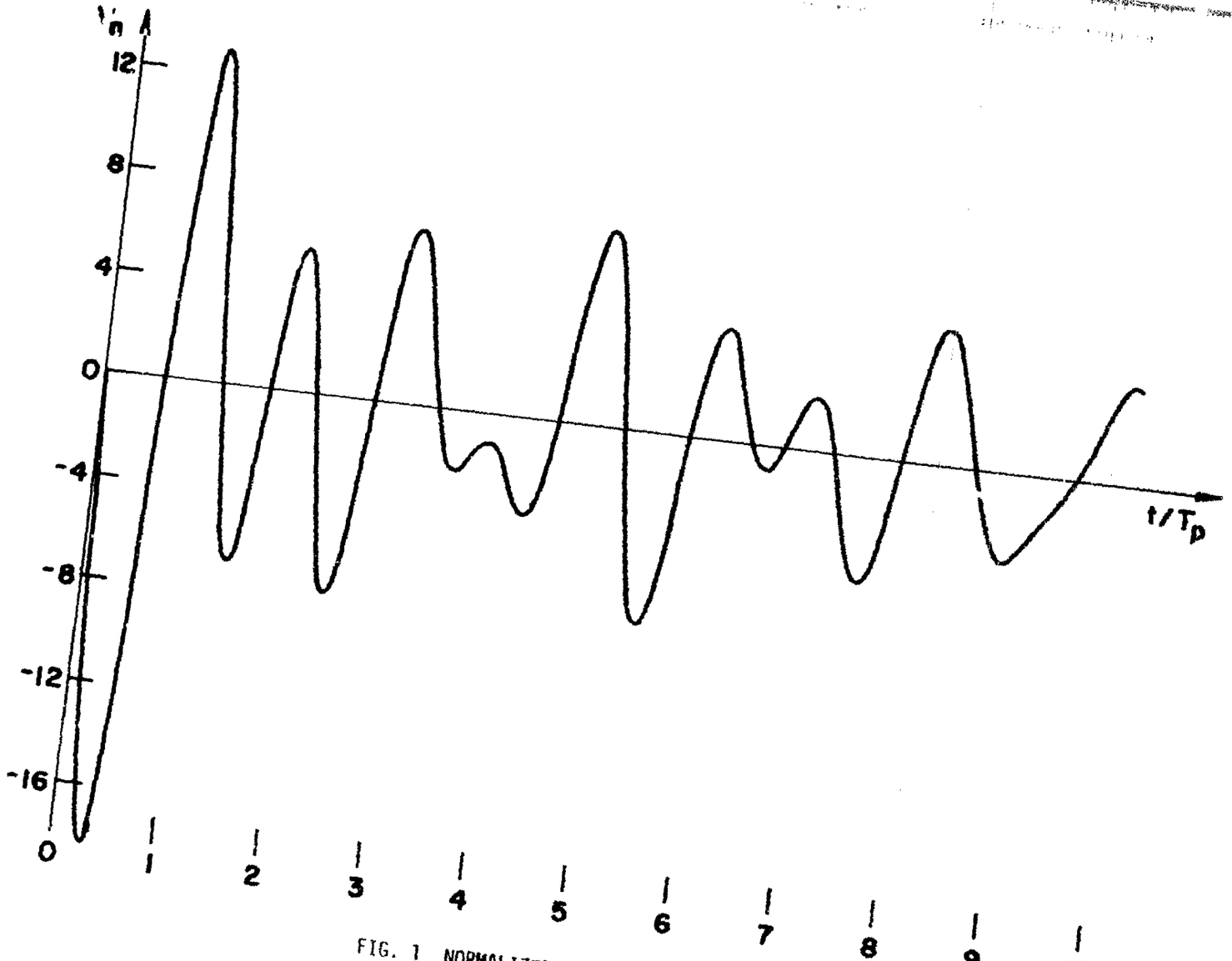

FIG. 1 NORMALIZED VOLTAGE VS. TIME
$a = 10^6$, $\epsilon = 10^5$, $d = 0.005$

Peaks of Normalized Voltage

$a = 10^6$, $u = 10^5$, $d = .004, .005, .007, .010$

d = 0.004		d = 0.005		d = 0.007		d = .010	
.287	-18.04	.287	-18.27	.291	-18.34	.294	-18.54
.853	+13.48	.853	+12.90	.853	+12.21	.853	+11.75
1.387	- 7.305	1.375	- 6.925	1.362	- 7.100	1.356	-7.610
1.856	+ 3.964	1.844	+ 5.587	1.850	+ 7.336	1.856	+8.095
2.319	- 6.104	2.353	- 7.649	2.372	- 7.521	2.375	-6.710
2.869	+ 8.571	2.912	+ 6.863	2.881	+ 4.351	2.862	+4.675
3.469	- 8.375	3.475	- 2.346	3.337	- 3.530	3.359	-5.925
4.137	+ 5.980	3.781	- 1.057	3.850	+ 6.432	3.884	+5.250
4.969	- 4.720	4.178	- 3.805	4.425	- 6.716	4.362	-2.604
5.656	- 4.464	4.781	+ 7.676	4.994	+ 2.096	4.825	+4.329
6.272	- 3.456	5.391	- 7.507	5.319	+ .607	5.370	-6.495
6.678	- .716	5.984	+ 4.351	5.766	+ 4.071	5.916	+3.387
6.978	- 1.594	6.475	- .965	6.372	- 6.031	6.344	-1.120
7.569	+ 4.920	6.903	+ 2.131	6.956	+ 3.596	6.819	+4.824
8.175	- 6.769	7.486	- 4.911	7.456	- .859	7.390	-6.030
8.787	+ 5.948	8.125	+ 5.288	7.925	+ 2.330	7.931	+3.150
9.430	- 3.389	8.825	- 3.448	8.531	- 3.099	8.406	-2.338
		9.994	+ 3.841	9.859	+ 2.542	8.909	+3.612
						9.403	-2.690
						9.881	+3.308

TABLE 3

peaks, henceforth called "peak-to-peak times", vary from 0.703 around t=4.0 to 1.869 at approximately t=9. One observes further that between the fourth and fifth negative peaks the voltage always remains negative; this remains so even after the dc bias in the data is removed. Examination of the voltage between the last negative and positive peaks of Fig. 1 reveals that the first difference passes through a minimum at approximately t=9 while remaining always positive.

This apparently erratic behavior could be suspected to be due to the numerical calculations and/or instabilities. A numerical experiment was performed with all parameters equal to those of the standard experiment except the stimulus reduced to $u=10^{4}$, 1/10 of the standard experiment. The voltage (after normalization) is identical to the one observed in the prior case except for a very small difference around t=10 where numerical instabilities begin in the case of the standard experiment (see Table 1). The voltage for this experiment with reduced excitation is plotted in Fig. 2. Extended observation is now possible. The same "erratic" behavior continues.

A numerical experiment was also performed for a plasma with a and d equal to the standard experiment and $u=5.10^{4}$. Results matched those of Table 3 and Figs. 1 and 2. Results are not shown since they contain no new information.

Fourier transformation of the data displayed in Figs. 1 and 2 presented significant results. It is however necessary to look at the transformation before attempting an interpretation of the results. As far as

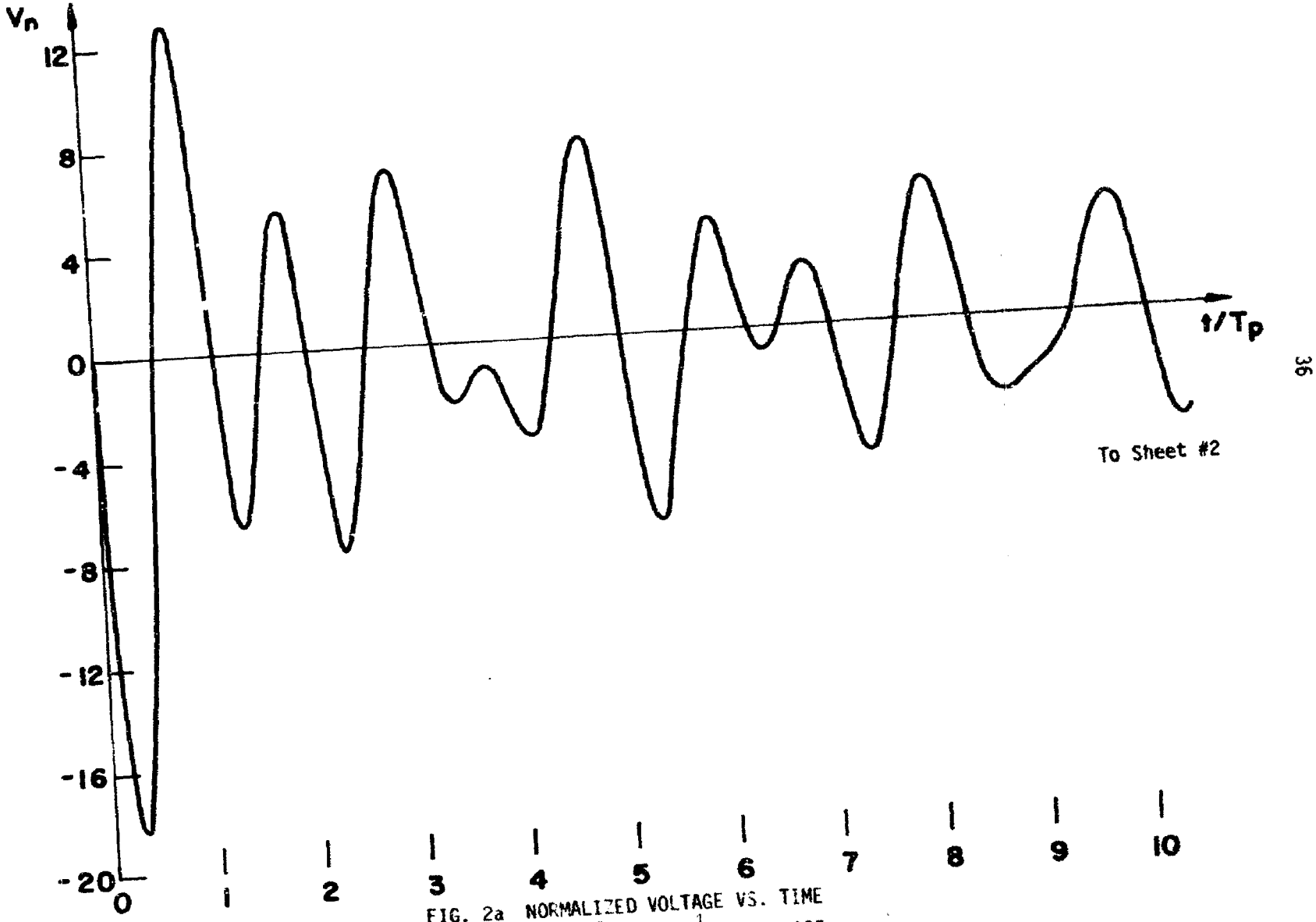

FIG. 2a NORMALIZED VOLTAGE VS. TIME
$a = 10^6$, $u = 10^4$, $d = 0.005$

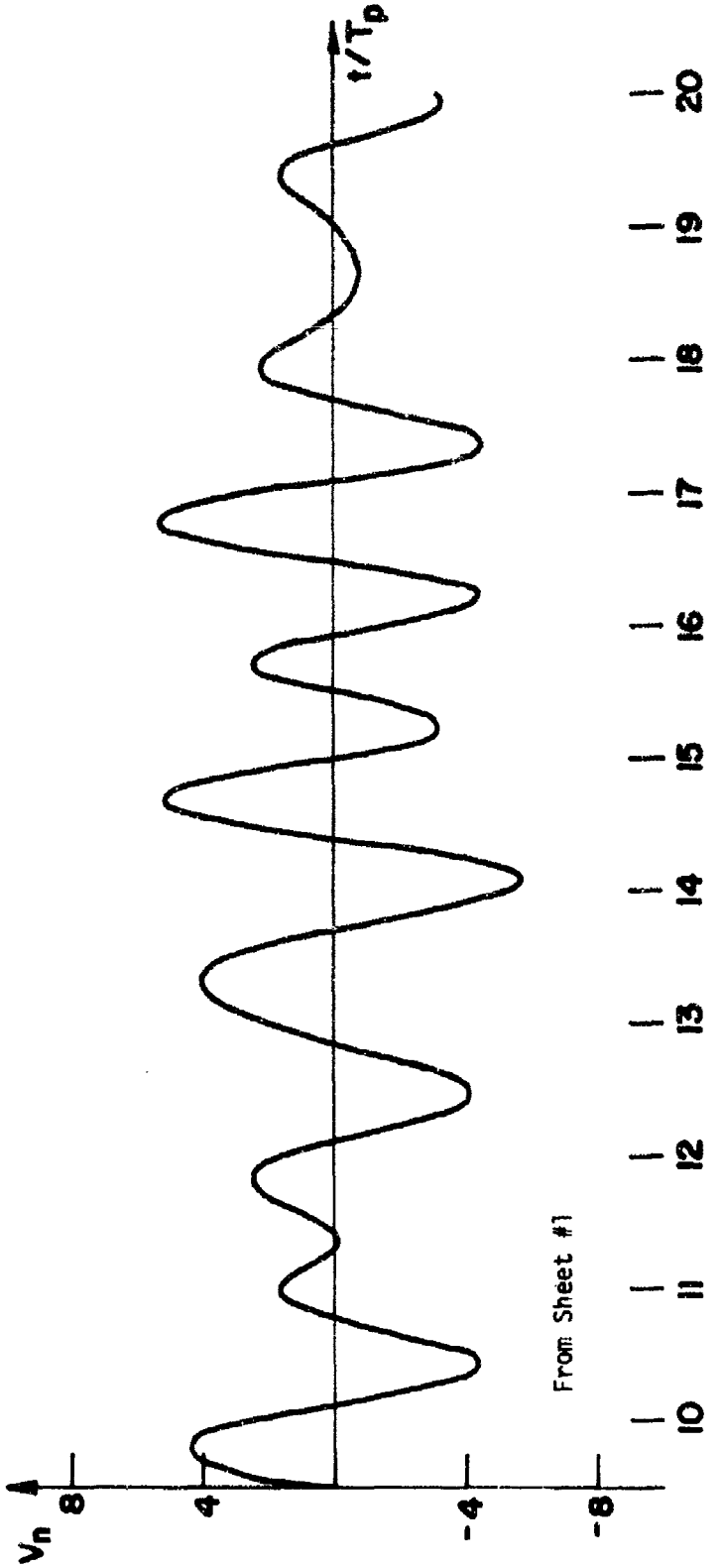

FIG. 2b NORMALIZED VOLTAGE VS. TIME
$a = 10^6$, $u = 10^4$, $d = 0.005$

the necessary numerical integration itself is concerned, trial computations showed that the use of 20 points per time unit (i.e., per plasma period) yielded a sufficiently good approximation (320 points per plasma period are available). A serious problem, however, is posed by the fact that the voltage is only known for a relatively short time period and not to infinity. Therefore the integration will not yield the Fourier Transform of the voltage but the Fourier Transform of the voltage multiplied by a truncation function $U(t) - U(t-t_m)$, where $U(t)$ is Heavyside's step function and t_m is the time limit up to which the function is known. The result of the transform thus will be the convolution of the voltage (known to infinity) with the capital function. In practice, one has to construct a curve through the local maxima of the obtained transform of the truncated voltage. It is also known that the number of local maxima per frequency unit is approximately the number of time units during which the voltage is known. In other words, if the voltage is known for 10 time units, one can expect 10 local maxima per frequency unit.

Since Fourier transform of voltages known over different time spans will have to be performed, it becomes necessary to renormalize the time scale. The normalization adopted herein practically results in the fact that the DC value of the Fourier transform equals the arithmetic mean of the voltage in the time domain.

Frequency normalization is imposed by (63). If $f_{po} = 1/T_p$ then

$$f_n = f/f_{po} = f \cdot T_p \tag{64}$$

is the normalized frequency. Again the term "frequency" henceforth will imply normalized frequency and the subscript "n" again will be dropped. (The angular velocity ω however will not be normalized). All tables and graphs of Fourier transforms display the amplitude versus normalized frequency.

In order to study the effect of truncation, the Fourier transforms using the numerical equivalent to Fig. 2 were performed based on the first 10, the first 15 and the first 20 time units. Results are listed in Tables 4 and shown in Fig. 3. First one notes, before attempting to interpret the results, that the agreement between the three curves is excellent; the difference in magnitudes results from the normalization process together with the attenuation to be expected with time. The main difference between the transform based on 10 time units as compared to the other two is that the valley around f=0.9 does not show up. This is due to the scarcity of local maximum points. Examination of the transform in this region shows the existence of a minimum value of the phase at which the absolute value has a magnitude very near to the one shown by the other transforms. Whenever the scarcity of local maxima will force the use of this procedure in order to obtain points of the Fourier transform, this will be noted in the tables as "phase reversal points" and this term also shall be used in the text whenever necessary.

In Table 5 the Fourier transform envelope points are listed for the standard experiment. Graphical representation is given in Fig. 4. Agreement with data of Table 4 and Fig. 3 is excellent. Note in particular the phase reversal point at f=0.855.

TABLE 4

Fourier Transform of V(t), over 10, 15 and 20 T_p

$a = 10^6$ $u = 10^4$ $d = .005$

10 T_p		15 T_p		20 T_p	
.000	.2855	.000	.2006	.000	.1797
.050	.4872	.035	.3103	.030	.2014
.150	.4918	.100	.3222	.075	.1997
.250	.5450	.165	.3031	.125	.2174
.345	.6351	.230	.3352	.180	.2157
.450	.8540	.300	.3632	.235	.2370
.570	2.0878	.360	.3900	.295	.2362
.695	.6610	.425	.4830	.330	.2536
.800	1.6282	.495	.7435	.385	.3007
.985	2.2913	.580	1.8835	.440	.3742
1.115	.8188	.655	.3413	.500	.5951
1.225	.4801	.720	.7155	.580	1.4761
1.330	.3420	.800	1.4657	.655	.1352
1.430	.2668	.875	.6747	.735	.5357
1.530	.2100	1.000	1.6245	.800	1.3965
1.630	.1735	1.095	.7668	.865	.7742
1.730	.1496	1.165	.4090	.925	.9057
1.830	.1281	1.230	.3250	.990	1.4140
1.930	.1147	1.300	.2517	1.115	.5163
2.030	.1033	1.365	.9889	1.175	.3673
2.130	.0913	1.435	.1738	1.235	.2686
2.225	.0816	1.500	.1405	1.320	.1857
2.325	.0781	1.565	.1323	1.380	.1852
2.425	.0683	1.635	.1141	1.435	.1587
		1.700	.0992	1.520	.1024
		1.765	.0891	1.580	.1257
		1.830	.0811	1.635	.1091
		1.900	.0782	1.690	.0652
		1.965	.0680	1.725	.0748
		2.035	.0631	1.780	.0913
		2.100	.0575	1.835	.0826
		2.165	.0580	1.890	.0550
		2.235	.0514	1.920	.0548
		2.300	.0472	1.980	.0733
		2.365	.0438	2.035	.0692
		2.430	.0443	2.090	.0456
		2.500	.0429	2.125	.0372
				2.180	.0577
				2.235	.0559
				2.290	.0358
				2.325	.0351
				2.380	.0458
				2.435	.0492
				2.495	.0331

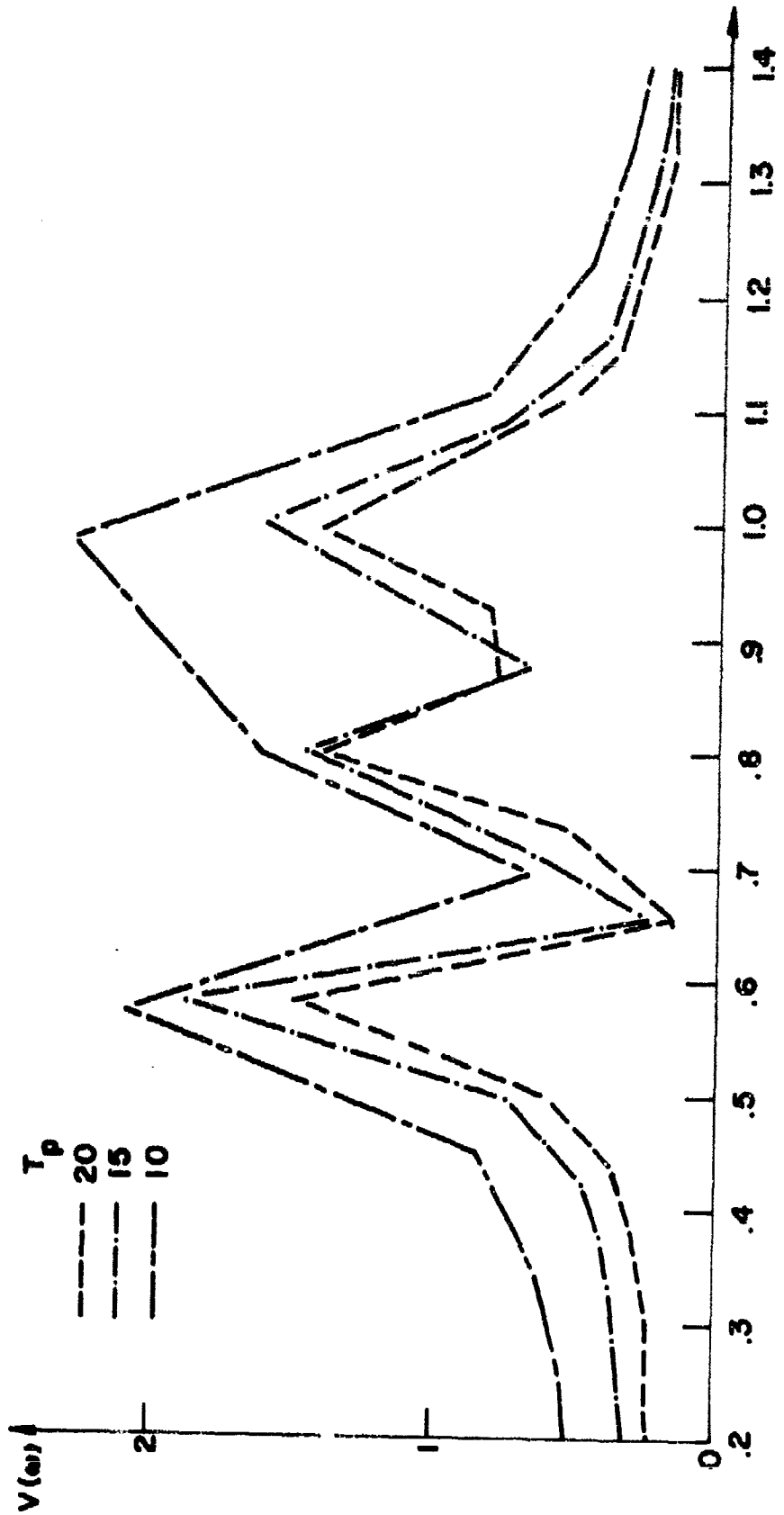

FIG. 3 FOURIER TRANSFORM OF V(t)
$a = 10^6$, $u = 10^4$, $d = 0.605$
Transforms based on response over 10, 15 and 20 T_p

Envelope points of Fourier Transforms of V(t)

$a = 10^6$ $u = 10^5$ d = .004, .005, .007, .010

d = .004		d = .005		d = .007		d = .010	
0.000	.4194	0.000	.3362	0.000	.3234	0.000	.3389
0.105	.4306	0.050	.4346	0.050	.4867	0.050	.5050
0.200	.4206	0.145	.4521	0.150	.4909	0.155	.5298
0.300	.4899	0.245	.4991	0.250	.5643	0.260	.6058
0.400	.5883	0.340	.5882	0.350	.7136	0.395	1.1047
0.505	.8393	0.440	.8149	0.475	1.5527	0.555	1.0411
0.635	2.3625	0.565	2.0802	0.680	1.1584	0.745	.8069
0.755	.6447	0.690	.5872	0.730*	.6605	0.855	1.2174
0.875	2.2793	0.800	1.6778	0.830	1.0965	0.885*	.9891
0.930*	1.2961	0.855*	.8657	0.860*	.9845	0.990	2.8101
1.010	1.8310	0.980	2.2452	0.985	2.3771	1.125	.7825
1.410	.2222	1.215	.4751	1.215	.4344	1.225	.4878
1.510	.1807	1.315	.3536	1.325	.3210	1.330	.3511
1.610	.1497	1.420	.2786	1.425	.2568	1.430	.2767
1.710	.1259	1.520	.2237	1.520	.1947	1.530	.2221
1.810	.1095	1.620	.1854	1.625	.1691	1.630	.1789
1.915	.0969	1.720	.1634	1.725	.1399	1.730	.1504
2.015	.0829	1.820	.1420	1.820	.1227	1.830	.1309
2.105	.0764	1.920	.1267	1.920	.1107	1.930	.1170
2.215	.0715	2.020	.1116	2.025	.0982	2.025	.1016
2.315	.0614	2.120	.1016	2.125	.0867	2.125	.0927
2.415	.0608	2.220	.0920	2.220	.0762	2.225	.0838
		2.320	.0871	2.320	.0724	2.325	.0763
		2.420	.0792	2.420	.0676	2.425	.0725

* Phase Reversal Point

TABLE 5

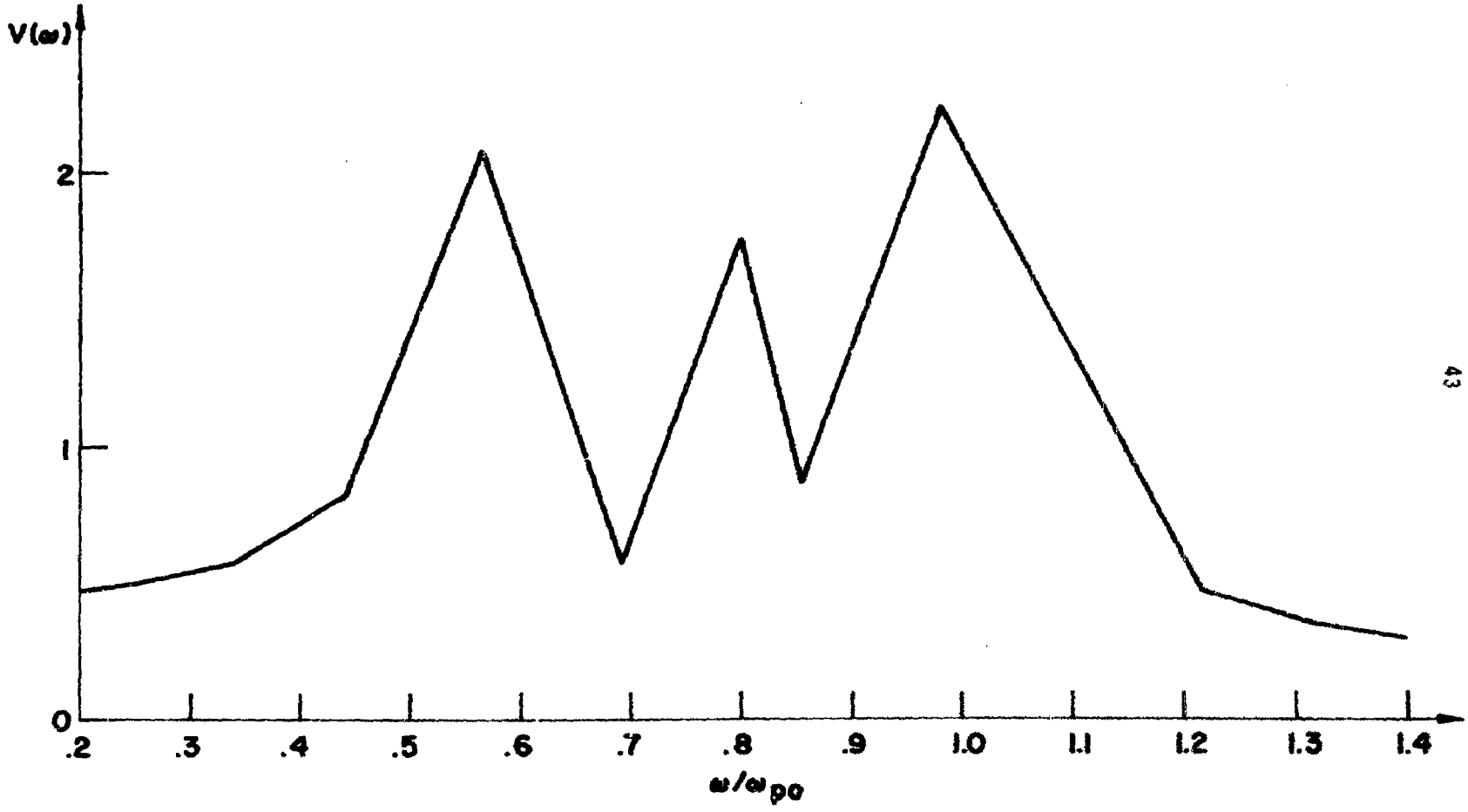

FIG. 4 FOURIER TRANSFORM OF V(t).
$a = 10^6$, $u = 10^5$, $d = 0.005$

Results shown graphically in Figs. 1-4 together with results for a plasma slab with identical a and d and u $=5\cdot10^{4}$ indicate that within this region the system operates linearly. Variation of the response as a function of a and d will be discussed in another section.

A typical behavior of Tonks-Dattner resonances is thus observed. Specifically, three high-amplitude peaks can be seen at

$$1 - f \cong 1.000$$

$$2 - f \cong 0.800$$

$$3 - f \cong 0.575$$

In addition, another set of resonances of smaller amplitude can be seen to exist at higher frequencies. The voltage for this range of frequencies is displayed in Fig. 5. These resonances clearly are thermal resonances. They do not show up in other voltages herein since the number of points per unit of frequency is too small to provide the necessary detail. While these resonances are easily explained and the resonance at approximately unit frequency is the main resonance, the resonances appearing at frequencies of approximately 0.8 and 0.575 necessitate further investigation. In order to present the necessary clarification, it is logical to study the behavior of the electric field within the plasma slab. This is carried out in the next section.

Some thermal resonances at frequencies above unity can be observed in Fourier transforms of the electric field or its deviation adduced in the next section. Since, however, they are not the object of this study, no further attention need be given to the same.

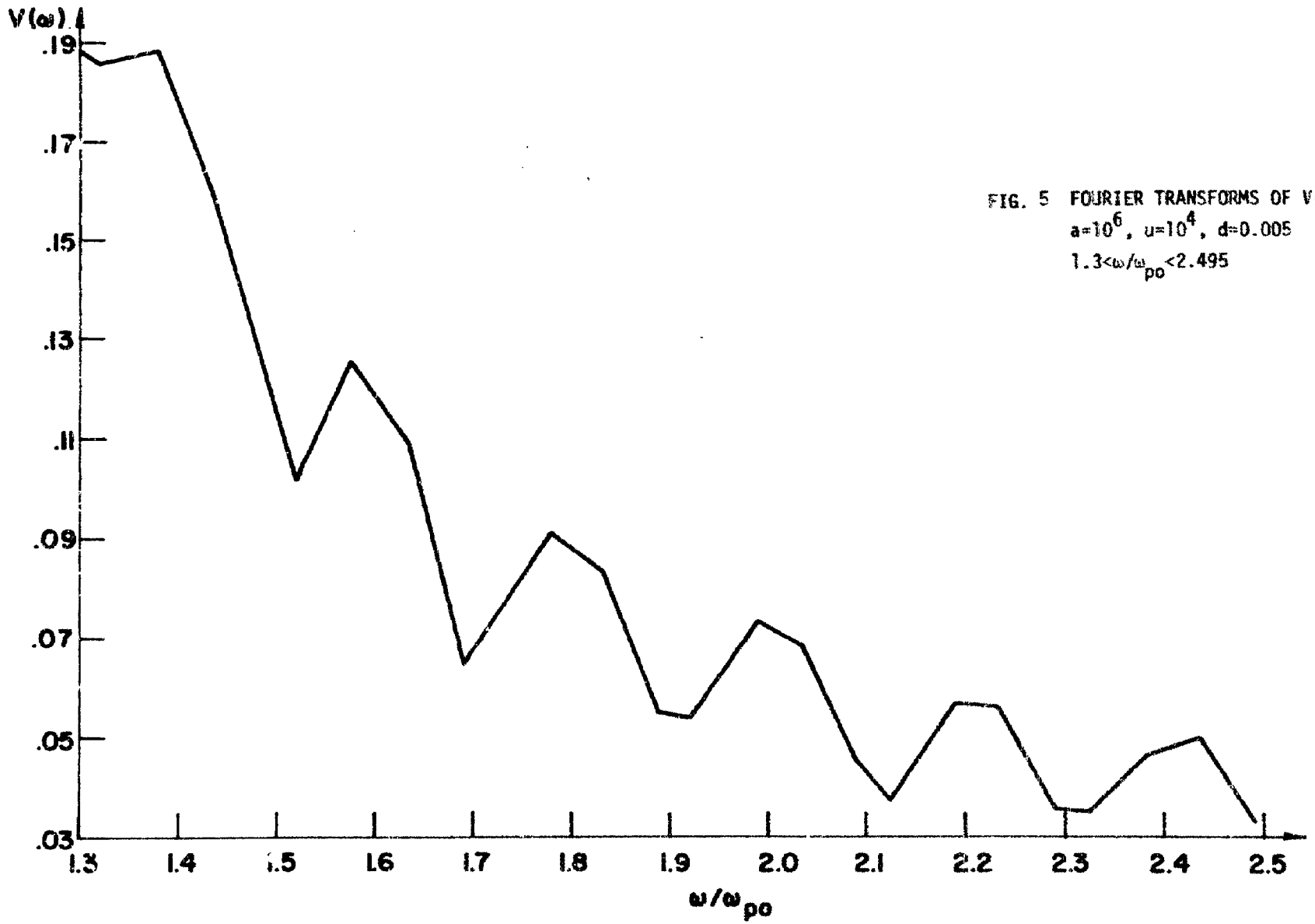

FIG. 5 FOURIER TRANSFORMS OF V(t).
$a=10^6$, $u=10^4$, $d=0.005$
$1.3<\omega/\omega_{po}<2.495$

B. The Electric Field and its Fourier Transform

In this section, the behavior of the electric field will be studied. Since the equilibrium electric field results in zero voltage, the investigation will be centered on the deviation $\Delta E(x/d,t)$. Results of computer calculations have shown that ΔE is approximately even. Thus studying this function in one half of the slab will be sufficient. Data obtained are shown and plotted only for $-d \leq x/d \leq 0.0$ unless noted (the "-" sign, however, will be omitted whenever convenient).

The deviation of the electron density Δn is also studied. This deviation is proportional to $-\Delta(\partial E/\partial x)$ as follows from (7) and yields therefore information on the behavior of ΔE. Further, the electron migration behavior is also of interest. The function Δn is odd in x/d to a very good approximation and thus practically zero at the center of the slab in the linear region. (In fact, one can almost define the linear region by this property of the electron density deviation at the center of the slab.)

Fig. 6 shows ΔE vs. time for x/d=0.0, 0.5, 0.8 for the standard experiment. Its three graphs bear no resemblance to each other. At the center of the slab, x/d=0.0, the electric field is an attenuated sinusoid at a frequency near unity, i.e., the local plasma frequency. Further towards the wall, at x/d=0.5, initially peak-to-peak times are slightly above unity, then become about 1.5, go back to unity, increase again. Near the wall, at x/d=0.8, peak-to-peak times are about 1.5 except for the "wiggle" between t=4.0 and t=5.0.

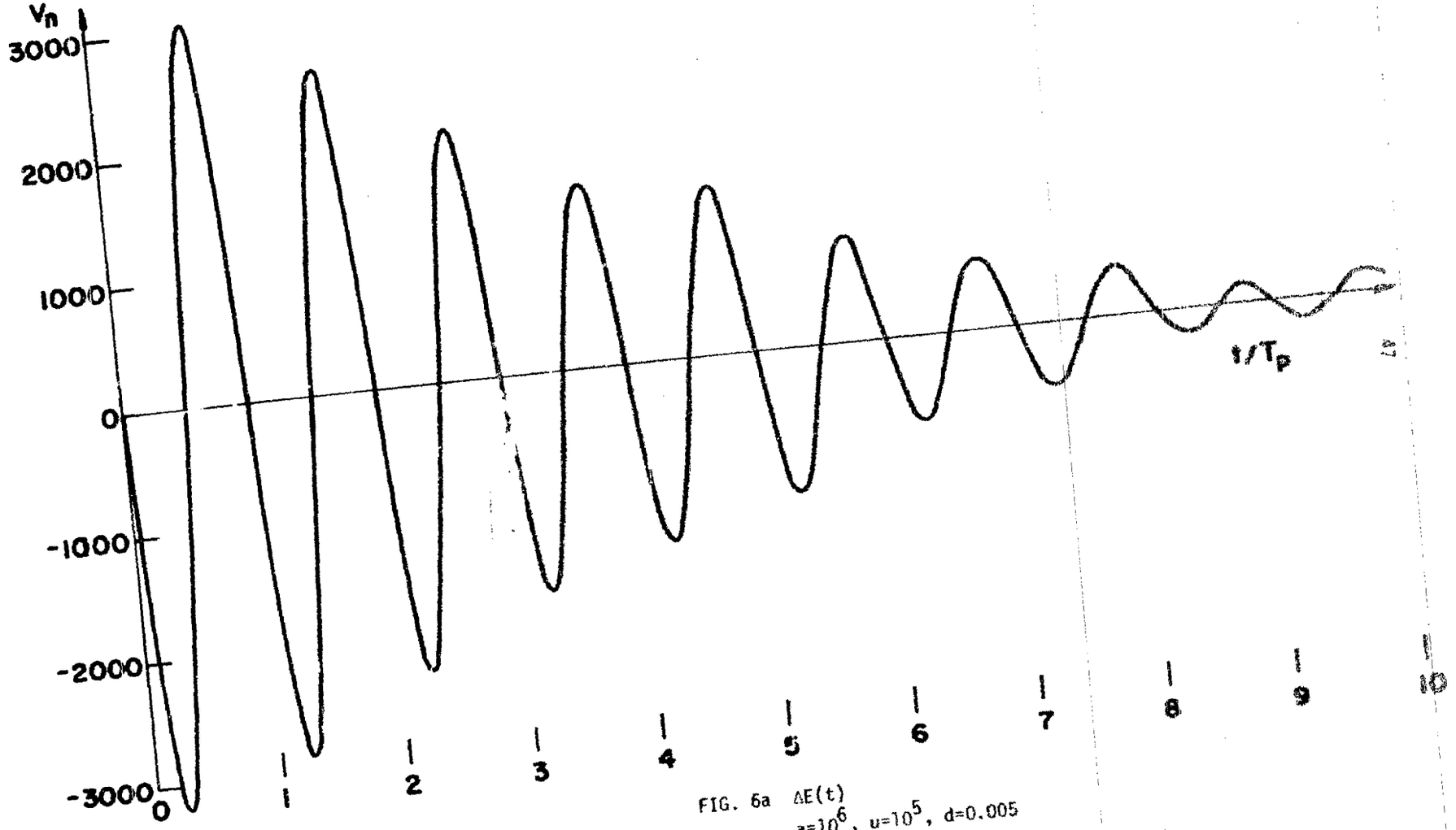

FIG. 6a $\Delta E(t)$
$a=10^6$, $u=10^5$, $d=0.005$
Sheet 1/3: $x/d=0.0$

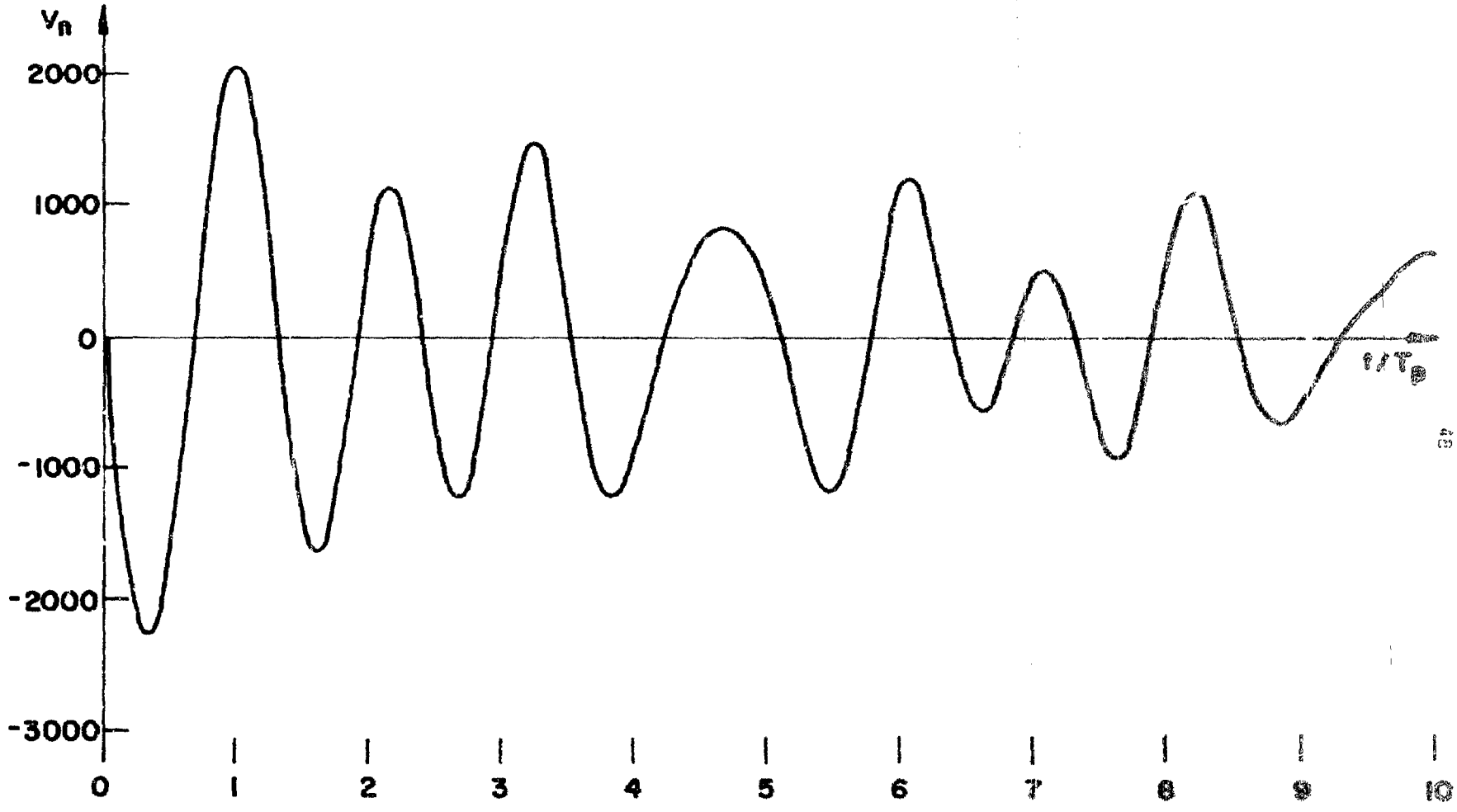

FIG. 6b $\Delta E(t)$
$\mu=10^6$, $u=10^5$, $d=0.005$
Sheet 2/3: $x/d=-0.5$

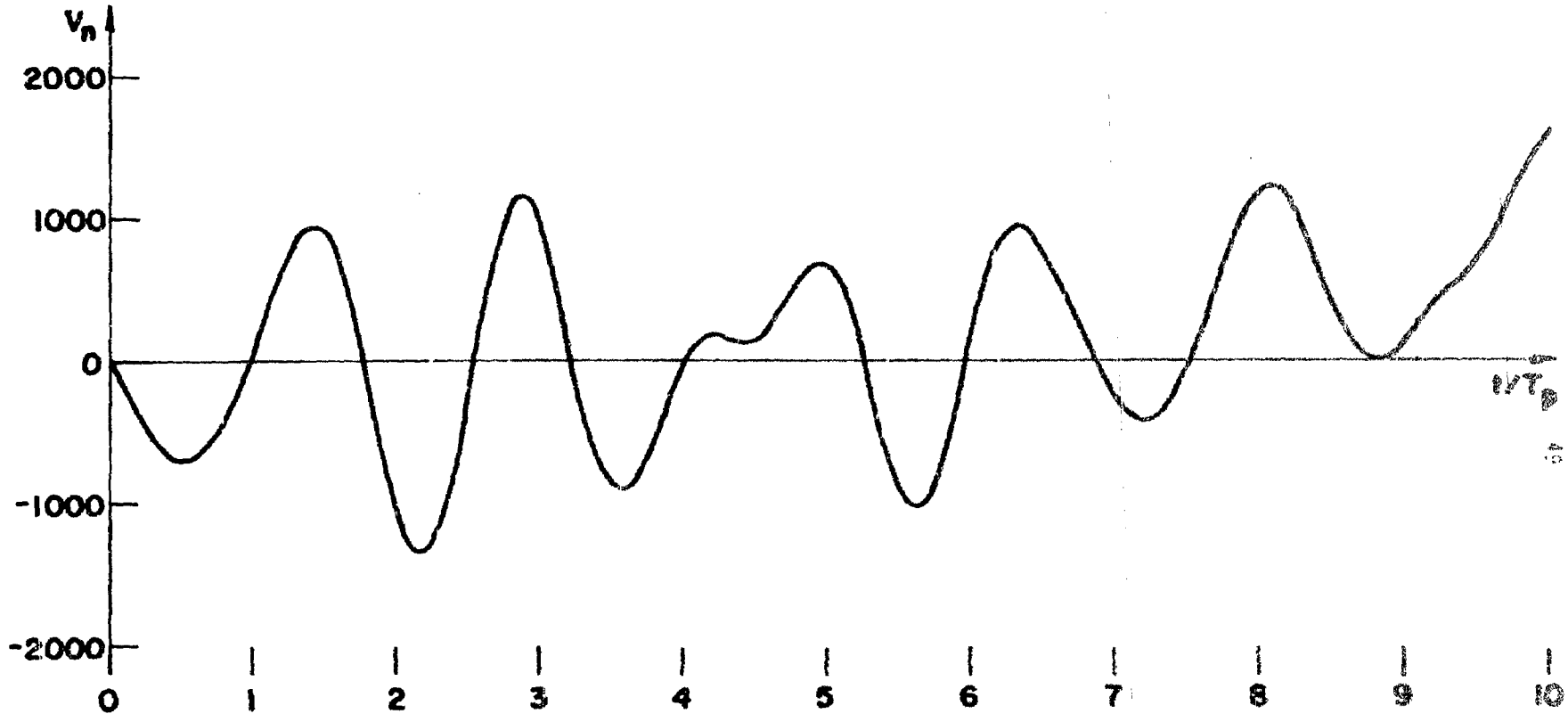

FIG. 6 $\Delta E(t)$
$a=10^6$, $u=10^5$, $d=0.005$
Sheet 3/3: $x/d=-0.8$

To look at the phenomena from a different viewpoint, Fig. 7 plots the quantized values of Δn vs. x/d and time, showing the electron migration pattern. Twelve discrete levels of quantization are chosen designated by "E", "D", "C", "B", "A", "+", "-", "1", "2", "3", "4", "5" in decreasing order with the zero located between "+" and "-". Occasionally the letter "X" is used to designate a level sufficiently near zero.

As mentioned before, $\Delta n \equiv 0$ at x/d=0.0. One observes that the first and second "positive" and the first "negative" peaks travel from the center of the slab towards the sheath. The second "negative" peak, however, does not reach x/d=0.8 anymore. It seems to dissipate itself at x/d=0.6, 0.7 around t=2.3. Some later peaks are seen to travel from the plasma sheath towards the center. One notes an almost continuous zero between x/d=0.5 and x/d=0.6 from t=3.5 to t=5.5. Of interest is also the "bunching" of particles at x/d=0.5 where Δn remains positive from t=5.2 to t=6.4.

Fig. 8 displays ΔE in a similar fashion. Similar to Fig. 1, one can see the first three electric field "peaks" (here the first one is "negative") travel towards the wall. The fourth peak (second "positive") which starts at the center around t=1.75 does not reach the wall. At x/d=0.6 there exists for about 0.5 time units a barrier which separates positive and negative values of ΔE at about t=2.5 and on both sides electric field waves seem to develop independently of each other. The positive peak near the wall then begins to travel towards the center and merges with another positive peak coming from the center of the slab. Another "barrier" can be observed at x/d=0.3 from t=4.3 to t=7.0. The oscillation

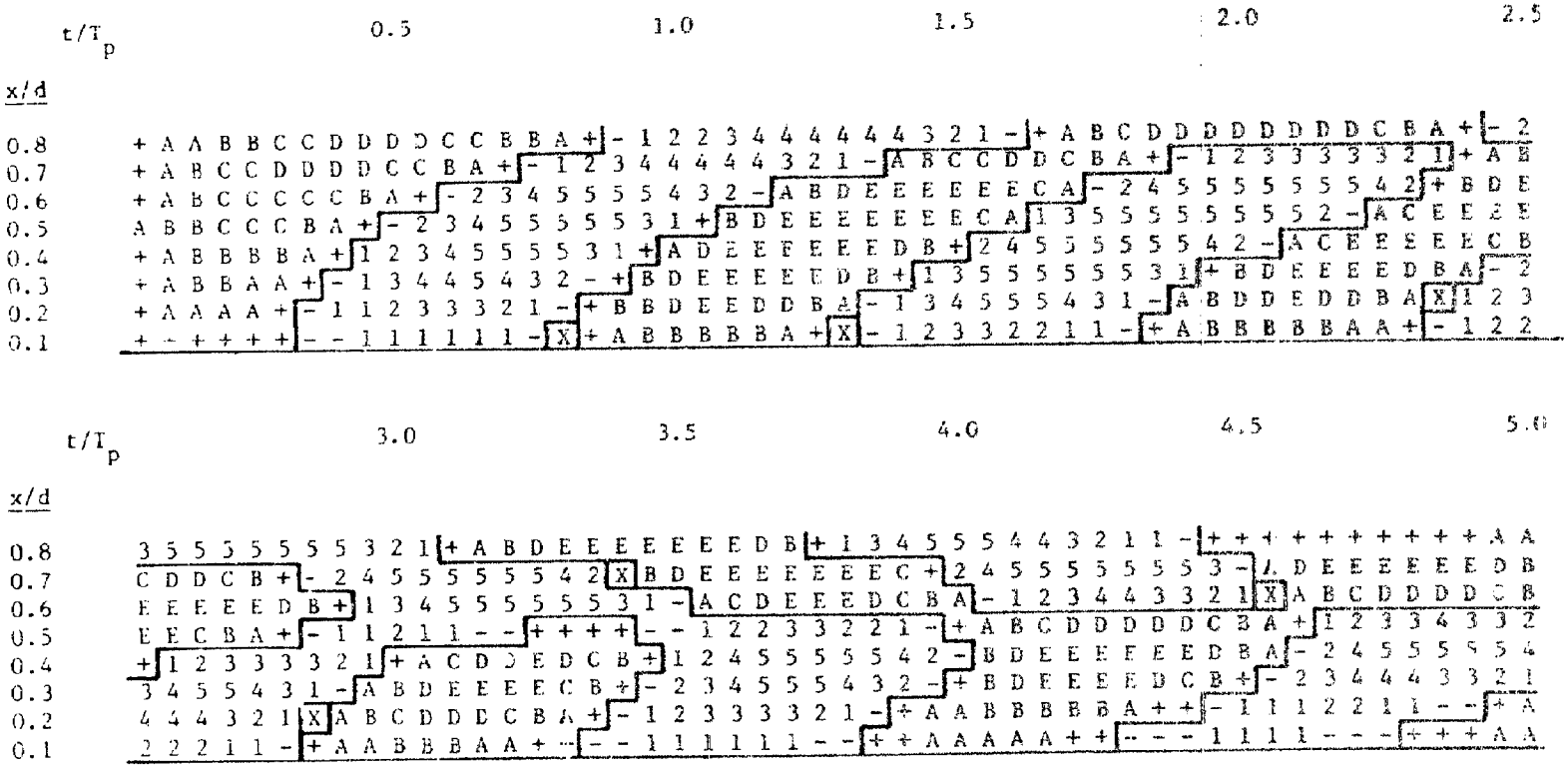

FIG. 7a QUANTIZED $\Delta n_e(t)$.

t/T_p=0.0(0.05)7.5 and x/d=0.0(0.1)0.8

$a = 10^6$, $u = 10^5$, $d = 0.004$

Sheet 1/2: t/T_p = 0.1(0.05)5.0

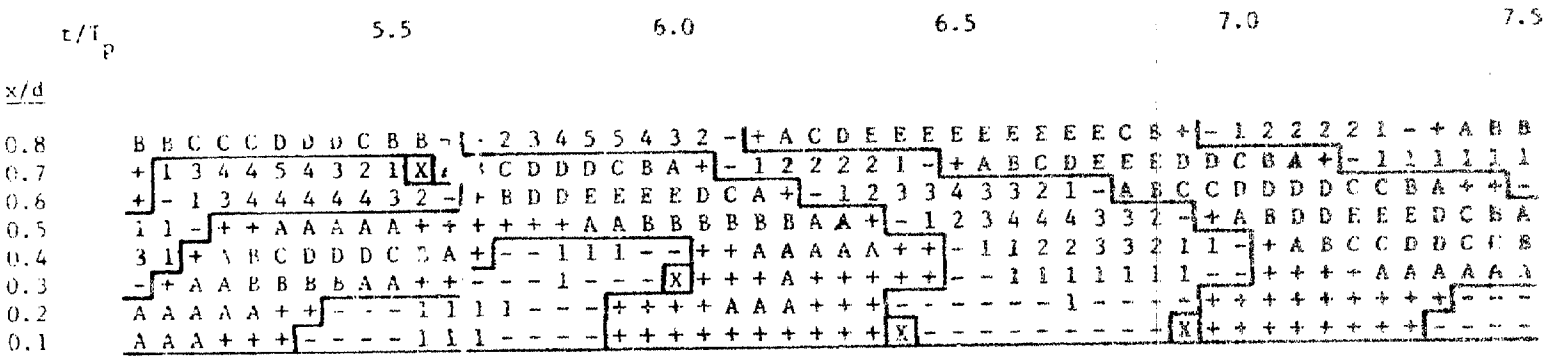

+1	–	+20	+		-1	–	-20	–
+21	–	+40	A		-21	–	-40	1
+41	–	+60	B		-41	–	-60	2
+61	–	+80	C		-61	–	-80	3
+81	–	+100	D		-81	–	-100	4
More	than	100	E		Less	than	-100	5

X = 0.0

Value relative to electron density 10^4 at center of slab

FIG. 7b QUANTIZED $\Delta n_e(t)$.

t/T_p=0.0(0.05)7.5 and x/d=0.0(0.1)0.8

a = 10^6, u = 10^5, d = 0.004

Sheet 2/2: 5.1(0.05)7.5

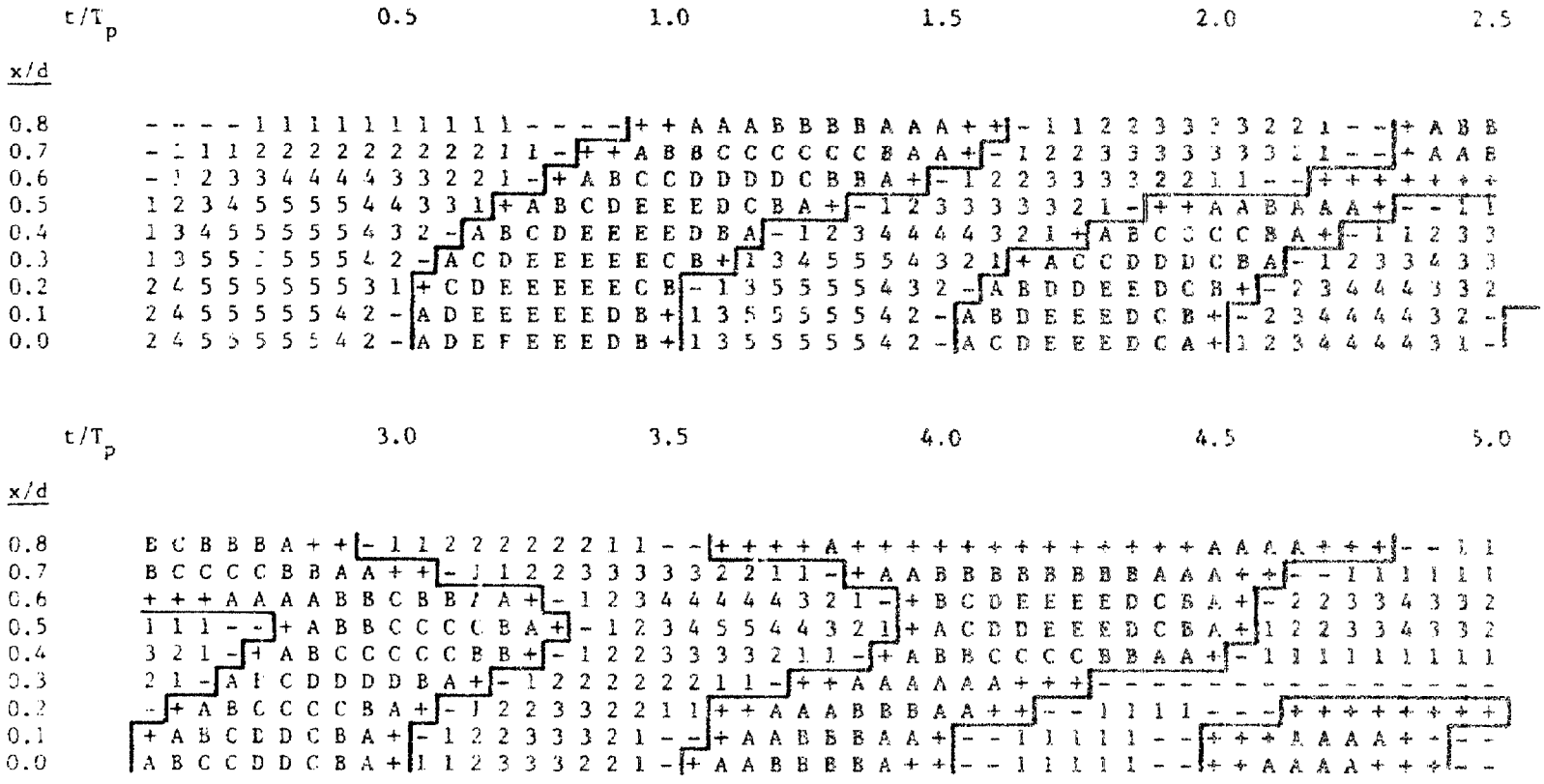

FIG. 8a: QUANTIZED $\Delta E(t)$

t/T_p=0.0(0.05)7.5, x/d=0.0(0.1)0.8

$a = 10^6$, $u = 10^5$, $d = .004$

Sheet 1/2: t/T_p=0.1(0.05)5.0

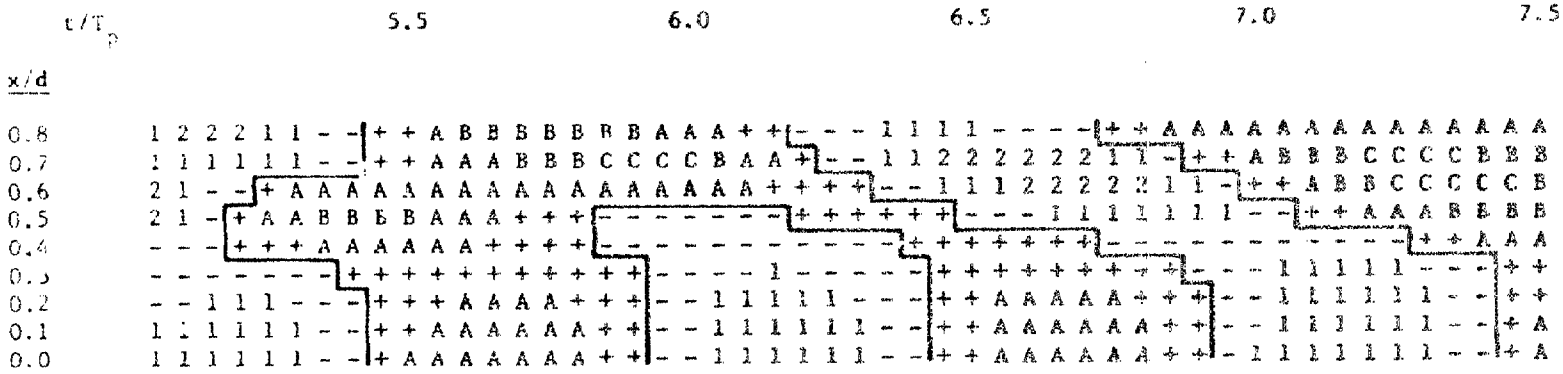

0	-	+400	+	0	-	-400	-
+400	-	+800	A	-400	-	-800	1
+800	-	+1200	B	-800	-	-1200	2
+1200	-	+1600	C	-1200	-	-1600	3
+1600	-	+2000	D	-1600	-	-2000	4
More than		2000	E	Less than		-2000	5

FIG. 8b: QUANTIZED $\Delta E(t)$

t/T_p =0.0(0.05)7.5, x/d=0.0(0.1)0.8

$a = 10^6$, $u = 10^5$, $d = .004$

Sheet 2/2: t/T_p=5.1(0.005)7.5

of ΔE at this point of the slab is small, while both towards the center and towards the wall more intense changes can be observed.

Fig. 9 presents in a different way the information contained in Figs. 1 and 8. ΔE and Δn are plotted vs. x/d at 12 different points per time unit for $0.0<t<3.0$ and $6.1<t<7.5$. Fig. 9 permits one to study the periodicity of ΔE and Δn throughout the slab and it becomes easy to see the differences of behavior in the two shown intervals. For instance, one notes that the oscillations of Δn in the region from x/d=0.0 to x/d=0.3 have become small with respect to the ones in the rest of the slab during $6.1<t<7.5$. Fig. 9 also permits one to follow the travel of the peaks in a clearer fashion than Figs. 7 and 8 especially the quantitative aspects involved in this "travel".

Analysis of Figs. 6-9 points to the existence of three characteristic regions within the slab (or five separate sectors, two pairs of which are symmetric with respect to the center of the slab, each pair forming a region).

This is most dramatically demonstrated by the Fourier spectra of the electric field (dynamic part) shown in Table 6 and Fig. 10. One recalls that in the voltage spectrum there are three high amplitude resonant peaks at $f\tilde{=}1$, $f\tilde{=}0.8$ and $f\tilde{=}0.575$ and a number of smaller peaks at higher frequencies. In Table 6 and Fig. 10 one observes that:

1 - For the region $0.0<|x/d|<0.3$, only the resonance at $f\tilde{=}1$ exists.

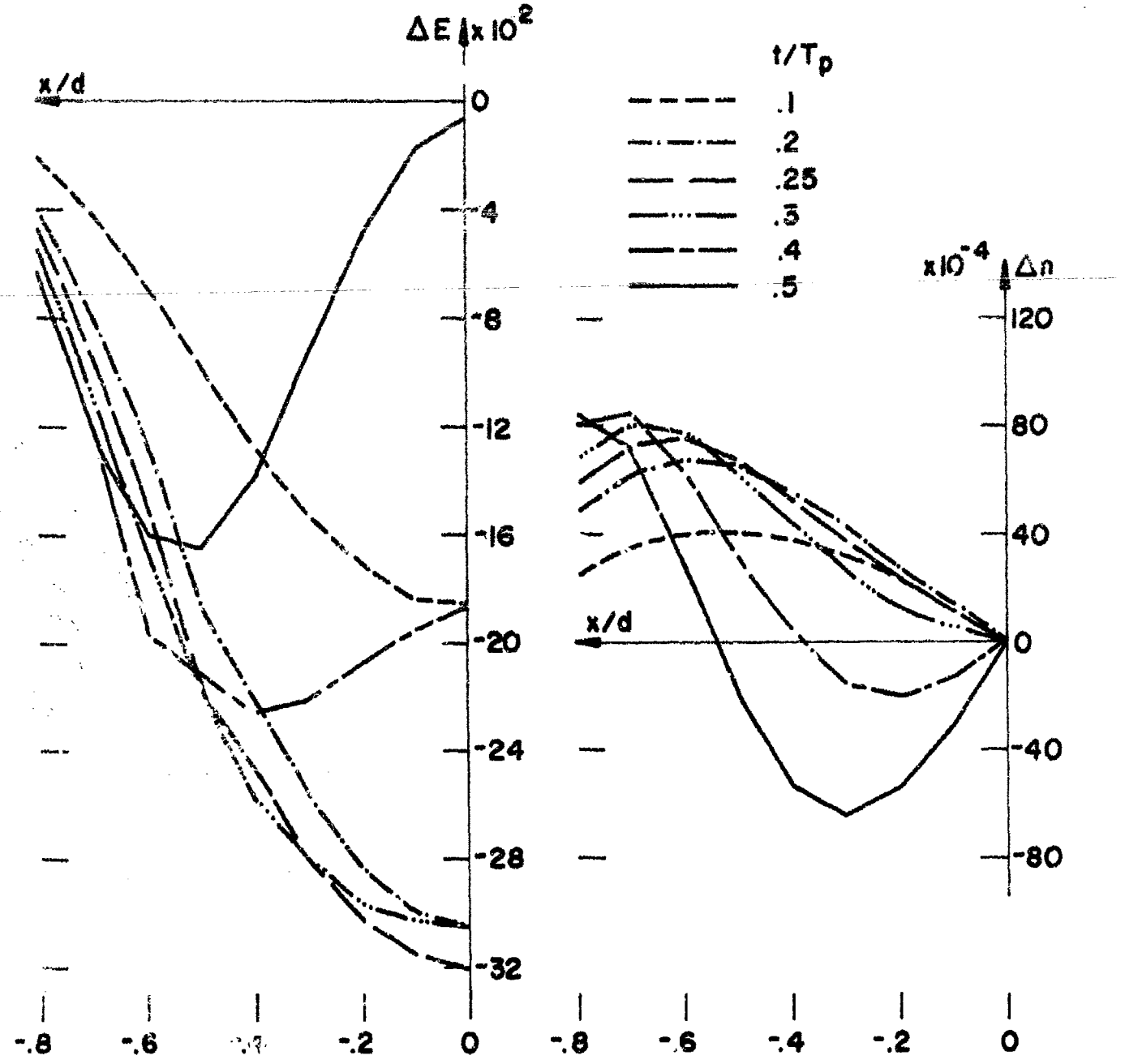

FIG. 9a ΔE and Δn vs. time
$a = 10^6$, $u = 10^5$, $d = 0.004$
Sheet 1/9: t/T_p=0.1, 0.2, 0.25, 0.3, 0.4, 0.5

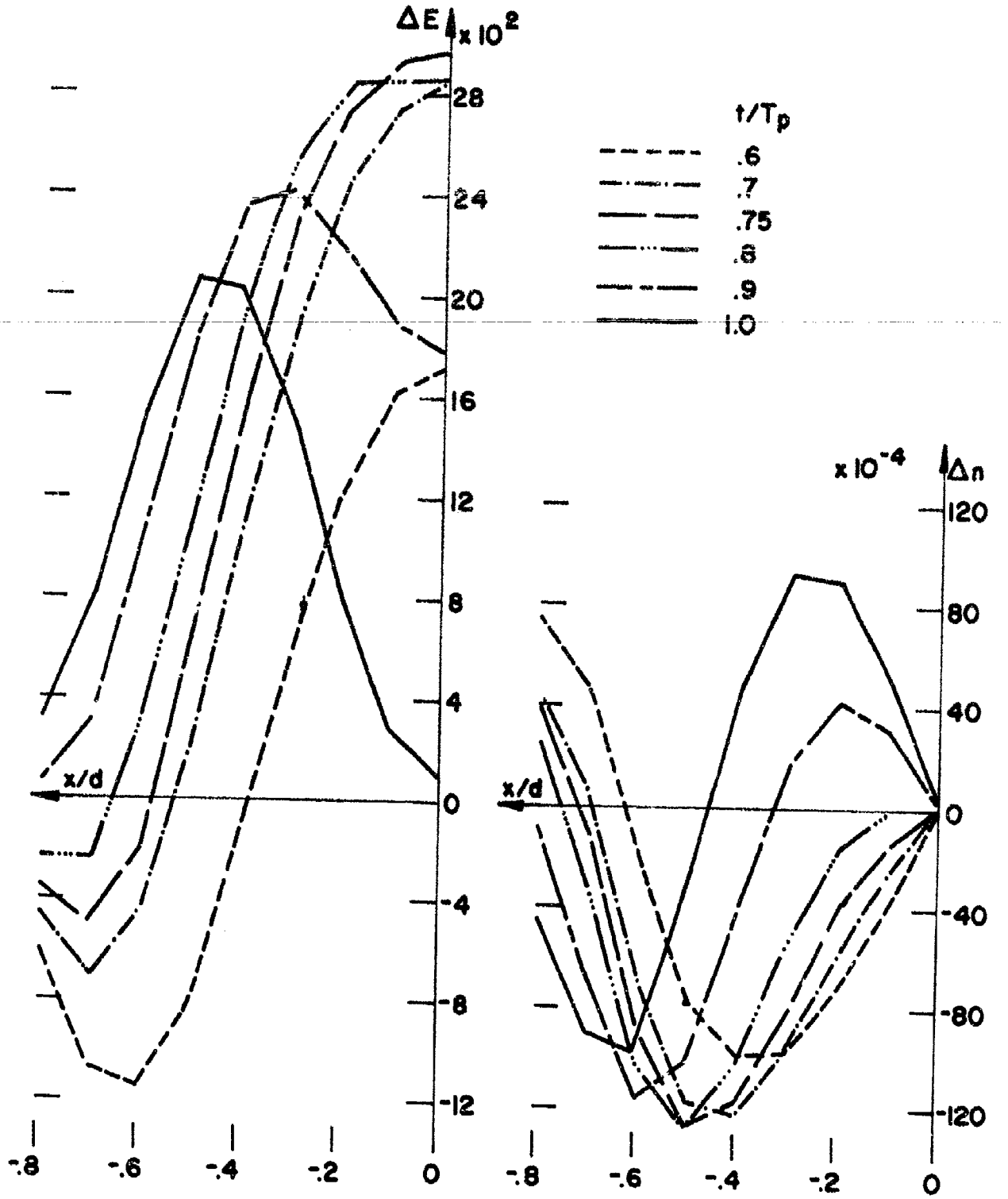

FIG. 9b ΔE and Δn vs. time

$a = 10^6$, $u = 10^5$, $d = 0.004$

Sheet 2/9: t/T_p=0.6, 0.7, 0.75, 0.8, 0. , 1.0

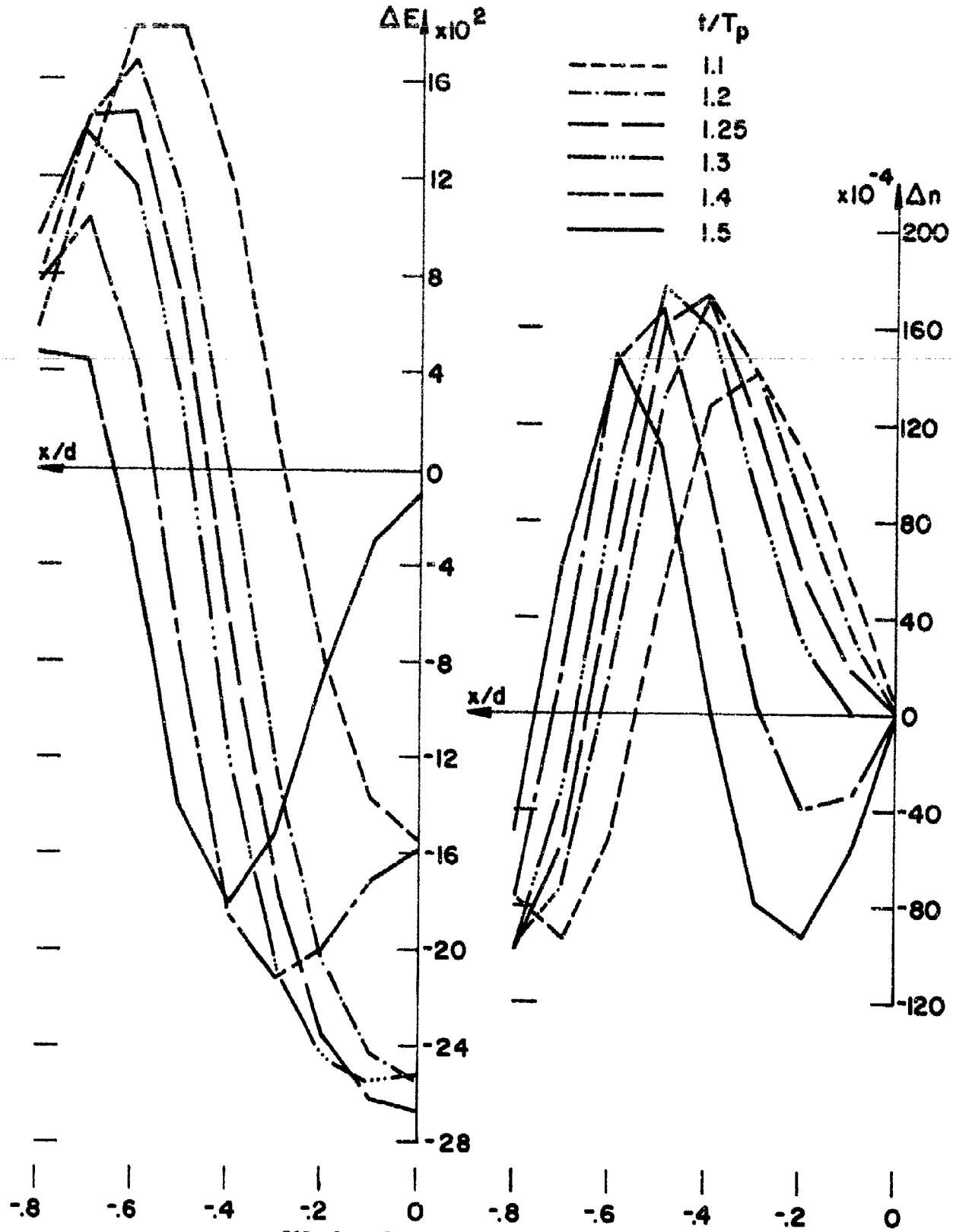

FIG. 9c ΔE and Δn vs. time
$a = 10^6$, $u = 10^5$, $d = 0.004$
Sheet 3/9: t/T_p= 1.1, 1.2, 1.25, 1.3, 1.4, 1.5

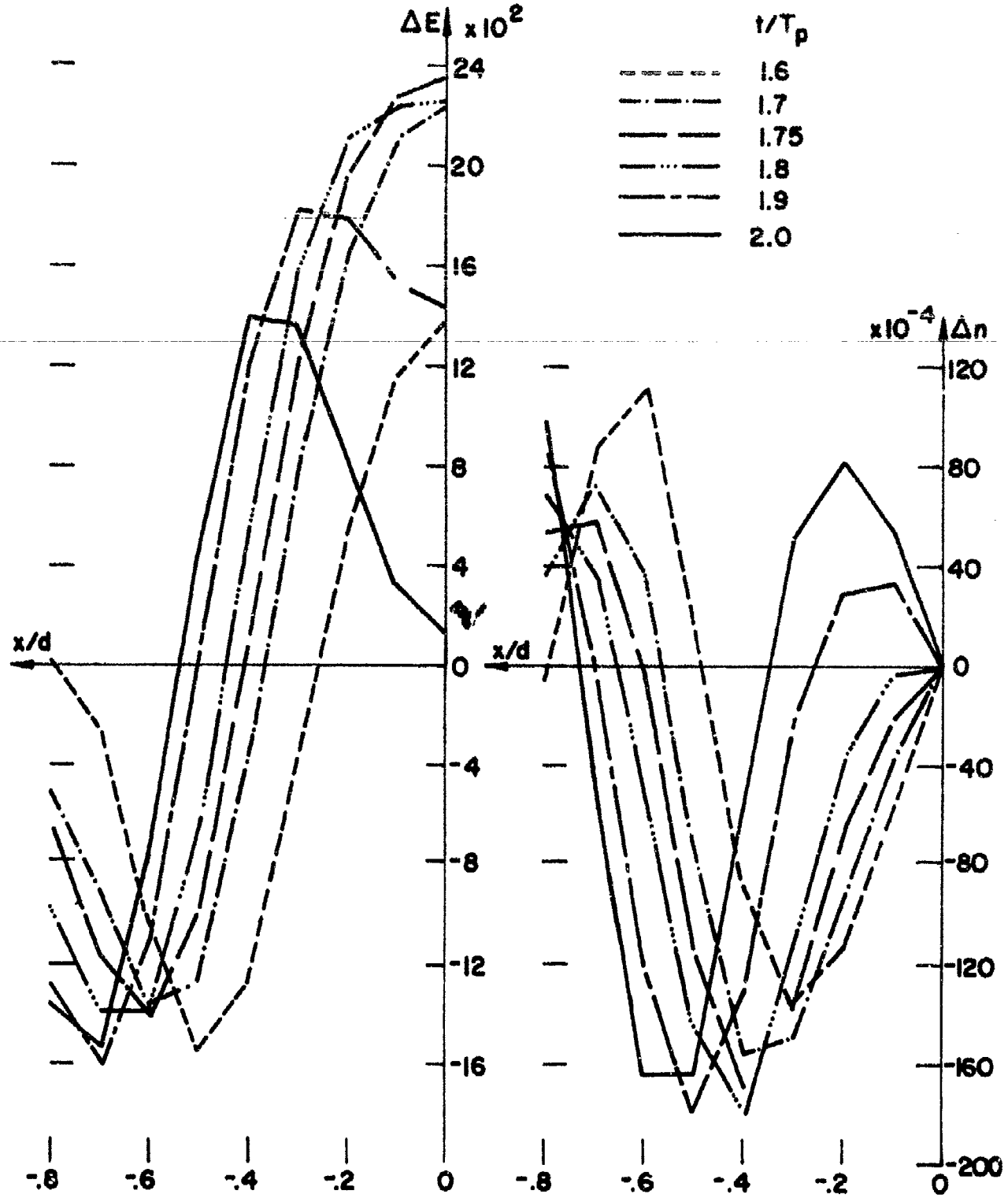

FIG. 9d ΔE and Δn vs. time
$a = 10^6$, $u = 10^5$, $d = 0.004$
Sheet 4/9: t/T_p=1.6, 1.7, 1.75, 1.8, 1.9, 2.0

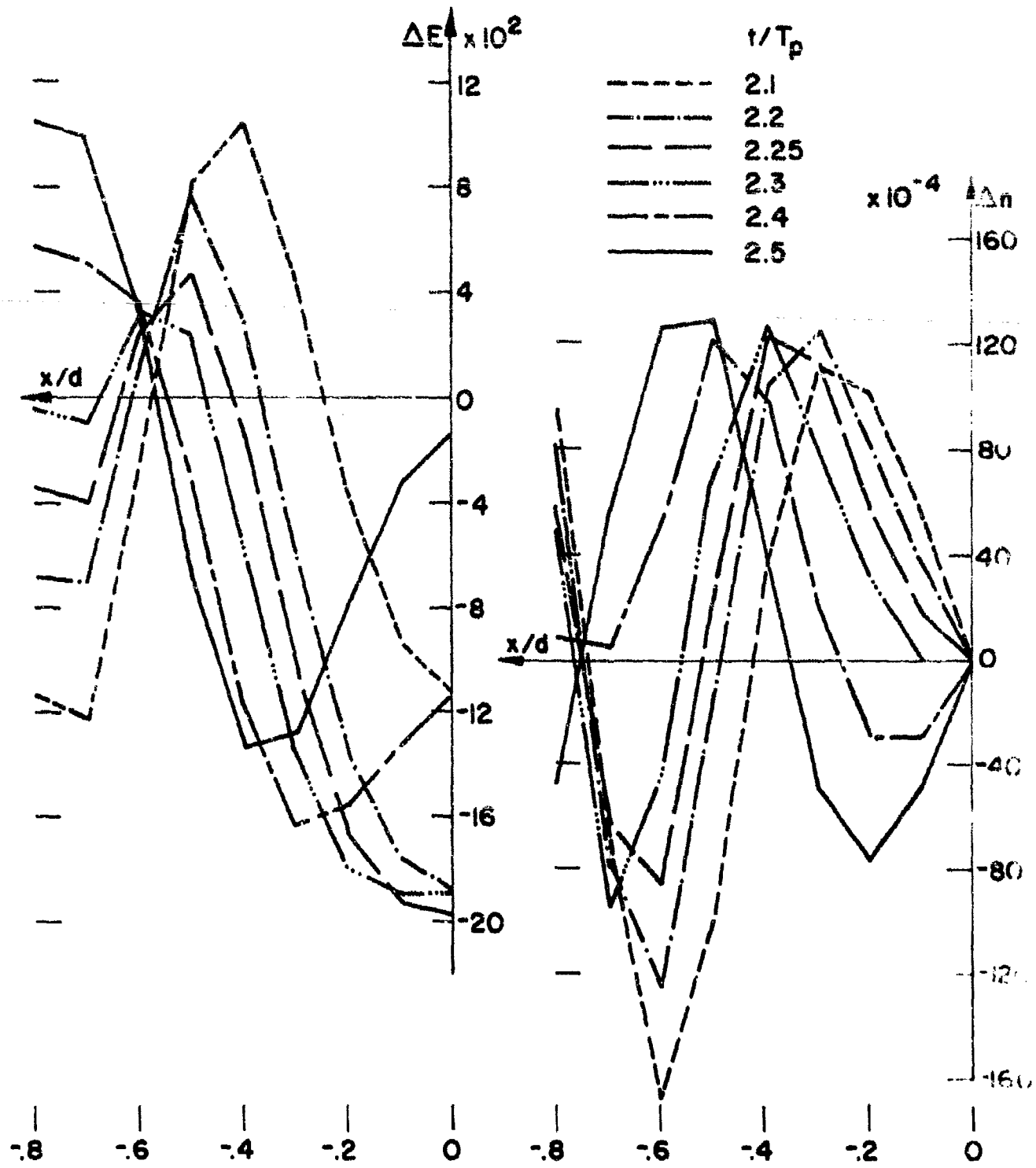

FIG. 9e ΔE and Δn vs. time
a = 10^6, u = 10^5, d = 0.004
Sheet 5/9: t/T_p = 2.1, 2.2, 2.25, 2.3, 2.4, 2.5

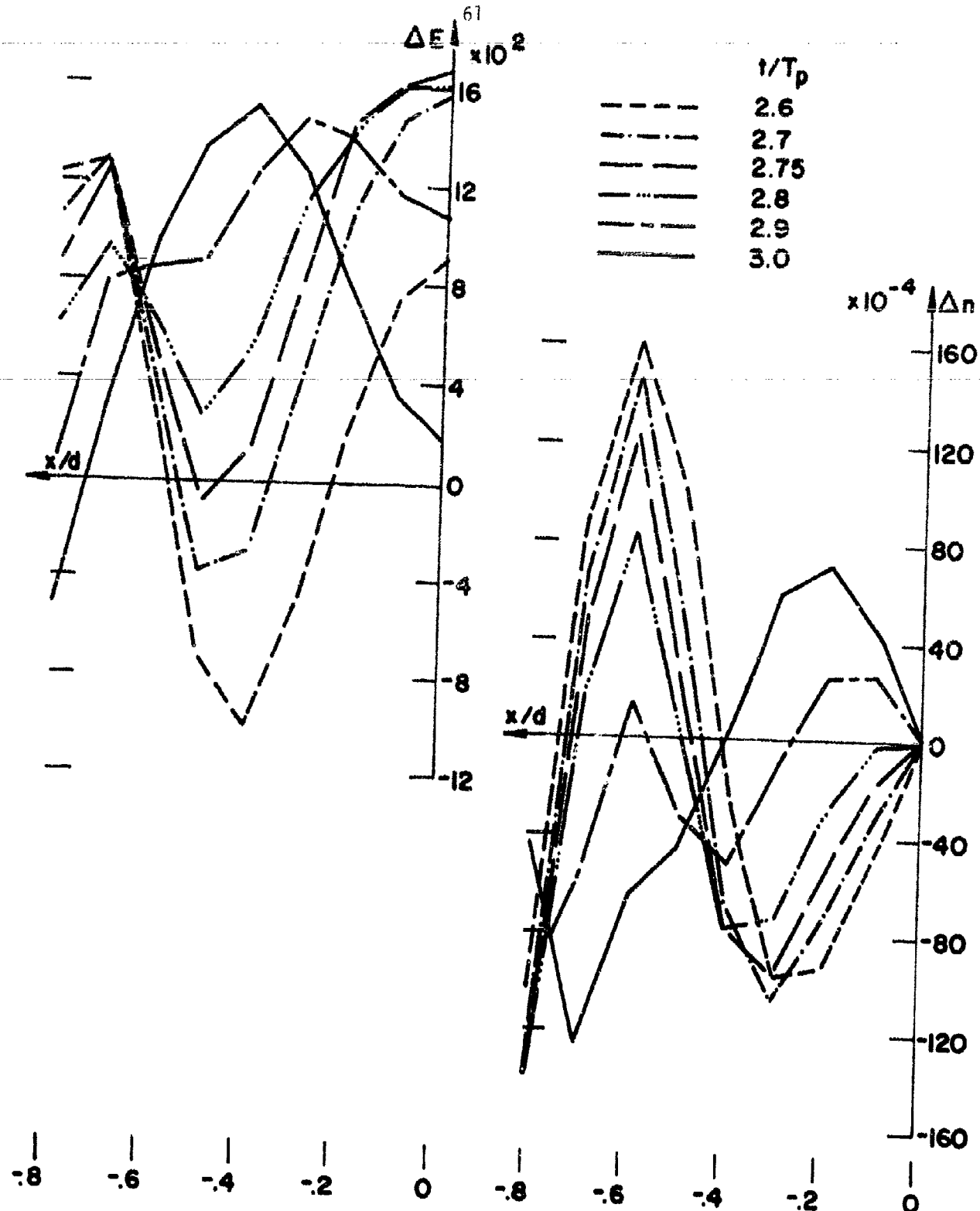

FIG. 9f ΔE AND Δn VS. TIME

$a = 10^6$, $u = 10^5$, $d = 0.004$

SHEET 6/9: $t/T_p = 2.6, 2.7, 2.75, 2.8, 2.9, 3.0$

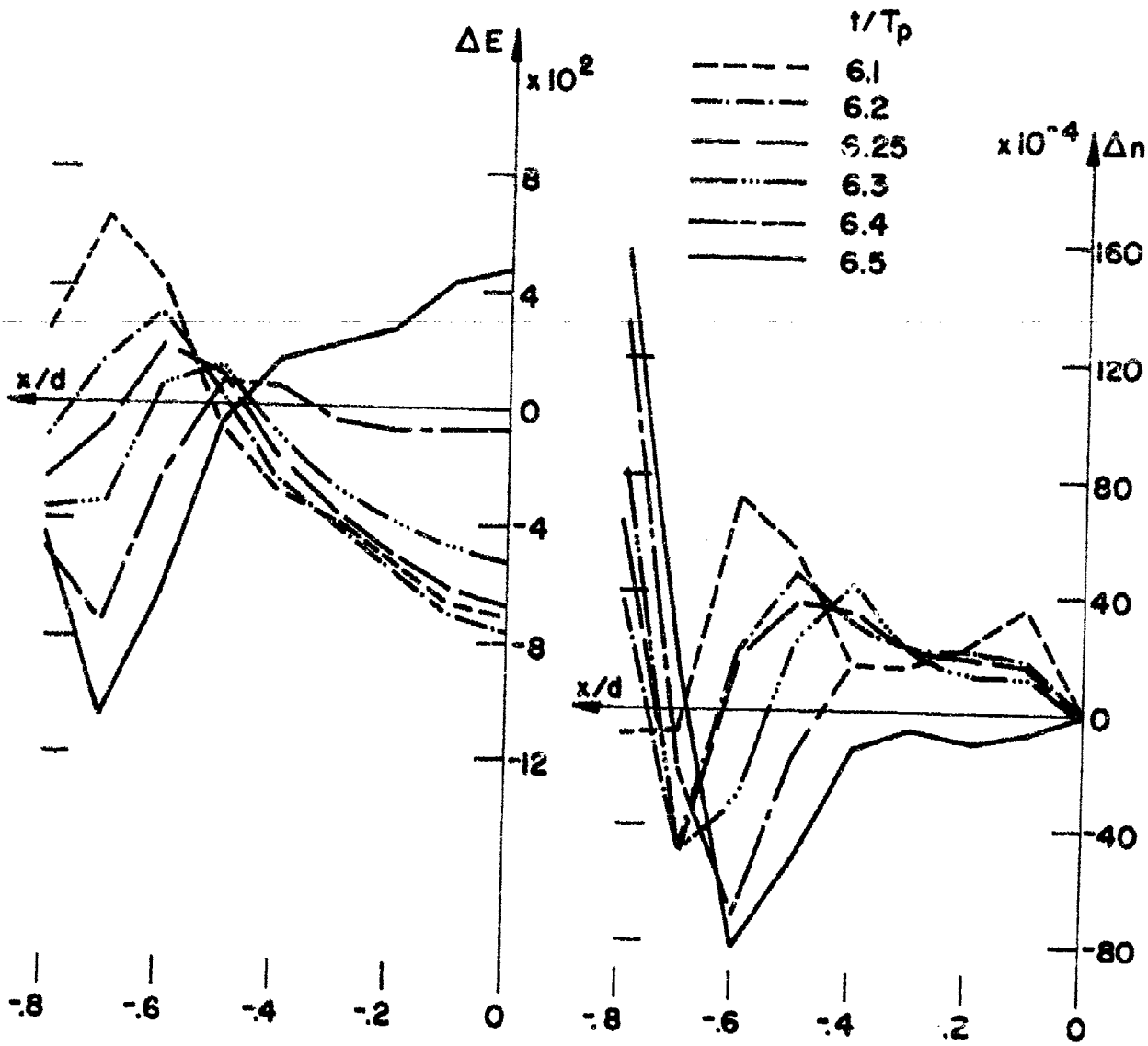

FIG. 9g ΔE AND Δn VS. TIME
$a = 10^6$, $u = 10^5$, $d = 0.004$
SHEET 7/9: t/T_p = 6.1,6.2,6.25,6.3,6.4,6.5

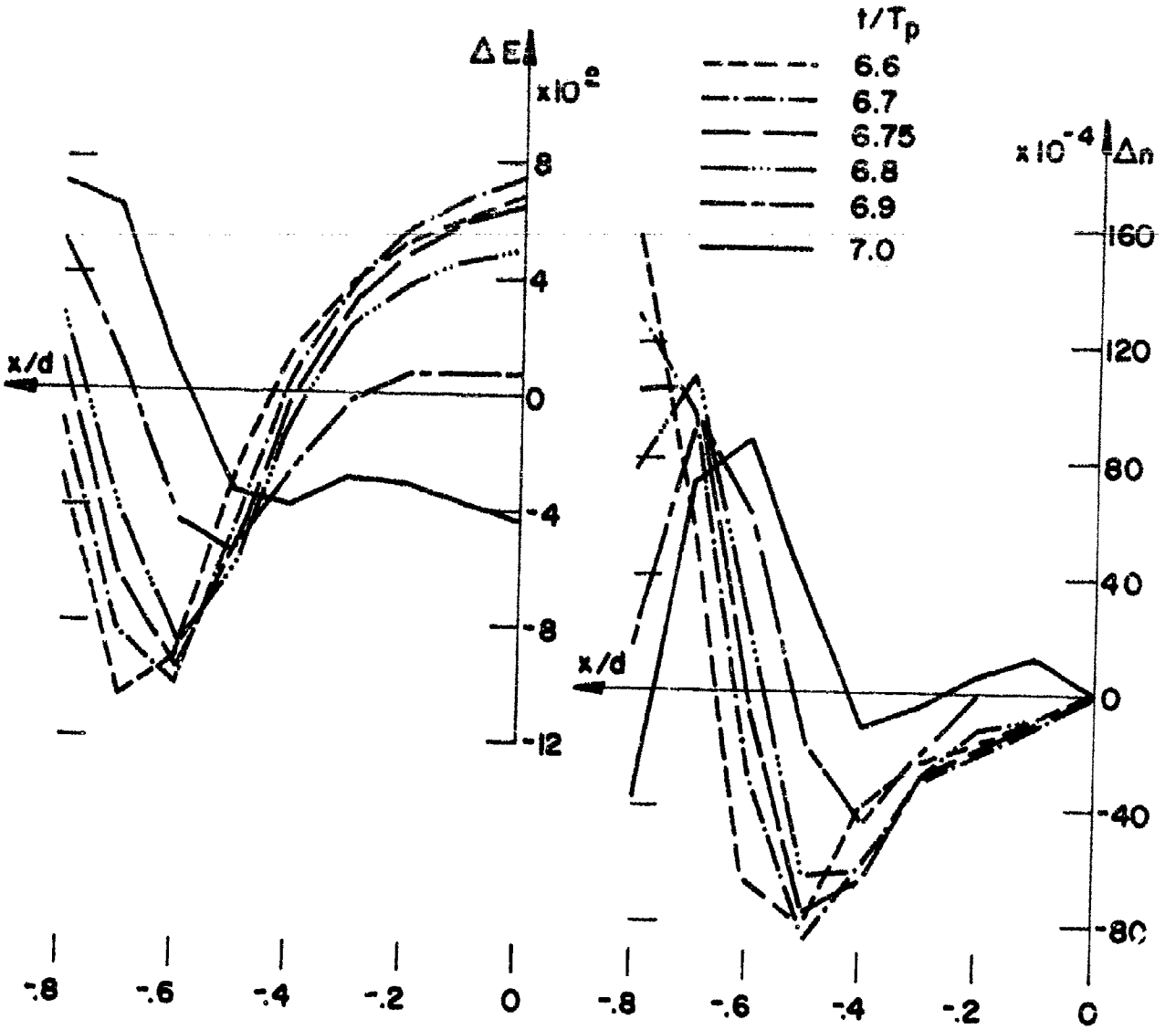

FIG. 9h ΔE AND Δn VS. TIME

$a = 10^6$, $u = 10^5$, $d = 0.004$

SHEET 8/9: t/T_p = 6.6,6.7,6.75,6.8,6.9,7.0

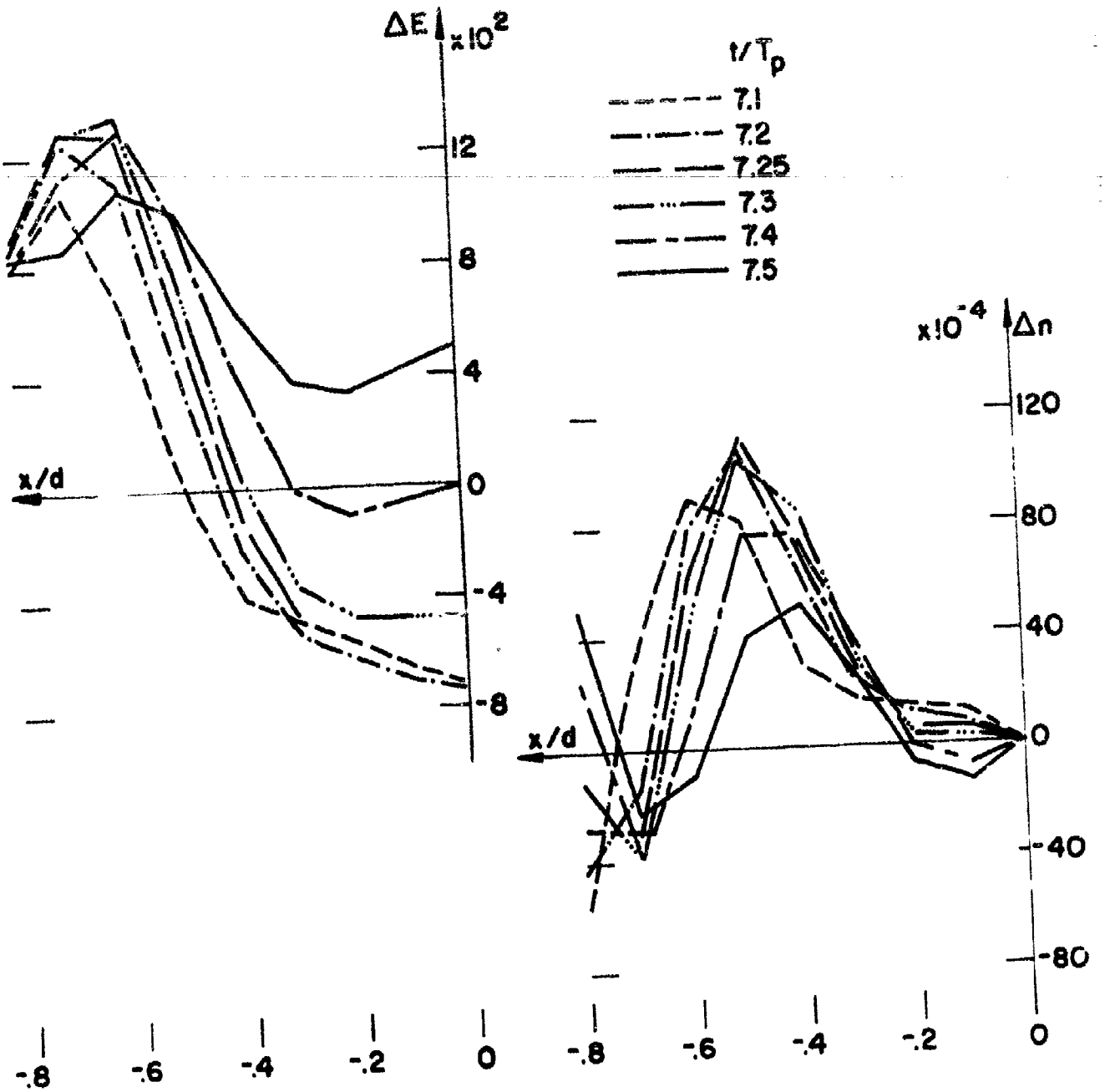

FIG. 9i ΔE AND Δn VS. TIME
$a = 10^6$, $u = 10^5$, $d = 0.004$
SHEET 4/9: t/T_p = 7.1,7.2,7.25,7.3,7.4,7.5

Envelope points of Fourier Transforms of ΔF

$a = 10^6$ $u = 10^5$ $d = 0.005$ $x/d = 0.0(0.1)0.8$

x/d = 0.0		x/d = 0.1		x/d = 0.2		x/d = 0.3	
0.000	96.20	0.000	97.10	0.000	88.20	0.000	49.57
0.050	107.84	0.050	106.87	0.085	97.20	0.175	259.71
0.160	112.48	0.160	111.61	0.235	122.80	0.555	325.31
0.250	117.28	0.250	116.46	0.340	114.68	0.820	593.98
0.340	125.62	0.340	125.79	0.605	200.90	0.970	1395.00
0.445	128.00	0.445	130.00	0.815	475.20	1.315	220.29
0.550	201.82	0.555	189.46	0.975	1330.27	1.410	226.26
0.810	345.36	0.815	326.02	1.195	210.28	1.735	200.17
0.985	1349.62	0.960	1345.52	1.310	129.02	2.035	172.72
1.415	108.30	1.305	146.11	1.420	96.98	2.110	172.78
1.525	83.64	1.420	106.33	1.529	87.85	2.415	172.68
1.625	65.48	1.520	81.20	1.615	68.22		
1.715	55.50	1.620	64.77	1.715	44.20		
1.825	47.58	1.720	55.58	1.820	46.98		
1.920	40.51	1.820	47.53	1.920	53....		
2.015	36.02	1.920	41.04	2.015	37.33		
2.120	23.89	2.020	35.90	2.120	19.21		
2.230	28.94	2.120	31.54	2.215	33.48		
2.325	25.18	2.215	28.33	2.315	38.95		
2.415	22.92	2.320	27.05	2.420	25.31		
		2.420	22.90				

TABLE 6a

Envelope points of Fourier Transforms of ΔT

$a = 10^6$ $u = 10^5$ $d = 0.005$ $x/d = 0.0(0.1)0.8$

x/d = 0.7		x/d = 0.8	
0.000	60.55	0.000	95.30
0.050	120.22	0.010	95.32
0.145	121.53	0.240	105.70
0.245	128.11	0.340	136.05
0.340	169.84	0.440	105.76
0.445	283.62	0.585	784.02
0.585	1192.86	0.755	316.20
0.720	263.92	0.980	161.70
0.820	176.73	1.210	85.79
0.945	417.10	1.365	71.71
1.125	65.53	1.525	73.91
1.235	40.46	1.690	65.06
1.335	33.70	1.840	65.91
1.425	25.16	2.005	63.67
1.510	26.68	2.115	61.12
1.615	31.03	2.315	64.02
1.720	33.89	2.475	58.10
1.830	32.40		
1.935	27.91		
2.050	20.00		
2.185	18.61		
2.305	20.17		
2.415	25.29		

TABLE 6c

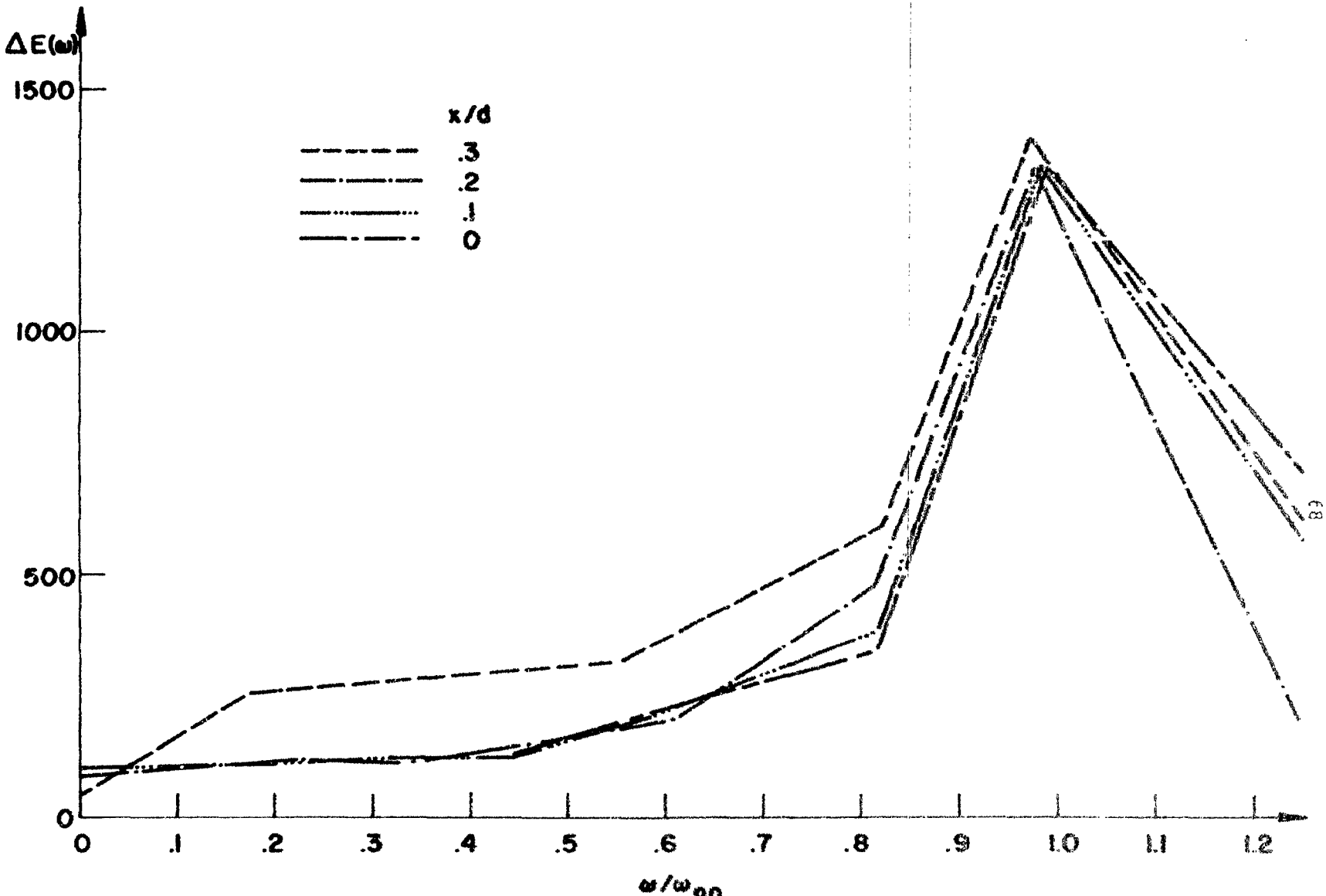

FIG. 10a FOURIER TRANSFORM OF ΔE(t)
$a = 10^6$, $v = 10^5$, $d = 0.005$
SHEET 1/3: x/d = 0.0, 0.1, 0.2, 0.3

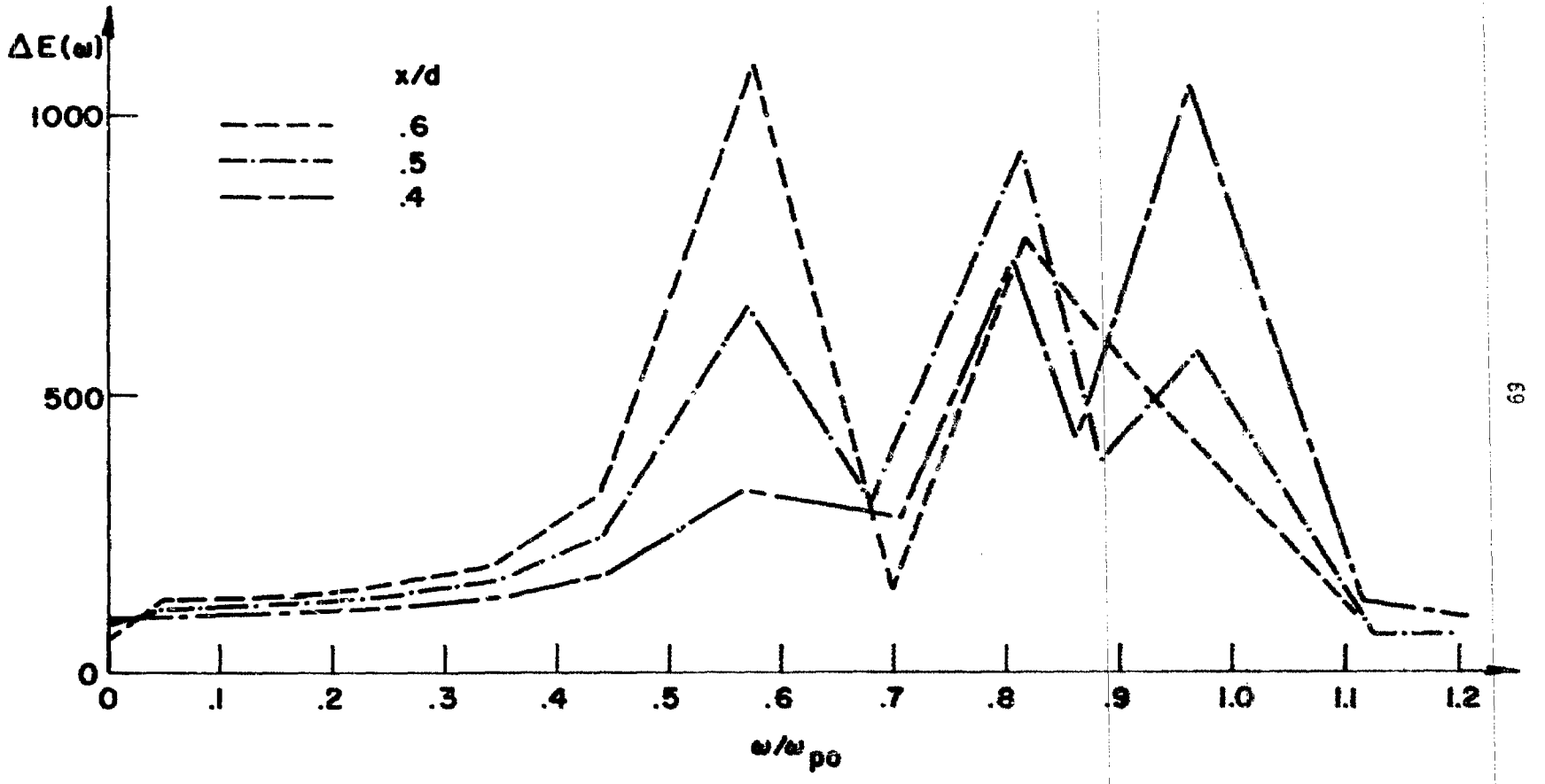

FIG. 10b FOURIER TRANSFORM OF $\Delta E(t)$
$a = 10^6$, $u = 10^5$, $d = 0.005$
SHEET 2/3: $x/d = 0.4, 0.5, 0.6$

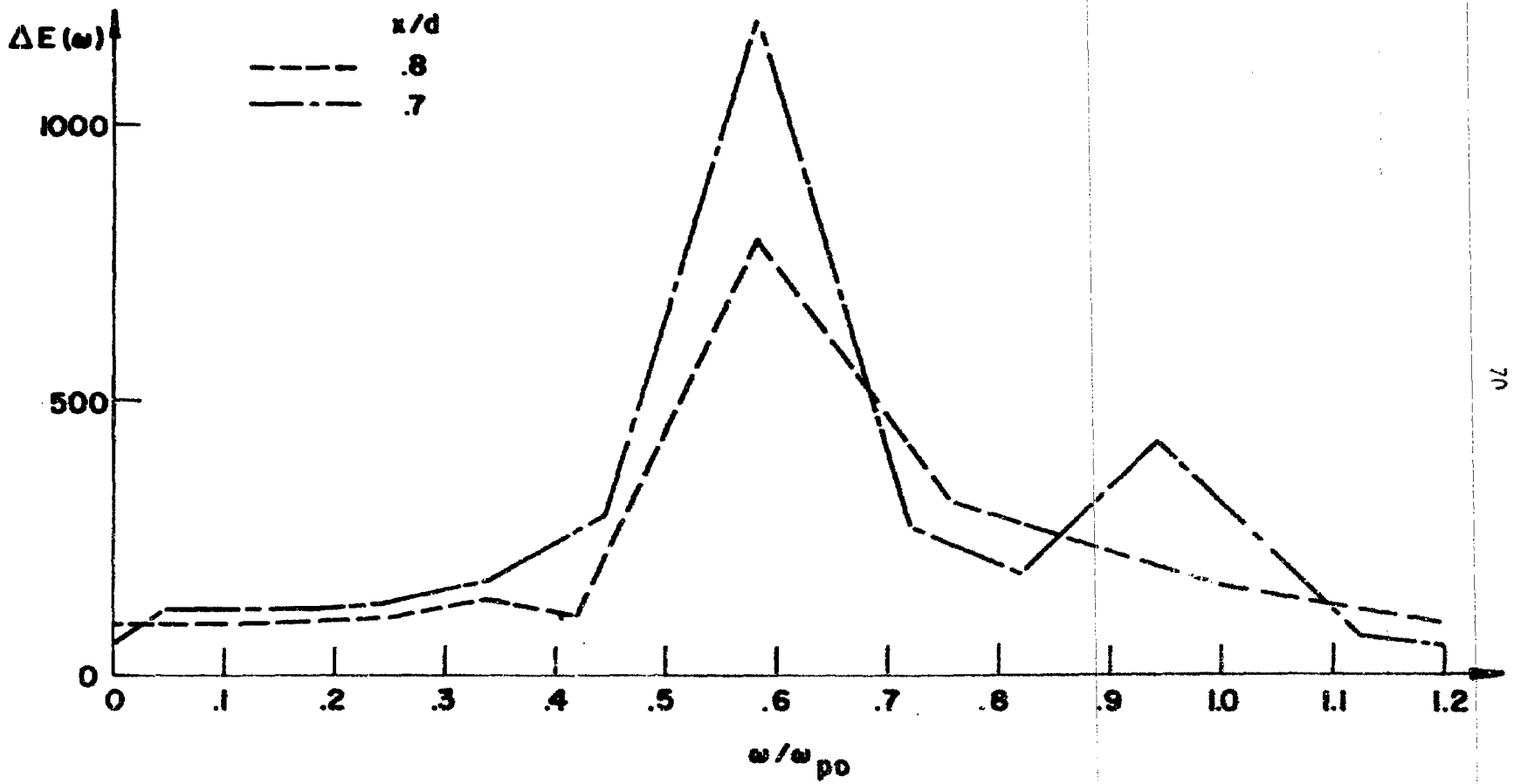

FIG. 10c FOURIER TRANSFORM OF E(t)
$a = 10^6$, $u = 10^5$, $d = 0.005$
SHEET 3/3: x/d = 0.7, 0.8

2 - At $|x/d| = 0.4$, the resonance at $f\tilde{=}0.9$ suddenly appears and the resonance at $f\tilde{=}0.575$ is noticeable. The resonance at $f\tilde{=}1$ has been reduced in amplitude.

3 - At $|x/d|=0.5$, the peak $f\tilde{=}1$ has been greatly reduced while the other resonances have been reinforced.

4 - At $x/d=0.6$, the resonance at $f\tilde{=}1$ does not show, the resonance at $f\tilde{=}0.8$ has begun to decrease in magnitude and the lowest resonance has become predominant.

5 - At $x/d=0.7$, the resonance at $f\tilde{=}0.8$ has disappeared, the resonance at $f\tilde{=}1$ shows a small remnant.

6 - At $x/d=0.8$, only the resonance at approximately $f=0.575$ remains.

Also worthy of note is the high magnitude of the Fourier spectrum at $x/d=0.3$ for frequencies below $f=0.8$. This tends to confirm the "barrier" behavior discussed previously. It is also possible that some small resonances are hidden in this part of the spectrum which cannot be seen due to the limited number of points available.

The two lower frequencies are both higher than the local cold plasma frequencies.

Thus the three regions are established and can be defined:

1 - Region #1, in the center of the slab, where only the resonance at $f\tilde{=}1$ is seen.

2 - Region #3, near the walls of the slab, where the resonance at $f\tilde{=}0.575$ is seen and only traces of the other two resonances are seen if they are seen at all.

3 - Region #2, between the previous two regions, where both the previous resonances can be seen plus a strong resonance at f≅0.8 which is characteristic of this region.

In this standard experiment, region #1 covers $0.0<|x/d|<0.3$. Region #2 consists of the two sectors $0.4<|x/d|<0.6$. Region #3 is formed by the two sectors defined by $0.7<|x/d|<0.8$.

The fact that only a limited number of points per frequency unit are available might of course hide some detail but this will not influence the above results to a significant degree.

C. Effect of Variation of Parameters of the Plasma Model

In order to establish that the two lower frequency peaks are thermal modes as conjectured in the preceding section, the effects of the variation of temperature and the slab width are investigated.

Computer runs were made for plasma slabs with a and u as for the standard experiment but with d=0.004(0.0005)0.006, 0.007(0.001)0.010. Results presented here are for d=0.004, 0.005, 0.007 and 0.010 only since these suffice to describe the effect of variation of d.

Figs. 11 and 12 show the voltage as a function of time for the slabs of halfwidth d=0.004 and d=0.010. While it is difficult to make a comparison between Figs. 1 and 11, one is able to notice a substantial difference between these two figures and Fig. 12. In the latter, the peak-to-peak times are much more uniform than in the former. Peak values of the voltage and times of occurrence are listed for all four widths in Table 3.

More interesting and informative are the Fourier transforms of the

FIG. 11 NORMALIZED VOLTAGE VS. TIME
$a = 10^6$, $u = 10^5$, $d = 0.002$

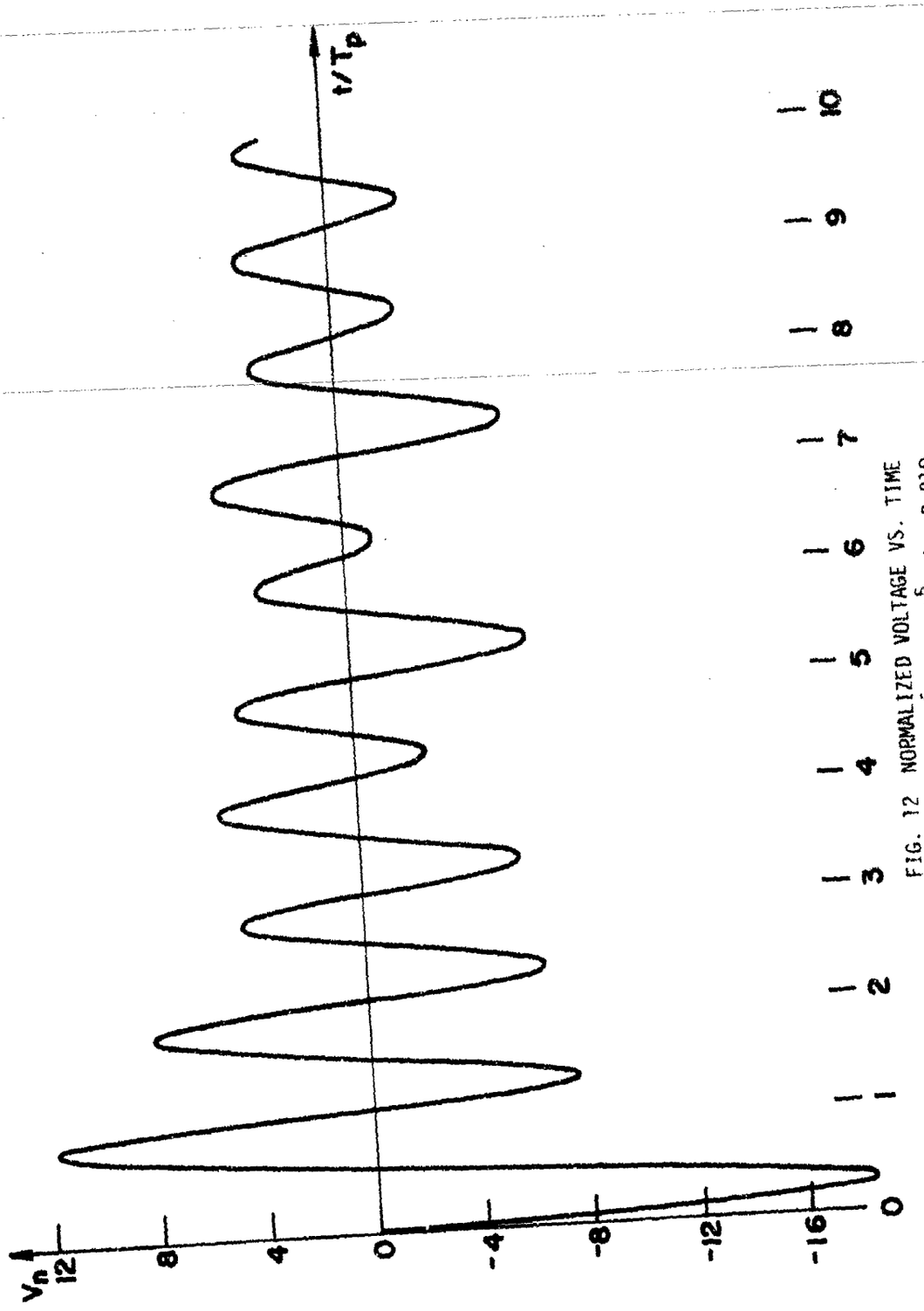

FIG. 12 NORMALIZED VOLTAGE VS. TIME
$a = 10^6$, $v = 10^5$, $d = 0.010$

voltages for the four plasma slabs under discussion. Results are shown in Table 5 and plotted in Fig. 13. One notices that

1 - The peak at $f \tilde{=} 1$ associated with the central region (region #1) increases in strength with increasing slab width, but with only a very slight shift of frequency, indicating a cold oscillation.

2 - The next peak associated with the "middle" region (region #2) decreases in strength with increasing slab width. For d=0.004, 0.005 a low shift is clear and one also notices a decrease in amplitude of the peak with increasing width. For d=0.007, 0.010 peaks are barely identifiable and no clear conclusion can be drawn.

3 - The lowest peak decreases in strength and broadens markedly as the slab widens. The low shifts of the peak towards lower frequency as the slab widens are clearly seen.

The low shift of the two lower frequency peaks as a result of the widening of the slab indicates the thermoresonance in the sense of Baldwin[27] and Ignat[28]. Or the thermomodes associated with a circular Tonks-Dattner structure are the acoustic wave resonances bounded between the sheath and a dense plasma region beyond which the low frequency oscillations cannot penetrate.

This is further confirmed by a study of the effect of varying the background temperature, i.e., the thermal velocity a. Experiments were performed for $u=10^5$, d=0.005 - the same stimulus and width of the standard

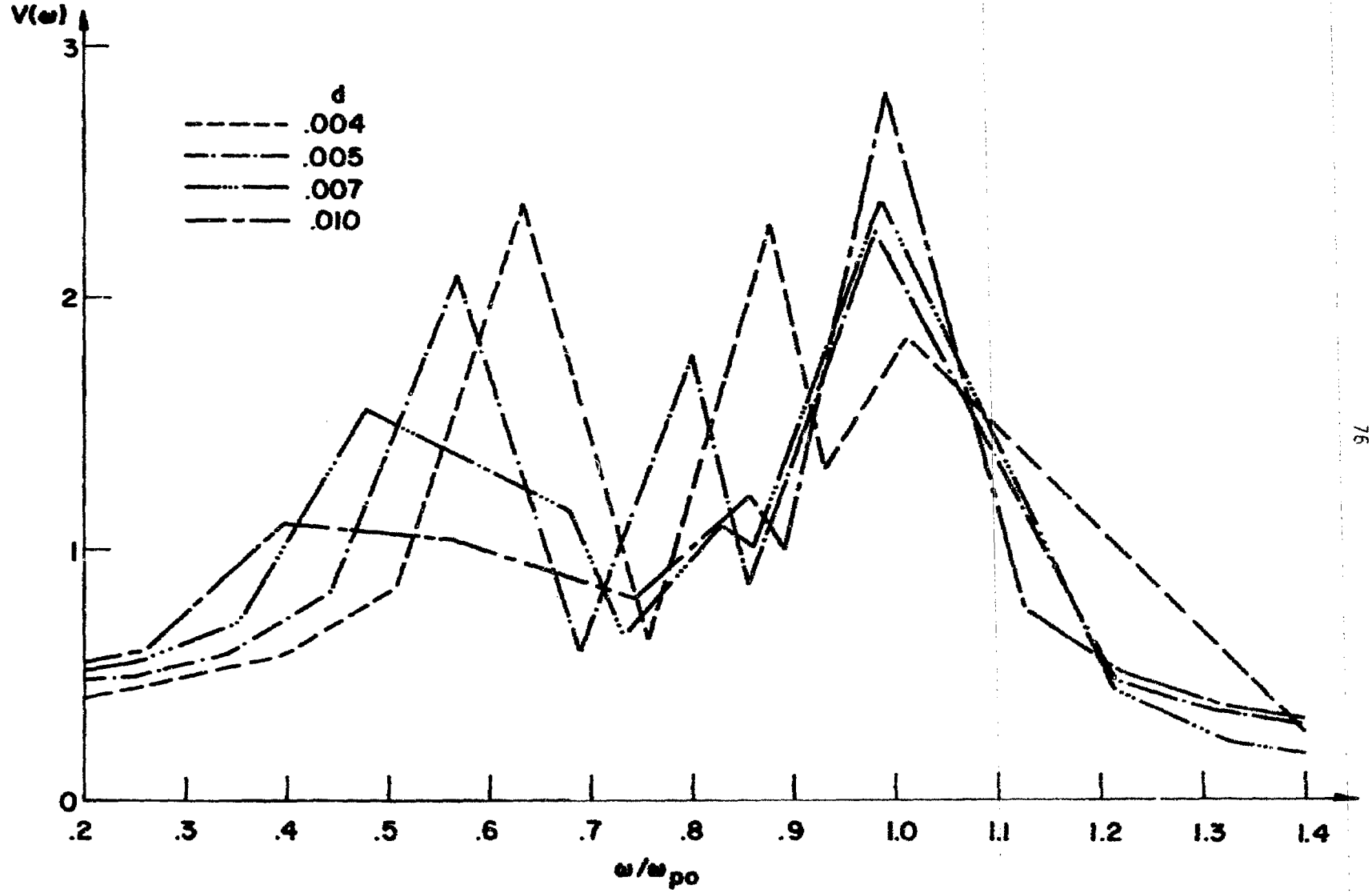

FIG. 13 FOURIER TRANSFORM OF V(t)
$a = 10^6$, $u = 10^5$, $d = 0.004, 0.005, 0.007, 0.010$

experiment - with $a=8\cdot10^5$, $9\cdot10^5$, $1.1\cdot10^6$, $1.2\cdot10^6$. Results of the Fourier transform of these experiments are listed in Table 8, together with the results of the standard experiment. Fig. 15 plots the Fourier transform for the highest and lowest thermal velocities and the Fourier transform of the standard experiment. One notices, by comparison with Table 5 and Fig. 13 that a decrease/increase in the temperature of the equilibrium slab has a very similar effect to the widening/narrowing of the plasma slab and in particular that the highest of the three high amplitude resonances shows a negligible frequency shift while the low shift of the two lower peaks is again clearly noticeable.

Thus the thermal character of the two lower high amplitude resonances as well as the cold character of the resonance at approximately $f\tilde{=}1$ has been clearly established.

The Fourier transform of $\Delta E(x/d,t)$ for $d=0.010$ was also obtained and has been tabulated in Table 7 and plotted in Fig. 14 for $x/d=0.0,0.5,0.8$. The behavior is in accordance with the result on the voltage. One notes the small peak around $f=0.7$ for the transform at $x/d=0.8$.

D. Summary of Results in the Linear Region

In the preceding sections it has been shown that the plasma model presented has a linear region and that in this region the Fourier spectrum of the impulse-response

1 - has three well-pronounced resonance peaks below and around the plasma frequency at the center of the slab, and that

Envelope points of Fourier Transforms of E(t)

$a = 10^6$ $u = 10^5$ $d = 0.01$ $x/d = 0.0, 0.5, 0.8$

x/d = 0.0		x/d = 0.5		x/d = 0.8	
0.000	28.22	0.000	39.90	0.000	24.22
0.050	73.66	0.050	61.80	0.055	52.66
0.150	76.50	0.150	63.09	0.165	65.87
0.250	76.40	0.250	74.90	0.275	92.36
0.350	87.98	0.355	88.43	0.420	399.54
0.450	98.17	0.455	108.31	0.565	67.34
0.550	105.44	0.570	195.07	0.695	130.32
0.650	126.31	0.605*	149.13	0.970	29.16
0.750	167.22	0.705	295.08	1.065	18.93
0.855	290.57	0.830	407.93	1.170	13.29
0.995	1145.78	1.030	132.02	1.270	11.95
1.135	244.64	1.155	48.37	1.370	11.24
1.240	135.20	1.255	35.14	1.470	10.26
1.39	90.24	1.355	27.58	1.570	9.42
1.44	67.61	1.455	23.54	1.670	8.48
1.54	53.75	1.555	20.64	1.765	7.72
1.64	42.83	1.655	17.25	1.865	7.52
1.74	35.27	1.755	14.60	1.970	6.78
1.84	30.57	1.860	13.03	2.065	6.43
1.94	26.83	1.960	11.02	2.170	5.88
2.04	23.64	2.050	9.85	2.265	5.70
2.14	20.72	2.160	9.50	2.370	5.32
2.24	18.38	2.260	7.84	2.465	5.46
2.34	16.47	2.355	7.254		
2.44	15.40	2.455	7.257		

* Phase reversal point

TABLE 7

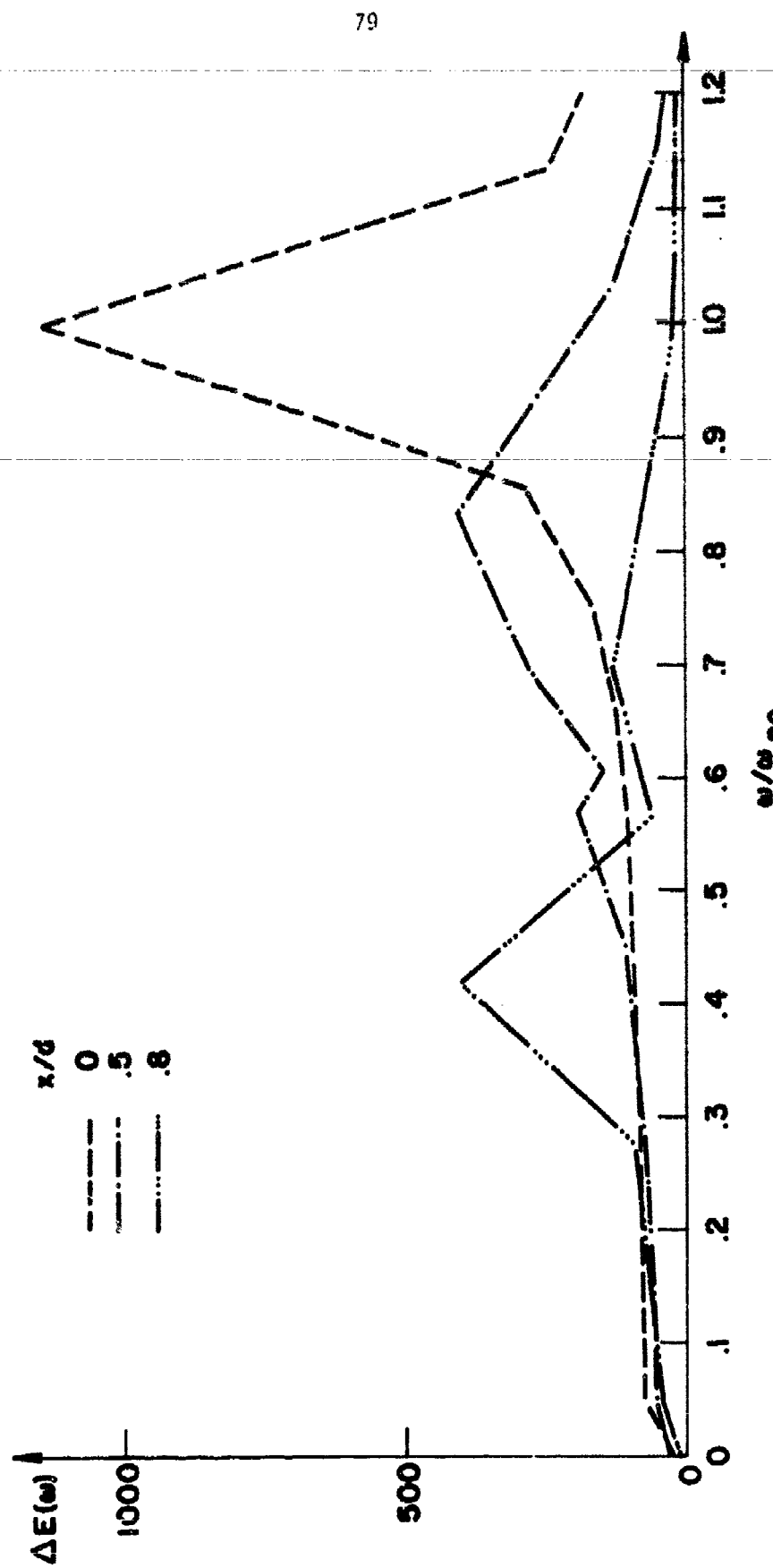

FIG. 14 FOURIER TRANSFORMS OF $\Delta E(t)$
$a = 10^6$, $u = 10^5$, $d = 0.005$, $x/d = 0.0, 0.5, 0.8$

Envelope points of Fourier Transforms of V(t)

$a = 8.10^5, 9.10^5, 10^6, 1.1.10^6, 1.2.10^6$ $u = 10^5$ $d = 0.005$

$a = 8.10^5$		$a = 9.10^5$		$a = 10^6$		$a = 1.1.10^6$		$a = 1.2.10^6$	
0.000	.3936	0.000	.4562	0.000	.3362	0.000	.3144	0.000	.3894
0.075	.4193	0.010	.4709	0.050	.4346	0.055	.4117	0.105	.4017
0.180	.4438	0.205	.4866	0.145	.4521	0.150	.4253	0.185	.3909
0.275	.5372	0.305	.5706	0.245	.4991	0.250	.4706	0.290	.4561
0.380	.7191	0.410	.7635	0.340	.5880	0.360	.5619	0.385	.7960
0.505	1.7279	0.535	1.8783	0.440	.8149	0.465	.7929	0.620	2.2559
0.720	1.4345	0.670	.5485	0.565	2.0802	0.595	2.1576	0.750	.6406
0.770*	.5811	0.765	1.5699	0.690	.5872	0.725	.6788	0.865	2.1677
0.845	1.2879	0.815*	.6824	0.800	1.6778	0.835	1.9573	0.915*	1.2256
0.875*	1.0528	1.000	2.0823	0.855*	.8657	0.885*	1.0232	1.005	2.0200
0.980	2.3285	1.230	.3995	0.980	2.2452	0.985	2.1604	1.125	.6858
1.135	.6046	1.330	.2799	1.215	.4751	1.355	.2652	1.240	.4171
1.260	.3885	1.435	.2217	1.315	.3536	1.465	.2034	1.345	.2764
1.365	.2932	1.535	.1731	1.420	.2786	1.560	.1620	1.450	.2154
1.465	.2261	1.635	.1439	1.520	.2237	1.660	.1396	1.550	.1742
1.565	.1922	1.730	.1202	1.620	.1854	1.760	.1207	1.650	.1470
1.670	.1645	1.825	.1040	1.720	.1634	1.860	.1056	1.750	.1238
1.770	.1416	1.925	.0914	1.820	.1420	1.965	.0934	1.855	.1093
1.870	.1252	2.02	.0808	1.920	.1267	2.065	.0848	1.960	.0930
1.970	.1132	2.12	.0741	2.020	.1116	2.165	.0752	2.055	.0828
2.070	.1025	2.22	.0673	2.120	.1016	2.260	.0669	2.160	.0766
2.170	.0917	2.33	.0608	2.220	.0920	2.365	.0627	2.260	.0648
2.270	.0844	2.43	.0546	2.320	.0871	2.460	.0599	2.355	.0636
2.370	.0760			2.420	.0792			2.460	.0577
2.470	.0725								

* Phase reversal point

TABLE 8

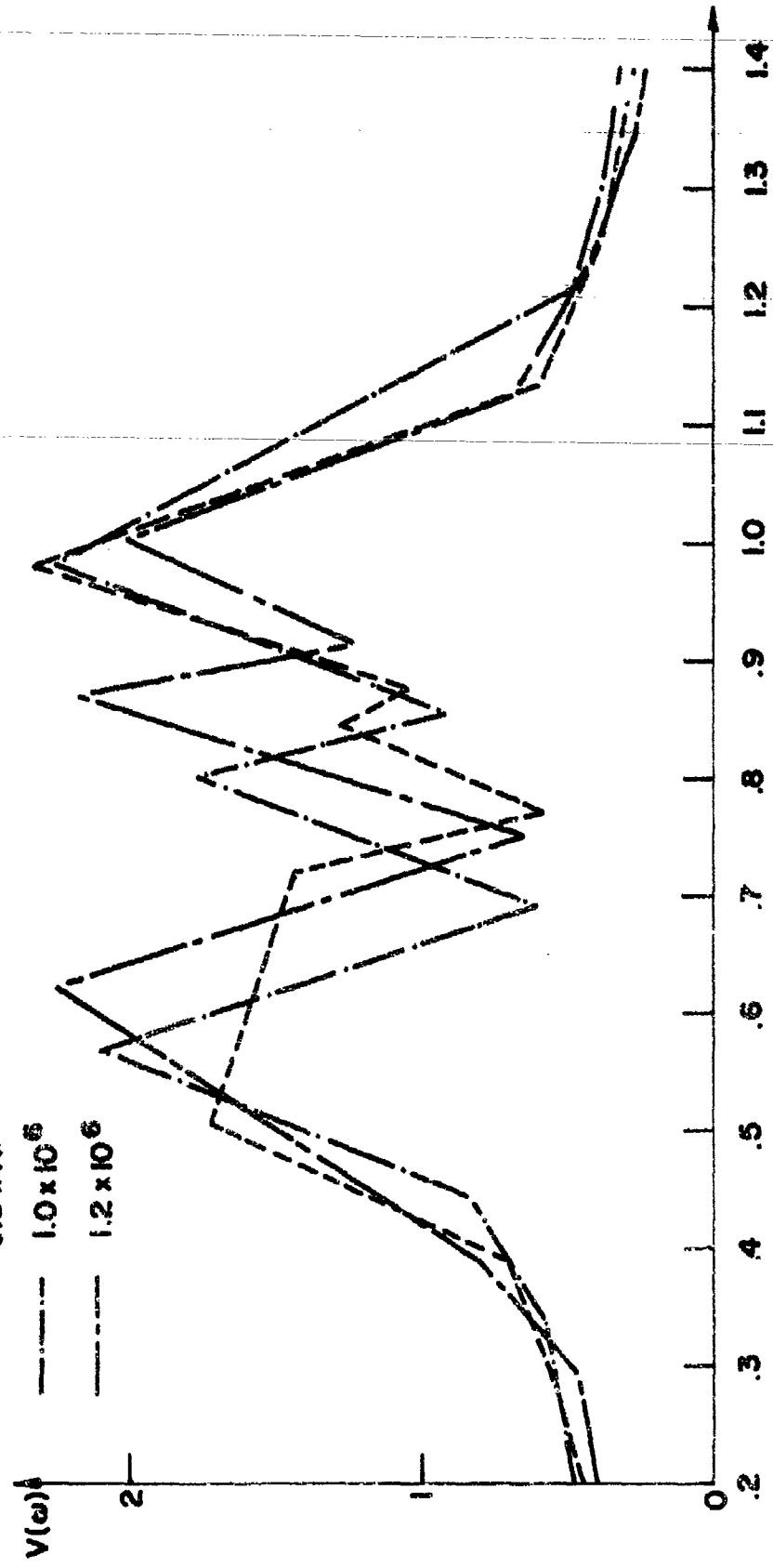

FIG. 15 FOURIER TRANSFORMS OF V(t)
$a = 8.10^5$, 10^6, $1.2.10^6$, $u = 10^5$, $d = 0.005$

2 - each of these frequencies is associated with a relatively well-defined region of the slab.

It has also been shown that the following associations can be made between the three resonances and areas of the slab:

1 - The highest of the three resonances belongs to a region located around the center of the slab. The amplitude and frequency are relatively independent of plasma temperature and width of slab. The value of the frequency of the resonance peak is at or slightly below the plasma frequency at the center of the slab.

2 - The lowest of the three resonances is associated with the region near the plasma sheath. The frequency of this resonance peak as well as its amplitude as well as the 3-db width of the resonance depend on both slab width and temperature. The frequency of the peak is above the local cold plasma frequencies in the region.

3 - The "middle" resonance is associated with the "middle" region located between the "center" region and the "wall" region. The amplitude of this resonance depends on slab width and temperature; the frequency of this resonance is also above the local cold plasma frequencies of this region.

Thus one is able to conclude that

1 - The resonance peak at $f \tilde{=} 1$ is a cold plasma resonance associated with the plasma frequency in the center of the plasma.

2 - The other two resonances are thermal resonances.

Table 9 shows local plasma frequencies and periods in the background plasma for x/d=0.0(0.1)0.9, normalized to center plasma frequency and period of unity.

It has further been shown that the three regions can be defined in the following manner through the Fourier transform of $\Delta E(x/d,t)$

1 - The central region contains only the resonance at f≅1. The other resonances cannot be seen in this region or are of negligible magnitude.

2 - The wall region shows the lowest resonance strongly predominant. The other resonances might or might not be noted in this region and are of small magnitude whenever noticed.

3 - The "middle" region contains all three resonances but only in this region is the "middle" resonance very strong, i.e., of the order or larger than any of the other two resonances.

TABLE 9

Local Plasma Frequencies and Periods
Normalized to 1 at Center of Slab

$\frac{x}{d}$	ω_{pn} or f_{pn}	T_{pn}
0.0	1.	1.
0.1	.9877	1.012
0.2	.9511	1.051
0.3	.8910	1.122
0.4	.8090	1.236
0.5	.7071	1.414
0.6	.5878	1.701
0.7	.4540	2.203
0.8	.3090	3.236
0.9	.1564	6.394

$$\omega_{pn} = \omega_{po} \cdot \cos \frac{\pi x}{2d}$$

V. RESULTS IN THE NON-LINEAR REGION

One of the goals of the present investigation was to device a numerical scheme to investigate the impulse-responses of a non-uniform bounded plasma with sheaths under strong excitations into the non-linear regime. The approach presented herein fulfills this goal to some extent. One recalls that the program is based on the non-linear Boltzmann-Vlasov equation with the imposed inhomogeneous background containing the singular fields at the slab boundaries simulating the sheath. The limitation imposed into this direction comes from the availability of computer time and of computer core. This has already been discussed in Section III.b.

The time during which the solution can be considered valid varies as a function of several parameters. One important factor causing the numerical instability is the singular sheath field. Thus in a different problem such as that of a unbounded plasma or a uniform plasma considered in most of the previous investigations, the numerical instability problem should be considerably relaxed. In fact, it is observed that, if the slab is widened, the situation improves.

With the computation resources available to the present study, the strength of the stimulus has been extended into the non-linear regime with some limited degree of success. For experiments defined by $a=10^6$ and $d=0.005$, i.e. the temperature and slab width of the standard experiment, the validity of data extends to about 7 plasma periods for an excitation $u=2.10^5$, to 3 plasma periods for $u=5.10^5$ and to 2 plasma periods for $u=10^6$. These times can be extended by refining the grid in all three dimensions

but, as mentioned, this will require more core space and availability of relatively large amounts of computer time. To give an idea os the volume of calculations involved, in the standard experiment 32.10^6 points of the electron distribution function are calculated for 10 plasma periods, each one requiring several additions, multiplications and of course requiring several data which have to be brought from memory to the arithmetic processor. Further developments in computer technology may alleviate the problem.

From the computations performed, the basic wave form of the voltage remains quite similar to linear results. Some of the obtained results are listed in Table 10 and 11. This listing of the voltage peaks and their time of occurrence permits to infer that the locations of the peaks, at least during the relatively early stages, will not change to a considerable amount but that the amplitudes at the peaks might change to some degree which at the moment is difficult to ascertain.

The Fourier transform of the voltage has been performed and results are given in Table 12 for the experiment defined by $a=10^6$, $u=2.10^5$, $d=0.005$ and shown, together with the Fourier transform of the voltage of the standard experiment, in Fig. 16. The qualitative behavior of the transforms is the same. A difference in magnitudes is expected due to the normalization process and due to the attenuation expected; one is in face of the same phenomenon discussed for results of Table 4 and Fig. 3. Briefly, one notes that:

1. The resonance of the peak corresponding to the region near the wall, at approximately $f=0.575$, shows an increase of approximately 10%.

Voltage Peaks

$a = 10^6$. $d = 0.005$

$u = 10^5$		$u = 2 \cdot 10^5$		$u = 5 \cdot 10^5$		$u = 10^6$	
.287	-18.27	-.290	-18.33	.290	-18.32	.290	-18.30
.859	+12.90	.853	+12.80	.855	+12.86	.855	+12.91
1.375	- 6.925	1.373	- 6.805	1.372	- 6.794	1.370	- 5.717
1.944	+ 5.587	1.842	+ 5.535	1.840	+ 5.560	1.835	+ 5.757
2.353	- 7.649	2.351	- 7.770	2.335	- 7.696	2.337	- 7.490
2.912	+ 6.863	2.914	+ 7.140	2.895	+ 7.614		
3.475	- 2.346	3.482	- 2.601	3.475	- 3.908		
3.781	- 1.057	3.802	- 1.105				
4.178	- 3.805	4.180	- 3.524				
4.781	+ 7.076	4.772	+ 7.660				
5.391	- 7.507	5.385	- 7.745				
5.984	+ 4.351	5.980	+ 4.867				
6.425	- .965	6.485	- 1.214				
6.903	+ 2.131	6.905	+ 1.670				
7.440	- 4.911	7.455	- 4.127				
8.125	+ 5.288						
8.825	- 3.488						
9.094	+ 3.841						

TABLE 10

Voltage Peaks, Varied Conditions

$a = 10^6$, $u = 10^5$, $d = .010$		$a = 10^6$, $u = 10^6$, $d = .010$		$a = 1.2 \cdot 10^6$, $u = 10^5$, $d = .005$		$a = 1.2 \cdot 10^6$, $u = 10^6$, $d = .005$	
.294	-18.54	.292	18.55	.287	-18.01	.287	-18.10
.853	+11.75	.852	11.70	.853	+13.36	.853	+13.84
1.356	- 7.610	1.360	- 7.606	1.361	- 7.293	1.387	- 7.145
1.856	+ 8.095	1.865	+ 8.140	1.850	+ 4.267	1.820	+ 3.905
2.375	- 6.710	2.368	- 6.145	2.325	- 6.544	2.300	- 5.894
2.862	+ 4.675	2.835	3.133				

TABLE 11

TABLE 12

Envelopt Points of the Fourier Transform of V(t)

$a = 10^6$, $u = 2.10^5$, $d = 0.005$

.000	.637
.013	.674
.265	.736
.395	.955
.560	2.2976
†	†
.790	1.7908
.850*	1.1364
.985	2.9311
1.145	.8480
1.285	.4974
1.415	.3430
1.550	.2759
1.680	.2154
1.810	.1866
1.940	.1494
2.075	.1382
2.200	.1128
2.335	.1118
2.465	.0859

† Results indicate probable existence of phase reversal point between 0.650 and 0.690. Exact position and absolute value at that point cannot be determined. In Figure No. 16, this phase reversal point is extrapolated with a certain arbitrarity to show the valley between the two resonances.

* Phase reversal point

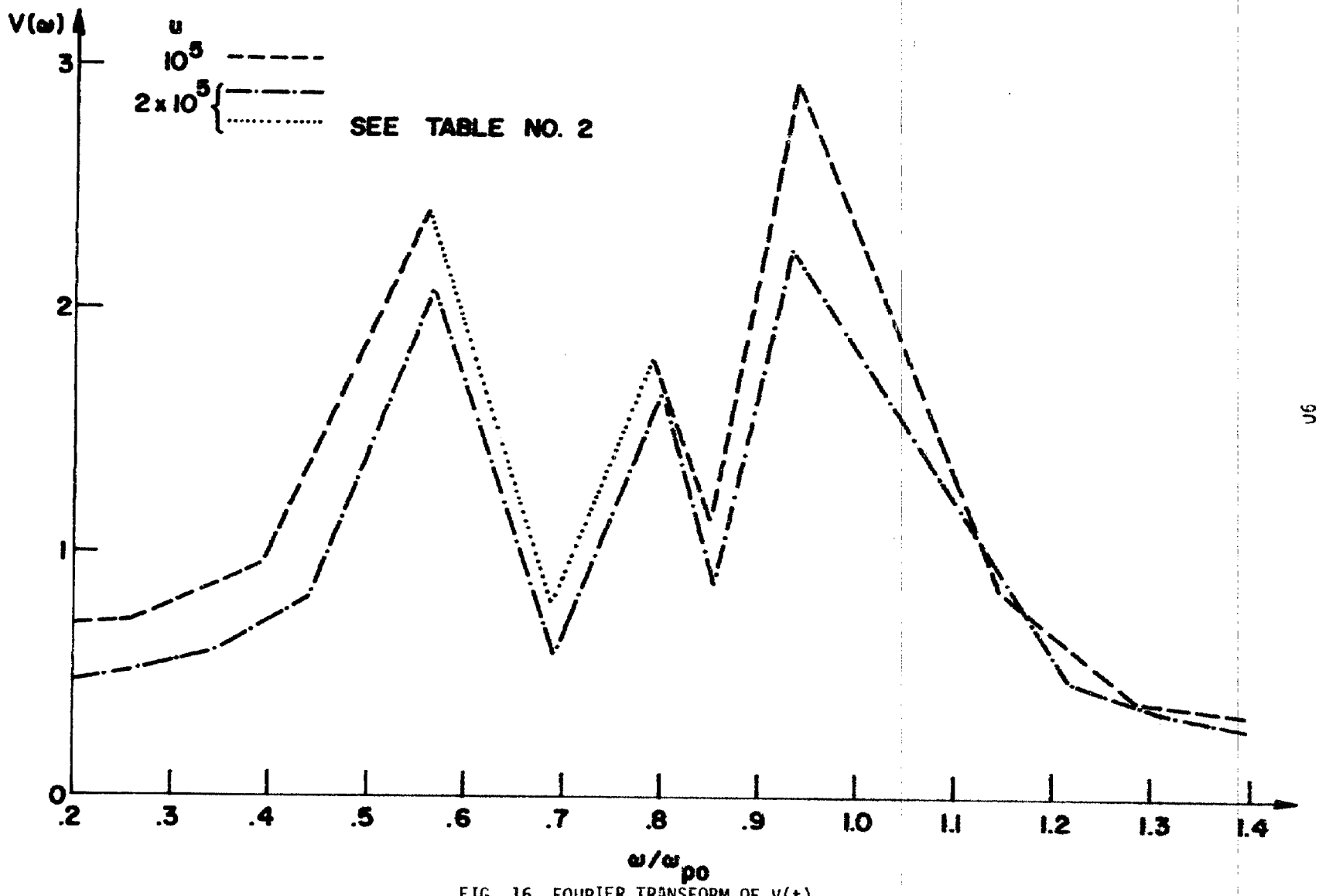

FIG. 16 FOURIER TRANSFORM OF V(t)
$a = 10^6$, $u = 10^5$, 2.10^5, $d = 0.005$

2. The resonance peak at approximately $\hat{f}=0.8$, generated in the intermediate region (region 2) shows an increase by about 6.5%.
3. The resonance corresponding to the region in the center of the slab is approximately 31% higher than that of the standard experiment.

It should be remembered that the results for the experiment under discussion had to be obtained from a time domain truncated to 7.5 plasma periods. Therefore the number of envelope points is rather small as can be seen from Fig. 16 and Table 12. The adduced results, however, permit to affirm that one has begun to penetrate the non-linear region.

As mentioned before, once one leaves the linear region Δn does not remain identically zero at the center of the slab. Variations of several percent of equilibrium density at the center of the slab are observed for $a=u=10^6$, $d=0.005$. The results are of the same magnitude if $d=0.010$. This implies that the particle migration pattern ar the origin will no longer have the "dipole characteristic" around the center of the slab. Further, Δn will no longer be essentially odd nor will ΔE be essentially even.

The non-linear interaction for the high-amplitude excitation is vividly shown in this study: Consider the case $a=u=10^6$, $d=0.005$, i.e. the configuration of the standard experiment with a ten times stronger stimulus. It is possible to see that a strong tendency to develop bunching is taking place at the very early stages. In Fig. 17, the total electric field (not its deviation) is plotted as a function of x/d. One observes initially the field at $t=0.3$ (at about the first voltage peak)

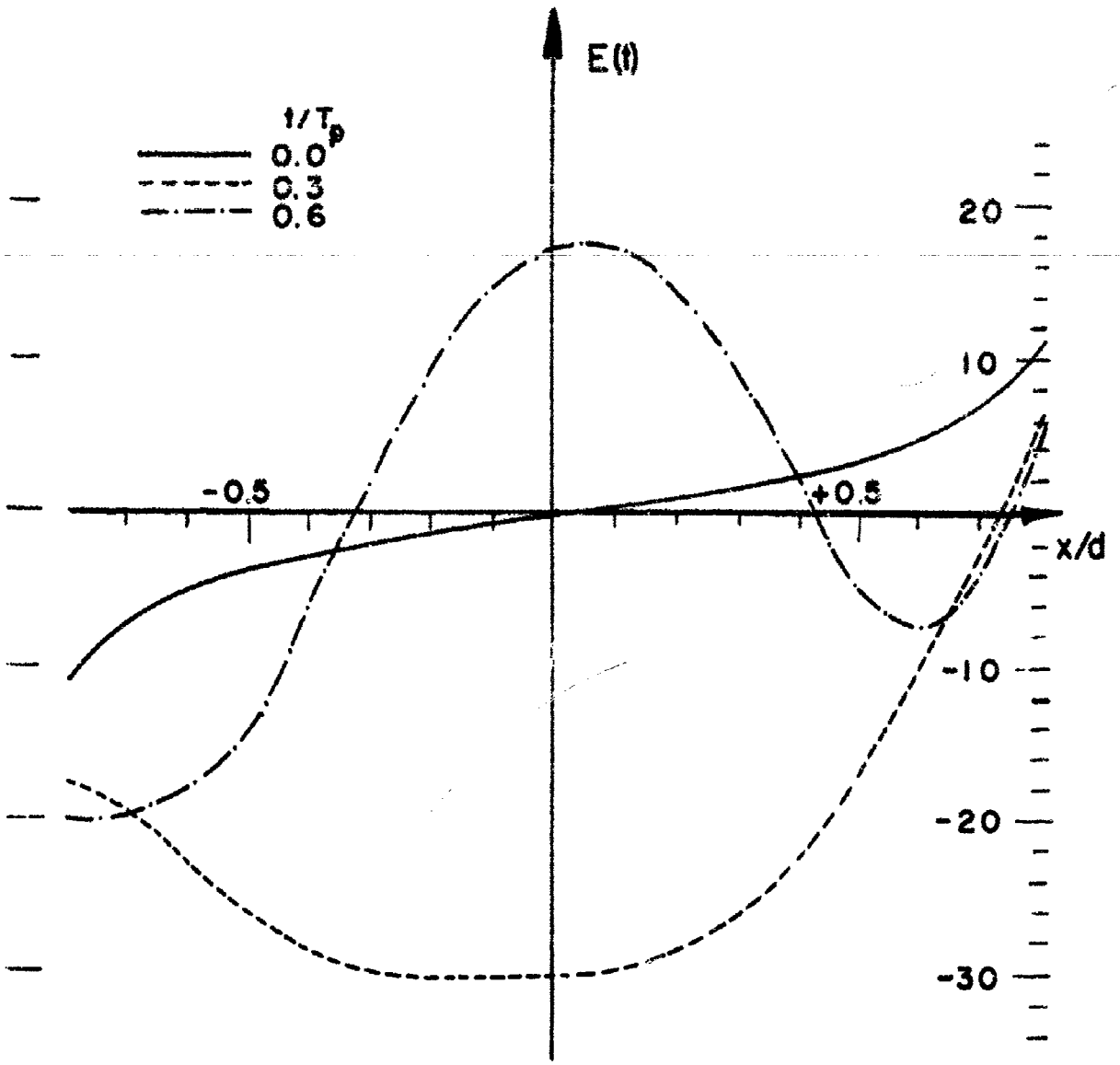

FIG. 17

E(t) vs. x/d
$a=10^6$, $u=10^6$, d=0.005
t- 0.0, 0.3, 0.6

which is characteristic for the electric field during the second quarter of the first plasma period, i.e. $0.25<t<0.5$. The electric field is negative everywhere except very near the wall $x=d$; practically all electrons which were accelerated by the initial impulse towards the wall at $x=-d$, now see a force which tries to restore them towards the wall at $x=d$. This is similar to the linear case. Next one observes the field at $t=0.6$ (at about the first voltage zero) which is characteristic for the electric field during the third quarter of the first plasma period, to be more exact, for the time $0.55<t<0.70$. One sees a positive region in the middle and a negative region between the center of the slab and the wall at $x=d$. One observes three zeros of the electric field while in the linear region one observes only one. The particle-wave interaction is now seen clearly; the electrons in the regions of positive electric field are accelerated towards the "left", i.e. the wall at $x=-d$ while electrons in the regions of negative electric field are accelerated towards the "right", i.e., towards the wall at $x=+d$. Thus bunching is produced around $x/d\approx-0.35$ and some around $z/d\approx+0.75$ while a depletion takes place around $x/d=+0.45$.

Also shown in Fig. 17 for comparison purposes is the electric field in the plasma in equilibrium.

Similar bunching and depletion areas are also observed at later times during the experiment. Similar results are observed for $a=u=10^6$, $d=0.010$.

APPENDIX I: THE GENERAL SYSTEM OF EQUATIONS FOR A COLLISIONLESS GASEOUS PLASMA. REDUCTION TO THE MONODIMENSIONAL (LONGITUDINAL) CASE.

The system of equations for a collisionless gaseous plasma formed by n kinds of particles is

$$\varepsilon_o \frac{\partial \underset{\sim}{E}}{\partial t} - \nabla \times \underset{\sim}{H} + \Sigma_\alpha q_\alpha \int f_\alpha \underset{\sim}{v} d\underset{\sim}{v} = 0 \qquad (I.1)$$

$$\nabla \times \underset{\sim}{E} + \mu_o \frac{\partial \underset{\sim}{H}}{\partial t} = 0 \qquad (I.2)$$

$$\frac{\partial f_\alpha}{\partial t} + \underset{\sim}{v} \cdot \nabla f_\alpha + \frac{q_\alpha}{m_\alpha}(\underset{\sim}{E} + \mu_o \underset{\sim}{v} \times \underset{\sim}{H}) \cdot \nabla_{\underset{\sim}{v}} f_\alpha = 0 \qquad (I.3)$$

$$\nabla \cdot \underset{\sim}{E} = \Sigma_\alpha \frac{q_\alpha}{\varepsilon_o} \int f_\alpha d\underset{\sim}{v} \qquad (I.4)$$

$$\nabla \cdot \underset{\sim}{H} = 0 (= \nabla \cdot \underset{\sim}{B}) \qquad (I.5)$$

$$\underset{\sim}{B} = \mu_o \underset{\sim}{H} \qquad (I.6)$$

$$\alpha = 1,2,3, \ldots, n$$

The 8+n scalar equations (I.1-5) relate the 6+n scalar functions $\underline{E}, \underline{H}, f_\alpha$ to the 7 independent variables $\underline{r}, \underline{v}, t$. The type of particle is characterized by the subscript α. ε_o and μ_o are the permeability and permittivity of free space. $\underline{E}$ and $\underline{h}$ are the usual field vectors, $\underline{B}$ being defined by (I.6) and the respective result used in (I.3). f_α is the distribution function

of the α-th type of particle. The system (I.1-6) refers the variables within the international M.K.S. (Giorgi) or similarly rationalized system.

Initially assume that one has a gaseous plasma composed of one element, the amount of impurities being negligible. This gas is fully ionized. It is not necessary to assume that the plasma is compensated. One has only electrons and ions; n=2. Assume that one is interested in a relatively short time span and that initially the ion velocity can be considered small; then the ions can be considered immobile. Thus the ion distribution function does not depend on velocity or time but on space only.

Consider now a plasma contained by the two walls $x = \mp d$. If one imposes translational invariance with respect to y and z and further imposes that the electrons move in the x-direction only, the electron distribution function will be function of the space coordinate x, the velocity v (in the x-direction) and time t only. From (I.4) follows that div $\underline{E}$ is a function of x and t only; assume the same to be true of the component E_x which one sets $E=E_x$ for notational simplicity. One notes further that (I.3) reduces to 0=0 for the ions and that the dot-cross product of the same equation for electrons vanished since the velocity gradient is collinear with $\underline{v}$ both being in the x-direction. Thus one has

$$\frac{\partial E}{\partial x} = -\frac{e}{\varepsilon_o} \int f \, dv + \frac{e}{\varepsilon_o} n \tag{I.8}$$

$$\frac{\partial f}{\partial t} + v\frac{\partial f}{\partial x} - \frac{e}{m} E\frac{\partial f}{\partial v} = 0 \tag{I.9}$$

f being the electron distribution function, n(x) the ion density and e now is the absolute value of the electron charge and it is assumed that the charge of an ion is e.

It should be mentioned once more that the plasma does not have to be compensated; in fact it is more convenient in further development to consider the plasma not compensated since this will lead to ease of language. One notes that (I.9) contains no information about the ions except through E. Thus the electron distribution function will not be affected if the term in n(x) be replaced by the x-derivative of a time-invariant external field. It is of course also possible that this external electric field has the x-derivative such that the plasma becomes compensated.

With these assumptions one recognizes in the system (I.8,9) equations for a longitudinal plasma behavior. It will be shown that (I.8,9) are in fact sufficient together with mixed initial value and boundary conditions to determine f and E.

APPENDIX II: PROOF OF THE SEPARABILITY OF VARIABLES OF THE DISTRIBUTION FUNCTION f(x,v) OF THE CONSIDERED PLASMA SLAB IN ITS EQUILIBRIUM STATE.

In this appendix we prove that for E(x) real analytic, the distribution function f(x,v) is separable, i.e., that $f(x,v) = \varphi(x)\psi(v)$ and that, further, $\psi(v)$ is Gaussian and that either $\varphi(x) > 0$ or $\varphi(x) < 0$ everywhere in the slab.

We consider the following equilibrium state of a Vlasov plasma

$$\frac{1}{C}\frac{\partial E(x)}{\partial x} = -\int_{-\infty}^{+\infty} f(x,v)dv + n(x) \qquad \text{(II.1)}$$

$$v\,\frac{\partial f(x,v)}{\partial x} - E(x)\,\frac{\partial f(x,v)}{\partial v} = 0 \qquad \text{(II.2)}$$

defined on the domain D

$$-d < x < d \qquad -\infty < v < \infty \qquad \text{(II.3)}$$

and subject to the boundary conditions

$$f(-d,v) = f(d,v) = f(x,-\infty) = f(x,+\infty) = 0 \qquad \text{(II.4)}$$

C is a real positive constant.

Lemma: Given f(x,v) differentiable everywhere on D, E(x) and n(x) are uniquely determined provided dE/dx exists for all $x \in D$ and the integral in II.1 exists.

Proof: f(x,v) is differentiable everywhere, the integral in (II.1) exists. The rest follows by inspection from (II.1,2).

Lemma: If f(x,v) is differentiable and separable in its variables, then, k and a being constants

$$f(x,v) = k\varphi(x)\exp(-v^2/2a^2) \tag{II.5}$$

Proof: Let $f(x,v) = \varphi(x)\psi(v)$. Then (II.3) yields

$$E = \frac{\frac{d\varphi}{dx}}{\varphi}\frac{v\psi}{\frac{d\psi}{dv}} \tag{II.6}$$

Since $E = E(x)$, the second fraction has to be a constant. Integrating the resulting ordinary differential equation with K and a constant

$$\psi(v) = K\exp(-v^2/2a^2) \tag{II.7}$$

and (II.5) results. It is convenient to choose K such that

$$\int_{-\infty}^{-\infty} \psi(v)\,dv = 1 \tag{II.8}$$

resulting in the Gaussian

$$\psi(v) = \frac{1}{a\sqrt{2\pi}}\exp(-v^2/2a^2) \tag{II.9}$$

It is also convenient to choose

$$\varphi(0) = 1 \tag{II.10}$$

Lemma: If f(x,v) is separable, i.e., $f(x,v) = \varphi(x)\psi(v)$, then

$$F(x) = -\frac{a^2}{\varphi}\frac{d\varphi}{dx} = -a^2\frac{d}{dx}(\ell n\varphi) \tag{II.11}$$

$$n(x) = \varphi - \frac{a^2}{C}\frac{d^2}{dx^2}(\ell n\varphi) \tag{II.12}$$

provided the derivatives in (II.11,12) exist.

Proof: One obtains E(x) be entering (II.5) into (II.2). Then, by entering (II.5,11) into (II.1), (II.12) follows.

THEOREM: Let E(x) be a real analytic function in D and let $\varphi(x)$ be a solution of the ordinary differential equation (II.11)

$$\frac{d}{dx}(\ell n\varphi) = -\frac{1}{a^2}E(x) \qquad \text{(II.13)}$$

satisfying $\varphi(-d) = \varphi(d) = 0$. Then $f(x,v) = K\varphi(x)\exp(-v^2/2a^2)$, i.e., f(x,v) is separable in its variables and its velocity dependence is Gaussian.

Proof: Let $\bar{f}(x,v) = \varphi(x)\psi(v)$ where $\psi(v)$ is given by (II.9) and $\varphi(x)$ is the solution of (II.13) satisfying $\varphi(d)=\varphi(-d) = 0$. $\bar{f}(x,v)$ together with the given E(x) satisfies (II.2) as well as the boundary conditions (II.4). But for E(x) analytic, the theorem of existence and unicity of the solution of quasi-linear partial differential equations of the first order in two variables certainly applies. Thus $\bar{f}(x,v) = \varphi(x)\psi(v)$ will also be the only solution of (II.2) with the given E(x). Q.E.D.

THEOREM: If E(x) is analytic in D, φ is either positive or negative everywhere in D.

Proof: From (II.11) follows, using (II.10), that

$$\varphi(x) = K\exp\left(-\frac{1}{2}\int_0^x E(x)dx\right) \qquad \text{(II.14)}$$

Since $E(x)$ is analytic, it is continuous and thus $\varphi(x)$ is continuous. But $E(x)$ also is finite in D and thus $\varphi(x)$ is non-zero in D as follows from (II.11). Therefore $\varphi(x)$ is either always positive or negative. Q.E.D.

One notes that if (II.10) is assumed, $\varphi(x)$ is positive everywhere in D.

BIBLIOGRAPHY

1. S.V. Klimontovich, "Statistical Theory of Non-Equilibrium in Plasma," MIT Press, Boston, 1967.
2. N. Marcuvitz, "Plasma Dynamics," Lecture Notes, New York University, 1970.
3. R. Davidson and P. Schramm, Nuclear Fusion, 8, 183 (1968).
4. P.E. Vandenplas and R.W. Gould, Plasma Physics, J. Nucl. En., Part C, 6, 449, 1964.
5. C.R. Obermann, Bull. Am. Phys. Society, Series 2, 5, 364, 1960.
6. M. Feix, "Mathematical Models of Plasma". In "Non-Linear Models of Plasma." Proc. 2nd Orsay Summer Institute, G. Kalman and M. Feix, eds., Gordon and Breach, New York 1969.
7. N.G. Van Kampen, Physica, 21, 949, 1955.
8. G. Georges, "Perturbation Theory for Non-Linear Systems," New York University Technical Memorandum, November 1969.
9. F. Einaudi and R.N. Sudan, Plasma Physics, 11, 359, 1969.
10. N. Marcuvitz, "Plasma Turbulence," Lecture Notes, New York University, 1969.
11. E.M. Barston, Phys. Fluids, 6, 828, 1964.
12. E.M. Barston, Ann. Phys., New York, 29, 282, 1964.
13. F.W. Crawford and G.S. Kino, Comp. Rend. Acad. Sc., Paris, 256, 1939 and 2798, 1963.
14. M. Trocheris, "On the Derivation of the 'Quasi-Linear' Equations," In Op. Cit. Reference #6.
15. J.F. Denisse et J.L. Delcroix, "Theorie des Ondes Dans Les Plasmas," Dunod, Paris, 1959.
16. V.L. Ginzburg, "Propagation of Electromagnetic Waves in Plasma," Fizmatgiz, Moscow, 1960; Eng. Tr., Gordon and Breach, New York.
17. P.E. Vandenplas, "Electron Waves and Resonances in Bounded Plasmas," John Wiley and Sons, London, 1968.
18. N. Marcuvitz, "Complete Set of Eigenmodes for a Collisionless Isotropic Maxwell-Vlasov Plasma." Communications in Electrophysics. Memorandum M-3, New York University, s.d
19. N. Marcuvitz, "Nonlinear Kinetically Described One-Component Plasma," Communications in Electrophysics, Memorandum M-1, New York University, October 1968.
20. R.A. Frisch, Prv. Comm., 1970.
21. N. Marcuvitz, "Quasi-Particle Descriptions in Classical Many-Particle Systems," Communications in Electrophysics. Memorandum M-5, New York University, s.d.
22. J.M. Dawson, Phys. Fluids, 5, 445, 1962.
23. A. Bers and H. Schneider, Quart. Prog., Report # 89, M.I.T., p. 123, April 15, 1968.
24. J. Brooks and B.S. Cheo, Priv. Comm., 1971.
25. T.P. Armstrong, Phys. Fluids, 10, 1269, 1967.
26. P. Pleshko, Ph.D. Thesis, New York University, 1969.
27. D.E. Baldwin, Phys. Fluids, 12, 279, 1969.
28. D.W. Ignat, Ph.D. Thesis, Yale University, 1969.